

Earth's Future

REVIEW ARTICLE

10.1029/2022EF003314

Special Section:

The Future of Critical Zone Science: Towards Shared Goals, Tools, Approaches and Philosophy

Key Points:

- Increasing remote sensing capabilities improve observations of disturbance severity and recovery in varying critical zone settings
- Case studies present how new approaches from multiple platforms and sensors better quantify post-disturbance recovery of montane forests
- We suggest integrating the new approaches to refine remote sensing capabilities and resolve critical zone processes at multiple scales

Correspondence to:

K. Hwang,
kyotaek.hwang@colorado.edu

Citation:

Hwang, K., Harpold, A. A., Tague, C. L., Lowman, L., Boisramé, G. F. S., Lininger, K. B., et al. (2023). Seeing the disturbed forest for the trees: Remote sensing is underutilized to quantify critical zone response to unprecedented disturbance. *Earth's Future*, 11, e2022EF003314. <https://doi.org/10.1029/2022EF003314>

Received 10 NOV 2022














Accepted 28 JUN 2023

Author Contributions:

Conceptualization: Kyotaek Hwang, Adrian A. Harpold, Christina L. Tague, Katherine B. Lininger, Pamela L. Sullivan
Formal analysis: Kyotaek Hwang, Adrian A. Harpold, Lauren Lowman, Gabrielle F. S. Boisramé, Aidan Manning, Louis Graup, Gabriel Lewis
Funding acquisition: Holly R. Barnard

© 2023 The Authors. Earth's Future published by Wiley Periodicals LLC on behalf of American Geophysical Union. This is an open access article under the terms of the [Creative Commons Attribution License](https://creativecommons.org/licenses/by/4.0/), which permits use, distribution and reproduction in any medium, provided the original work is properly cited.

Seeing the Disturbed Forest for the Trees: Remote Sensing Is Underutilized to Quantify Critical Zone Response to Unprecedented Disturbance

Kyotaek Hwang¹ , Adrian A. Harpold² , Christina L. Tague³ , Lauren Lowman⁴ , Gabrielle F. S. Boisramé⁵ , Katherine B. Lininger⁶ , Pamela L. Sullivan⁷ , Aidan Manning⁸ , Louis Graup³ , Marcy Litvak⁹ , Gabriel Lewis² , Kate Miller², Paul D. Brooks¹⁰ , and Holly R. Barnard^{1,6} 

¹Institute of Arctic and Alpine Research, University of Colorado Boulder, Boulder, CO, USA, ²Department of Natural Resources and Environmental Science, University of Nevada, Reno, Reno, NV, USA, ³Bren School of Environmental Science and Management, University of California, Santa Barbara, Santa Barbara, CA, USA, ⁴Department of Engineering, Wake Forest University, Winston-Salem, NC, USA, ⁵Division of Hydrologic Sciences, Desert Research Institute, Las Vegas, NV, USA, ⁶Department of Geography, University of Colorado Boulder, Boulder, CO, USA, ⁷College of Earth, Ocean and Atmospheric Science, Oregon State University, Corvallis, OR, USA, ⁸Graduate Program of Hydrologic Sciences, University of Nevada, Reno, Reno, NV, USA, ⁹Department of Biology, University of New Mexico, Albuquerque, NM, USA, ¹⁰Department of Geology and Geophysics, University of Utah, Salt Lake City, UT, USA

Abstract Understanding the severity and extent of near surface critical zone (CZ) disturbances and their ecosystem response is a pressing concern in the face of increasing human and natural disturbances. Predicting disturbance severity and recovery in a changing climate requires comprehensive understanding of ecosystem feedbacks among vegetation and the surrounding environment, including climate, hydrology, geomorphology, and biogeochemistry. Field surveys and satellite remote sensing have limited ability to effectively capture the spatial and temporal variability of disturbance and CZ properties. Technological advances in remote sensing using new sensors and new platforms have improved observations of changes in vegetation canopy structure and productivity; however, integrating measures of forest disturbance from various sensing platforms is complex. By connecting the potential for remote sensing technologies to observe different CZ disturbance vectors, we show that lower severity disturbance and slower vegetation recovery are more difficult to quantify. Case studies in montane forests from the western United States highlight new opportunities, including evaluating post-disturbance forest recovery at multiple scales, shedding light on understory vegetation regrowth, detecting specific physiological responses, and refining ecohydrological modeling. Learning from regional CZ disturbance case studies, we propose future directions to synthesize fragmented findings with (a) new data analysis using new or existing sensors, (b) data fusion across multiple sensors and platforms, (c) increasing the value of ground-based observations, (d) disturbance modeling, and (e) synthesis to improve understanding of disturbance.

1. Introduction

The critical zone (CZ—the terrestrial Earth's surface above the base of actively circulating groundwater) determines how forest ecosystems and streams will respond to drought, warming temperatures, and disturbances (Condon et al., 2020; Keller, 2019). Because of the high spatial and temporal variability of CZ structure and function, understanding the links and feedbacks among a myriad of CZ processes remains a challenge in Earth Science. Vegetation connects the atmosphere and the subsurface, and simultaneously responds to atmospheric and subsurface conditions. This interaction among plants and the surrounding environment exerts strong controls on hydrologic, geomorphic, and biogeochemical fluxes. Consequently, vegetation disturbance has important cascading impacts on the functioning of key CZ ecosystem services, including the provisioning of natural resources, erosion and weathering, biogeochemical cycling, and maintenance of biota over instantaneous to decadal time frames (Field et al., 2015; Green et al., 2019; Minor et al., 2020; Peterson et al., 2021; Rasmussen et al., 2015).

Montane forests in the western United States (US) provide important CZ services, including regulation of water, wildlife habitat, biodiversity, and carbon sequestration (Field et al., 2015). However, these forests are facing persistent and increasing pressures from climatic and human-driven disturbances. Monitoring and understanding

Investigation: Kyotaek Hwang, Lauren Lowman

Project Administration: Holly R. Barnard

Resources: Adrian A. Harpold, Marcy Litvak

Supervision: Holly R. Barnard

Visualization: Kyotaek Hwang, Adrian A. Harpold, Lauren Lowman, Gabrielle F. S. Boisramé, Aidan Manning, Louis Graup, Kate Miller

Writing – original draft: Kyotaek Hwang, Adrian A. Harpold, Christina L. Tague, Lauren Lowman, Gabrielle F. S. Boisramé, Katherine B. Lininger, Pamela L. Sullivan, Aidan Manning, Louis Graup, Marcy Litvak, Gabriel Lewis, Holly R. Barnard

Writing – review & editing: Kyotaek Hwang, Adrian A. Harpold, Christina L. Tague, Lauren Lowman, Gabrielle F. S. Boisramé, Katherine B. Lininger, Pamela L. Sullivan, Aidan Manning, Louis Graup, Marcy Litvak, Gabriel Lewis, Paul D. Brooks, Holly R. Barnard

disturbance-driven changes to the forest ecosystems is challenging due to the complex spatio-temporal patterns involved. Montane forested ecosystems have large elevation gradients, with higher elevations being generally cooler and wetter than lower elevations, and corresponding shifts in vegetation composition adapted to those climate and CZ conditions. Higher biomass and more precipitation variability also make montane ecosystems more susceptible to chronic and acute disturbances, such as multi-year droughts (Clark et al., 2016; Young et al., 2017), extreme flooding (Anderson et al., 2015), insect outbreaks (Meddens et al., 2012), wildfire (Dennison et al., 2014), and expansion of the wildland-urban-interface (Radeloff et al., 2018). Complex topography (e.g., steep slopes and convergent areas) also leads to greater heterogeneity in climate and vegetation, thereby posing significant challenges in prediction of disturbance response. Disturbances are an important part of CZ evolution in forests and other ecosystems, altering the co-evolution of vegetation, subsurface properties, and water storage (Pelletier et al., 2013; Troch et al., 2015). The recent increases in intensity and spatial extent of wildfires and insect outbreaks have altered the CZ services in many montane forests that remain hard to monitor and predict (Bales et al., 2018; Mildrexler et al., 2016; Thorne et al., 2018).

Disturbance often changes the structure and composition of both above- and belowground ecosystems, which ultimately affects carbon and water budgets (Hicke et al., 2012; Keller, 2019; Williams et al., 2014). For example, high severity wildfire can remove much of the overstory biomass, whereas widespread tree die-off from drought, disease, and insects is likely to leave standing dead trees that can persist for decades (Stephens et al., 2018). Similarly, high-severity wildfire can reduce water storage by removing much of the organic matter from the soil surface and temporarily reducing infiltration capacity (Ebel, 2020; Ebel & Moody, 2017; Moody et al., 2019; Shakesby & Doerr, 2006). The vegetation succession and species change after disturbance will depend not only on local ecosystem resilience, but also on climate (Rother & Veblen, 2016, 2017) and on existing CZ structure (i.e., deep and porous soils vs. low subsurface storage) (Tague & Moritz, 2019). Over long periods of time, disturbance severity and return intervals can govern processes such as weathering fluxes, subsurface porosity development (Navarre-Sitchler et al., 2009, 2013, 2015), and surface erosion (Orem & Pelletier, 2015, 2016). One commonality across disturbance vectors for montane forests is an expectation that climate change will increase the occurrence, severity, and extent of disturbance (Dale et al., 2001; Loehman et al., 2017; Tague et al., 2019). For example, increasing air temperature and vapor pressure deficit (VPD) are expected to increase drought mortality, and weaken resistance to insects and disease (Hartmann et al., 2022). Similarly, warming climate and poor fuel management are expected to increase wildfire severity and extent into the mid-21st century (Abatzoglou & Williams, 2016). Future precipitation changes are highly uncertain, but increased warming is expected to drive atmospheric patterns that produce additional intense and extreme weather events (Mallakpour & Villarini, 2016) that will impact flood frequencies.

Satellite remote sensing platforms have served as the workhorse for forest change detection, with the ability to determine global forest loss (Hansen et al., 2010, 2013), land cover conversion (Curtis et al., 2018), and post-disturbance recovery of forest ecosystems (White et al., 2017). Chronic disturbance (e.g., drought), which needs regional observations with a long record of several decades, has benefited from continuous satellite-based spectral observations (e.g., Landsat and Moderate Resolution Imaging spectroradiometer; MODIS) (Frolking et al., 2009; Kennedy et al., 2012; Okin et al., 2018). Similarly, current research has used multi-decade satellite data to determine not only the type and extent of disturbance (Hislop et al., 2019; White et al., 2017), but also a wide variety of post-disturbance vegetation attributes such as forest structure, species composition and establishment (Bolton et al., 2015; Hermosilla et al., 2019; Matasci et al., 2018; Savage et al., 2017; Senf et al., 2019; Vanderhoof et al., 2021; White et al., 2018). Remote sensing platforms have also been used to assess the impact of human activities such as river and floodplain restoration through the re-introduction of beaver and the installation of beaver mimicry structures (i.e., beaver dam analogs) and other restoration approaches (Hausner et al., 2018; Melesse et al., 2007), highlighting human actions aimed at enhancing landscape resiliency in the CZ. However, many CZ processes that may be influenced by disturbance, occur at spatial and temporal scales that cannot be effectively captured with conventional coarse scale, multispectral remote sensing (e.g., Landsat has 30-m and MODIS has 500-m resolution). For example, the ability of forest structure mapping that can separate overstory and understory, identify species, and estimate evapotranspiration and productivity is still limited. At the same time, emerging remote sensing platforms and sensors have new capabilities to observe CZ response to disturbance at finer spatial and temporal scales.

The potential to utilize new sensing platforms has many benefits for understanding CZ response to disturbance that have yet to be fully realized (Figure 1). Higher-resolution observational capabilities from satellites, aircrafts,

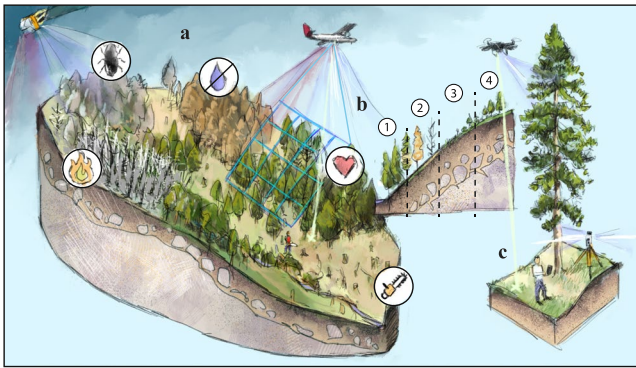


Figure 1. Conceptual description of remote sensing applications in evaluating vegetation response to disturbances. Subpanels indicate different capabilities of remote sensing platforms (i.e., satellite, airborne, unmanned aerial vehicle, and ground) in quantifying CZ structure and inferring CZ processes across the spatial coverage: (a) catchment, (b) hillslope, (c) individual tree. The hillslope scale inset (b) presents post-disturbance vegetation succession stages with (1) pre-disturbance, (2) disturbed, (3) understory regrowth (grass/forb/shrub), (4) overstory regrowth to intermediate height. (image credit: Eric Parrish).

and uncrewed aerial vehicles (UAVs), can fill this observational gap from 0.1 m² to 1 km² that is critical to CZ processes and disturbance heterogeneity (Figure 1). Different disturbance types and intensities require different observation strategies in terms of resolution, extent, and repeatability (Figure 2). For example, higher-resolution observations from newer platforms (e.g., airborne, UAV, and ground) may be more effective for lower-intensity and smaller-extent disturbances that will have slower recovery. Similarly, more conventional remote sensing platforms (e.g., satellite) have evolved to increase spatial, temporal, or spectral coverage (Figure 2). For example, small, geostationary satellites are able to capture multispectral images at the scale of 50–200 cm (Frazier & Hemingway, 2021; Kimm et al., 2020). The fixed wing aircraft continues to remain critical to sensor technology that is not satellite ready (i.e., active energy sources) or where higher spatial resolution is required. UAV platforms have become much more common with recent advances in sensors and reductions in sensor size and weight. At these scales, remote sensing can be effectively linked and verified with field observations for integrating subsurface and ecological processes that are not observable with satellite remote sensing. With these new platform technologies, experimental design trade-offs between spatio-temporal coverage, resolution, and costs need to be considered for different disturbance extents and severity (Figure 2).

A suite of different sensing technologies exists or is near deployment that can be developed into a variety of data products relevant to CZ disturbance and vegetation recovery (Table 1), yet most are rarely utilized in a coordinated way to monitor CZ disturbance. Remote sensing products across different sensor types can either supplement data coverage (e.g., lidar, photogrammetry, and radar) (Qi et al., 2019) or relate estimated variables to extent and intensity of disturbance (e.g., imaging spectrometer and lidar) (Bolton et al., 2015; Kane et al., 2014; Meng et al., 2018; Viana-Soto et al., 2022; White et al., 2022). Importantly, co-located sensors in the same platform result in development of new algorithms to estimate new variables (e.g., canopy water content and biomass) that could only be acquired from destructive measurements previously (Asner et al., 2015; Paz-Kagan et al., 2018). However, these attempts are not producing reliable information for post-disturbance monitoring as they are lacking thorough validation efforts.

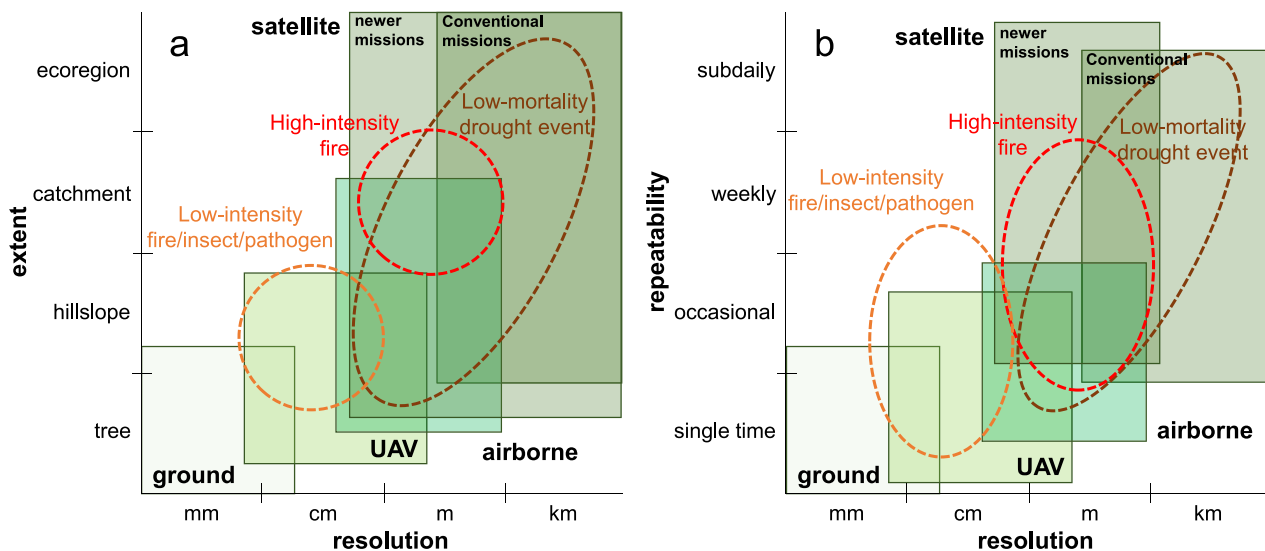


Figure 2. Conceptual diagrams of remote sensing capabilities in (a) extent, and (b) repeatability for disturbance evaluation. Different remote sensing platforms provide complementary spatio-temporal coverages that have varying suitability for disturbance type and intensities.

Table 1
Observational Capabilities of Remote Sensing Sensors in Disturbance Assessment

Sensor type	Direct observation	Derived quantity	Disturbance evaluation				
			Flooding	Wildfire	Harvest/ thinning	Drought	Insect/ pathogen
Spectral Imaging	Spectral traits of land surface	Land cover classification		0		0	0
		Surface moisture index			0		
		Snow albedo, snow aridity index	0	0	0	0	
	Spectral traits of vegetation canopy	Burn severity index, burn ratio		0			
		Fraction of absorbed photosynthetically active radiation				0	
		Vegetation index		0	0	0	0
		Tree health/mortality				0	0
		Disease/infestation stage					0
Lidar and Photogrammetry	Land surface elevation	Sediment yield, erosion/deposition	0	0			
		Snow cover/depth	0	0	0	0	
	Vegetation structure	Vegetation height/density, species composition, wood volume, basal area, diameter at breast height, species type, canopy size		0	0		
Thermal Sensing	Land surface temperature	Soil surface temperature		0		0	
		Land surface energy balance	0	0	0	0	
	Leaf surface temperature	Evapotranspiration	0	0	0	0	
		Stomatal conductance, vegetation water stress					0
Radar	Vegetation structure	Aboveground/underground biomass, forest carbon storage	0	0	0	0	
		Foliage volume		0	0		
	Water content	Soil/vegetation water content					0
		Snow water equivalent		0	0	0	0

In this focused review, we call attention to an opportunity in CZ science: how modern remote sensing platforms and sensors (Table 1, Figures 1 and 2) could advance our understanding of disturbance impacts and recovery across scales. Although disturbances have been studied for decades (Frolking et al., 2009; Huang et al., 2019; Jiao et al., 2021; Senf et al., 2017; Szpakowski & Jensen, 2019), the quality of remote sensing has reached a threshold that can better inform our predictive models. However, integration of different remote sensing datasets and platforms, coordination with field observations, and experimental design remain key challenges. Several knowledge gaps persist including the assessment of CZ changes and their drivers/impacts, and elucidating how disturbance impacts carbon and water storage and fluxes (Bloschl et al., 2019). Specifically, montane forests need better predictions of post-disturbance changes in CZ services such as carbon sequestration, water supply and quality, and risk mitigation for people and property. We focus on three topics relevant to the CZ science and remote sensing communities:

1. How can we improve our evaluation of disturbance extent and severity over different time periods following disturbance?
2. What combination of sensors, platforms, and data fusion will most improve the characterization and modeling of the post-disturbance CZ processes?
3. How can resources be mobilized and coordinated to apply better remote sensing observations following disturbance?

Our primary focus is to explore sensor-platform combinations that can transform our understanding of CZ response, with the goal of highlighting how new sensor technologies can contribute to advances in our knowledge. Section 2 briefly reviews recent remote sensing applications for disturbance evaluation using different sensor-platform combinations. Our aim is to analyze the strengths and weaknesses of these combinations and identify the most effective approaches for tracking individual disturbance types. Section 3 presents five prevailing disturbance cases from the western montane forests that demonstrate how both old and new sensor-platform combinations are utilized for different spatio-temporal scales and disturbance types. These case studies identify effective methods for evaluating CZ processes. Finally, based on the knowledge gained from these studies, Section 4 presents a vision for leveraging these advances, in combination with current observation capabilities, to enhance our understanding of CZ processes.

2. Sensors and Platforms for Observing CZ Disturbance

A suite of remote sensing platforms and sensors can provide snapshots of CZ structure useful for inferring processes at multiple spatio-temporal scales. Compared to mature and obsolete missions, cutting-edge platforms and sensors from recently launched and upcoming missions facilitate improved observations with enhanced resolutions of space, time, and wavelength/bandwidth (Table 2). Opportunities exist to evaluate transferability of the new platforms and sensors including (a) more specific wavelength/bandwidth combinations to measure vegetation attributes that were not detected before, (b) existing algorithms to be either used or refined to retrieve variables in greater detail, and (c) spatial scales and temporal intervals to best describe CZ processes and vegetation responses (Table 1). In this section, we review platforms (i.e., satellite, airborne, UAV, ground) and sensor types (i.e., spectral imaging, lidar and photogrammetry, thermal sensing, radar) associated with recent advances and how they were used to address ecosystem response to environmental disturbances. Strengths and weaknesses of each platform and sensor are discussed with examples of how these are used to evaluate post-disturbance forest changes.

2.1. Satellite-Based Sensors

Satellite remote sensing with more than 50 years of regular data acquisition across the globe has great value in assessment of disturbance. This data is uniquely useful in disturbance-prone areas that lack any in-situ or airborne measurements. A wide variety of sensor instruments have recorded the land surface over five decades, along with dozens of pioneering missions (Lettenmaier et al., 2015). Non-commercial satellite datasets are publicly available with standardized image process and centralized data management through dedicated agencies, including National Aeronautics and Space Administration (NASA) and the US Geological Survey (USGS). Despite advances in platform and sensor technologies, relatively low-resolution images still constrain small scale observations (e.g., from leaf to tree scale) (Table 2).

Table 2
Specifications of Satellite and Airborne Remote Sensing Missions in Forest Disturbance Evaluation

Platform	Mission name	Temporal coverage	Spatial resolution	Overpass interval	Sensor type (Band width)	Observational capability			
						Geomorphology	Forest structure	Physiology	Hydrology
Satellite	Landsat	1972–present	30 m	16 days	Multispectral (VIS-MIR), TIR			O	O
	MODIS	2000–present	250, 500, 1,000 m	1 day	Multispectral (VIS-MIR), TIR			O	O
	SPOT	2012–present	1.5, 6 m	1–5 days	Multispectral (VIS, NIR)			O	
	Sentinel-2	2015–present	10, 20, 60 m	10 days	Multispectral (VIS-NIR, SWIR)			O	
	PlanetScope	2016–present	3 m	1 day	Multispectral (VIS, NIR)			O	
	WorldView-4	2016–present	1.24 m	1 day	Multispectral (VIS, NIR)			O	

Table 2
Continued

Platform	Mission name	Temporal coverage	Spatial resolution	Overpass interval	Sensor type (Band width)	Observational capability			
						Geomorphology	Forest structure	Physiology	Hydrology
	Hyperion	2000–2017	30 m	16–30 days	Hyperspectral (220 bands in 357–2,576 nm)			O	
	VIIRS	2011–present	375, 750 m	16 days	Hyperspectral (22 bands in 0.412–12.01 μm)			O	
	HISUI	2019–present	20, 30 m	33 days	Hyperspectral (185 bands in 400–2,500 nm)			O	
	PRISMA	2019–present	5, 30 m	29 days	Hyperspectral (238 bands in 400–2,500 nm)			O	
	EnMAP	2022–present	30 m	4 days	Hyperspectral (230 bands in 420–2,450 nm)			O	
	HyTI	2022 (planned)	60 m	6U Cubesat	Hyperspectral (25 bands in 8–10.7 μm), TIR			O	O
	SBG	2022 (planned)	30, 60 m	5, 19 days	Hyperspectral (210 bands in 350–2,510 nm), TIR			O	O
	FLEX	2025 (planned)	300 m	27 days	Hyperspectral (>250 bands in 500–780 nm)			O	
	CHIME	2029 (planned)	20, 30 m	10–12.5 days	Hyperspectral (400–2,500 nm)			O	
	HiTeSEM	Planned	20, 60 m	5 days	Hyperspectral (75 bands in 7.2–12.5 μm), TIR			O	O
	ICESat	2003–2010	70 m	8 days	Lidar	O	O		
	ICESat-2	2018–present	20 m	91 days	Lidar	O	O		
	GEDI	2019–present	25–1,000 m	4 days	Lidar	O	O		
	ECOSTRESS	2018–present	30, 70 m	1–7 days	TIR, SWIR			O	O
	Envisat ASAR	2002–2012	30–150 m	35 days	Radar (C band)		O		
	Sentinel-1	2014–present	5 m	12 days	Radar (C band)		O		
	ALOS-PALSAR	2006–2011	10–100 m	46 days	Radar (L band)		O		
	ALOS-2 PalSAR	2014–present	3–10 m	14 days	Radar (L band)		O		
	NISAR	2023 (planned)	5–10 m	5–8 days	Radar (L band, S band)		O		
	BIOMASS	2023 (planned)	200 m	3 days	Radar (P band)		O		
	TerraSAR-X	2008–present	16 m	2–3 days	Radar (X band)		O		
	TanDEM-X	2010–present	1–16 m	11 days	Radar (X band)		O		
	GRACE	2002–2017	300–400 km	30 days	Radar (K band)				O
	GRACE-FO	2018–present	300–400 km	30 days	Radar (K band)				O
	QuikSCAT SeaWinds	1999–2018	25 km	4 days	Radar (Ku band)				O
	SWOT	2023 (planned)	50 m	21 days	Radar (Ka band, Ku band, microwave)				O
	AMSR-E	2002–2016	4–43 km	1–2 days	Radar (microwave)				O
	AMSR-2	2012–present	3–35 km	1 day	Radar (microwave)				O
	SMAP	2015–present	1–3 km	2–3 days	Radar (microwave)				O

Table 2
Continued

Platform	Mission name	Temporal coverage	Spatial resolution	Overpass interval	Sensor type (Band width)	Observational capability			
						Geomorphology	Forest structure	Physiology	Hydrology
Airborne	MASTER	1998–present	5–50 m	-	Multispectral (VIR-MIR), TIR			O	O
	NAIP	2003–present	1 m	-	Multispectral (VIS, NIR)			O	
	AVIRIS	1986–present	20 m	-	Hyperspectral (224 bands in 400–2,400 nm)			O	
	AVIRIS-NG	2014–present	0.3, 4 m	-	Hyperspectral (600 bands in 380–2,510 nm)			O	
	NCALM	2003–present	0.2 m	-	Lidar, VIS	O	O	O	
	GAO	2006–present	0.25–2 m	-	Lidar, Hyperspectral (>400 bands in 380–2,510 nm)	O	O	O	
	G-LiHT	2011–present	1 m	-	Lidar, Hyperspectral (402 bands in 400–1,000 nm), TIR	O	O	O	O
	ASO	2013–present	1.5 m	-	Lidar, Hyperspectral (72 bands in 380–1,050 nm)	O	O	O	
	NEON AOP	2013–present	1 m	-	Lidar, Hyperspectral (426 bands in 380–2,510 nm)	O	O	O	

Note. Abbreviated missions and campaigns include MODIS (Moderate Resolution Imaging Spectroradiometer), SPOT (Satellite Pour l'Observation de la Terre), VIIRS (Visible Infrared Imaging Radiometer Suite), HISUI (Hyperspectral Imager Suite), PRISMA (Hyperspectral Precursor of the Application Mission), EnMAP (Environmental Mapping and Analysis Program), HyTI (Hyperspectral Thermal Imager), SBG (Surface Biology and Geology), FLEX (FLuorescence EXplorer), CHIME (Copernicus Hyperspectral Imaging Mission for the Environment), HiTeSEM (High resolution Temperature and Spectral Emissivity Mapping), ICESat (Ice, Cloud, and Land Elevation Satellite), GEDI (Global Ecosystem Dynamics Investigation), ECOSTRESS (Ecosystem Spaceborne Thermal Radiometer Experiment on Space Station), ASAR (Advanced Synthetic Aperture Radar), ALOS-PALSAR (Advanced Land Observing Satellite-Phased Array type L-band SAR), NISAR (NASA-ISRO SAR), TanDEM-X (TerraSAR-X add-on for Digital Elevation Measurements), GRACE (Gravity Recovery and Climate Experiment), GRACE-FO (GRACE Follow-on), QuikSCAT (Quick Scatterometer), SWOT (Surface Water and Ocean Topography), AMSR-E (Advanced Microwave Scanning Radiometer for Earth Observing System), SMAP (Soil Moisture Active Passive), MASTER (MODIS/ASTER Airborne Simulator), NAIP (National Agriculture Imagery Program), AVIRIS (Airborne Visible/Infrared Imaging Spectrometer), AVIRIS-NG (AVIRIS-Next Generation), NCALM (National Center for Airborne Laser Mapping), GAO (Global Airborne Observatory), G-LiHT (NASA Goddard's LiDAR, Hyperspectral and Thermal), ASO (Airborne Snow Observatory), and NEON AOP (National Ecological Observatory Network Airborne Observation Platform). Note abbreviated sensor types include VIS (visible), MIR (mid infrared), TIR (thermal infrared), NIR (near infrared), SWIR (shortwave infrared).

2.1.1. Satellite Spectral Imaging of Disturbance

Satellite-based spectral data that have either a long history of observation (e.g., Landsat; over 50 years) or a frequent overpass (e.g., MODIS; once a day) are widely used for continuous monitoring of the land surface and vegetation cover. In particular, many vegetation indices have been developed to characterize physiological activities from a local to regional scale (Cuevas-Gonzalez et al., 2009; Jin & Sader, 2005). Combinations of spectral bands are sensitive to specific disturbance types, such as normalized difference vegetation index (NDVI) (Gabban et al., 2006), normalized difference burn ratio (Miller & Thode, 2007; van Wagtenonk et al., 2004), and normalized difference moisture index (Wilson & Sader, 2002), or combinations of all such indices (Kennedy et al., 2010). In chronic drought assessment, sensitivity of canopy water loss to precipitation and soil moisture can be indirectly induced from satellite-based NDVI (Gu et al., 2007, 2008; Karnieli et al., 2010; Pettorelli et al., 2005; Williams et al., 2013). More broadly, vegetation health and mortality can be estimated with various approaches including vegetation indices (Meddens et al., 2011; Spruce et al., 2019; Verbesselt et al., 2009; Walter & Platt, 2013), statistical classification models (Garrity et al., 2013), empirical classification models (Fassnacht et al., 2014; Hart & Veblen, 2015; Meddens & Hicke, 2014), and object-based approaches (Freeman et al., 2016). These applications suggest the potential to provide warning signals of drought-induced mortality (Liu et al., 2019) and insect infestation stages (Meddens et al., 2011). Recently launched (e.g., Hyperspectral Precursor of the Application Mission, Hyperspectral Imager Suite; PRISMA, HISUI) and planned (e.g., Hyperspectral Thermal Imager, Copernicus Hyperspectral Imaging Mission for the Environment; HyTI, CHIME) hyperspectral missions resolve sensitive

spectrum ranges of species composition and physiological response to disturbance (Fassnacht et al., 2014; Lausch et al., 2017; Veraverbeke et al., 2018). In particular, hyperspectral vegetation indices detect detailed physiological response of specific species to environmental stress (Gamon et al., 2016). However, inherent constraints of the satellite products prohibit observation of understory attributes due to canopy obstruction and coarser resolution.

2.1.2. Satellite Lidar and Photogrammetry of Disturbance

Satellite-based laser scanning and photon counting has a relatively short record of use in geoscience research (Frolking et al., 2009) but demonstrates the ability to assess post-disturbance forest regrowth (Dolan et al., 2009; Goetz et al., 2010). Recently launched active remote sensing missions such as the Advanced Topographic Laser Altimeter System (ATLAS) onboard ICESat-2 and NASA's Global Ecosystem Dynamics Investigation (GEDI) are expected to improve our ability to quantify post-disturbance vegetation regrowth and carbon transport at sub-meter to a few meter resolution (Boucher et al., 2020; Francini et al., 2022). In particular, the GEDI data has showed potential in disturbance assessment with biomass (Dorado-Roda et al., 2021; Qi et al., 2019), canopy structure (Marselis et al., 2022), and canopy height (Dorado-Roda et al., 2021) estimations over various biomes. Challenges of this platform-sensor combination include uncertainty in determining land surface elevation over sloping areas because of difficulties in separating mixed signals from the ground and understory vegetation (Rosette et al., 2008).

2.1.3. Satellite Thermal Sensing of Disturbance

Thermal infrared sensors can effectively indicate drought conditions using vegetation water stress and retrieval of biophysical parameters (Otkin et al., 2013; Seyednasrollah et al., 2019), often combined with either spectral vegetation indices (Karnieli et al., 2010) or soil moisture data from microwave sensors (Hao & Singh, 2015; Jiao et al., 2019). Widely used water stress indices include the crop water stress index (CWSI), which is based on a linear relationship between temperature difference from the leaf to the atmosphere, and VPD (Idso et al., 1981). However, this approach has limited application to forests because variables that are needed to translate thermal measurements into water stress indices (e.g., aerodynamic resistance, stomatal conductance, soil moisture) are difficult to estimate over heterogeneous landscape (Liu et al., 2020). Besides, the coarse-resolution thermal information of vegetation canopy is often interfered with background soil emissivity for low canopy density (Neinavaz et al., 2021). The recently launched Ecosystem Spaceborne Thermal Radiometer Experiment on Space Station (ECOSTRESS) mission provides daily estimation of water use and demand (i.e., evapotranspiration and evaporative stress index) based on the frequent image acquisition (i.e., multiple times of day with a return frequency of 1–5 days) (Fisher et al., 2020). Despite a short term-deployment on the space station, ECOSTRESS can help us understand pre- and post-disturbance diurnal ecosystem processes related to vegetation water stress (Pascolini-Campbell et al., 2022) and productivity (Poulos et al., 2021).

2.1.4. Satellite Radar Remote Sensing of Disturbance

Backscattered radiation from the radar system is closely related with scattering surface properties to render a 3D structure of the land surface and tree canopy (Treuhaft et al., 2004) and estimate vegetation attributes using allometric or empirical relationships (Saatchi et al., 2007). Satellite radar data from past (e.g., Advanced Land Observing Satellite-Phased Array type L-band Synthetic Aperture Radar, Envisat-Advanced Synthetic Aperture Radar, Advanced Microwave Scanning Radiometer for Earth Observing System, Quick Scatterometer SeaWinds; ALOS-PALSAR, Envisat-ASAR, AMSR-E, QuikSCAT SeaWinds), current (e.g., Sentinel-1, AMSR-2), and planned (e.g., BIOMASS, NASA-ISRO SAR, Surface Water and Ocean Topography; NISAR, SWOT) missions can be used to quantify disturbance-induced change in forest structure (Musthafa et al., 2020; Tanase et al., 2018), foliage volume (Bae et al., 2022; Tanase et al., 2019), vegetation water content (Anderegg et al., 2018; Konings et al., 2019), biomass (Jones et al., 2013; Konings et al., 2021; Lucas et al., 2010; Momen et al., 2017), leaf water stress (Frolking et al., 2011; Saatchi et al., 2013), fire extent (Tanase et al., 2011), burn severity (Tanase et al., 2010), and tree mortality (Rao et al., 2019). This approach is especially useful in detecting substantial change in forest structure (e.g., deforestation, high severity fire) with stronger electromagnetic returns, that is, less scattering from the canopy layer (Almeida et al., 2007). However, challenges including high spatial and temporal variability in backscatter signals (Ruetschi et al., 2019) and weak penetration of the radar pulses for assessing understory changes (Bouvet et al., 2018; Lohberger et al., 2018) exist for the satellite data. In addition,

predictability declines for high biomass forests and increasing soil moisture (Lucas et al., 2010) due to signal saturation, that is, decreased sensitivity of electromagnetic return to aboveground biomass (Joshi et al., 2017).

2.2. Airborne- (Fixed Wing/Helicopter) Based Sensors

Starting with aerial photogrammetry, airborne remote sensing has a long history of observing the Earth's surface in many parts of the globe. Having relatively fewer technological and operational challenges than satellites, this platform is specialized in high spatial resolution sensing (submeter to a few meters) of the land surface at a landscape scale. In particular, intensive airborne campaigns such as MODIS/Advanced Spaceborne Thermal Emission and Reflection (ASTER) Airborne Simulator (MASTER) possess unique value as a precursor to satellite missions with (a) calibration of satellite sensors, (b) validation of the geophysical retrieval algorithms for target platform/sensor combinations, and (c) collection of higher spatial, temporal, or spectral resolution data to bridge the coarser satellite data to ground-based observations (Harris et al., 2011; Hook et al., 2001; Veraverbeke et al., 2011) (Table 2, Figures 1 and 2).

2.2.1. Airborne Spectral Imaging of Disturbance

Airborne imaging spectroscopy is widely known as an effective tool to map the spatial distribution of physiological and biophysical status of vegetation species (Asner et al., 2014, 2015). The fine spatial resolution products facilitate tree-level assessment of multi-scale disturbances (Arnett et al., 2014; Lewis et al., 2012) and disaggregate satellite images (Gartner et al., 2016; Latifi et al., 2018). In particular, recently available hyperspectral imagery provides new opportunities in finding sensitive spectral ranges for forest health analysis (Huesca et al., 2021; Veraverbeke et al., 2018). A combined use of the imaging spectroscopy and lidar links forest structure to drought susceptibility with examples of strong relationships between tree mortality and tree height (Baguskas et al., 2014; Stovall, Shugart, & Yang, 2019), elevation (Baguskas et al., 2014), and canopy water content (Brodrick & Asner, 2017; Martin et al., 2018; Paz-Kagan et al., 2018). Post-disturbance studies of fire severity (Kokaly et al., 2007; Robichaud et al., 2007; Veraverbeke et al., 2014) and tree mortality (Fassnacht et al., 2014; Tane et al., 2018) show the value of hyperspectral imagery from pre- and post-disturbance (Veraverbeke et al., 2018). Contrary to satellite platforms, however, tracking a pathway of physiological and biophysical responses with high temporal resolution (e.g., less than a few days) is generally not feasible with airborne sensing due to constraints in costs and labor.

2.2.2. Airborne Lidar and Photogrammetry of Disturbance

Airborne laser scanning has the great potential in monitoring spatial dynamics of forest structure at local to regional scales with respect to disturbance (Newton et al., 2009). The structural properties of segmented trees (e.g., tree height, wood volume, biomass, species type, canopy size, canopy density, basal area, and diameter at breast height) enhance the conventional method that empirically estimates biomass (Chen et al., 2007; Yu et al., 2011; Zolkos et al., 2013). The airborne active sensing substantially increases the accuracy of understory vegetation cover measurements (Hamraz et al., 2017; Wing et al., 2012) that is important for understanding post-disturbance vegetation reestablishment and succession stages (Chen et al., 2008; Falkowski et al., 2009; Kane et al., 2010, 2011; van Ewijk et al., 2011). However, differentiation of understory vegetation depends on canopy obstruction (e.g., dense/sparse, short/tall canopy) with respect to the orientation of the lidar sensor (Campbell et al., 2018). In this case, allometric modeling could alternatively estimate understory tree size distribution using lidar-based overstory inventories (Swetnam et al., 2014).

2.2.3. Airborne Thermal Sensing of Disturbance

Airborne thermal sensing provides direct information of how disturbance and plant response progress to refine satellite analysis with disaggregated observation (Allison et al., 2016; Hook et al., 2001). This zoom-in product is essential in calibration and correction of satellite products for atmospheric attenuation, cloud contamination, and background emissivity (Ackerman et al., 1998). Airborne thermal information indicates physiological state of trees with less atmospheric interference (Virlet et al., 2014) so that water stress (Gerhards et al., 2018) and drought impacts (Coates et al., 2015) are assessed at a canopy level. The tree-scale analyses have revealed that different tree sizes (Junttila et al., 2017) and species (Scherrer et al., 2011) have different drought susceptibility and adaptation strategies to drought conditions. These findings highlight a need for high resolution data on the

hillslope terrain where plant water availability is heterogeneous. Extra care should be taken for a shade impact on the thermal image especially when the flights are at different times of the day.

2.2.4. Airborne Radar Remote Sensing of Disturbance

Dense observation of the forest structure from the airborne radar links the catchment- (i.e., satellite) to tree-scale (i.e., ground) measurement (Lucas, Lee, & Williams, 2006) (Figure 1). Some intensive regional radar campaigns (e.g., AirSWOT) are dedicated to refining existing and upcoming satellite altimetry missions (e.g., SWOT) as precursors (Altenau et al., 2017; Pitcher et al., 2019; Wang et al., 2022). These airborne data can potentially assist the utility of satellite missions in disturbance assessment with regard to tracking long-term changes over decades. Detailed observation of structural attributes contributes to evaluation of aboveground biomass change due to thinning and typhoons (Takahashi et al., 2011), forest cover change (Ningthoujam et al., 2016), and forest regrowth (Lucas, Cronin, et al., 2006; Lucas, Lee, & Williams, 2006). Nevertheless, more studies on identification of backscatter sensitivity over forest types, species compositions, and climate settings are needed for reliable forest change assessment.

2.3. UAV

UAV-based environmental remote sensing has developed a substantial number of applications in the last decade related to CZ disturbance (Vivoni et al., 2014). The advent of UAVs led to land surface observation with operational benefits such as repeat imagery at very high spatial resolution (<1 m), flexibility in flight scheduling, affordable on-demand surveys, and reduced technical and operational barriers for individual investigators. The flights can be operated from the ground with user-defined spatial resolution and scale. A wide range of existing sensors onboard airborne and satellite platforms, including digital photogrammetry, spectroscopy, and laser scanning, can be readily transferred to UAVs. UAVs are especially useful to link satellite to field data by (a) complementing the field data in space and time, and (b) calibration and validation of satellite products (McCabe, Rodell, et al., 2017). However, the diverse use of these arrays may need standardization in observation and application, especially for multidisciplinary collaborations (Tang & Shao, 2015). In disturbance assessment, real-time monitoring of ongoing disturbance (e.g., insect outbreaks and wildfire) with UAVs can increase availability, affordability, and efficiency of data acquisition compared with other platforms (Arroyo et al., 2008; Wulder et al., 2006). The research-grade capabilities of autonomous UAVs have been increasingly demonstrated from environmental studies with spectral imaging (Section 2.3.1), lidar and photogrammetry (Section 2.3.2), and thermal sensing (Section 2.3.3) to link satellite and airborne observations to ground data. Multiple-band radar sensors on UAVs have been applied for forest mapping in the last decade (Y. W. Chen et al., 2017) but forest change was hardly assessed due to a relatively short record of use.

2.3.1. UAV Spectral Imaging of Disturbance

In disturbance characterization, spectral characteristics are leveraged to identify tree health and physiological response (Abdollahnejad & Panagiotidis, 2020; Dash et al., 2017; Lehmann et al., 2015). The spectral traits from UAV images are useful to distinguish infested and dead trees from healthy trees (Kloucek et al., 2019). In particular, UAV-based hyperspectral data may be the best way to classify infestation stages of individual trees rather than the conventional pixel-based approach from coarser-resolution satellite images. Hyperspectral information from UAVs is especially useful in mapping forest health stages (e.g., healthy, infested, dead) (Nasi et al., 2015, 2018) and physiological stress (e.g., vegetation indices) (Dash et al., 2017) of individual trees with a few pioneer studies. Compared with airborne images, UAV hyperspectral images better predicted individual spruce health associated with bark beetle infestation (Nasi et al., 2018). The tree-scale analysis demonstrated that the optimal spatial resolution of imagery would be acquired at scales as fine as 1 m (Dash et al., 2017).

2.3.2. UAV Lidar and Photogrammetry of Disturbance

Although not widely employed in disturbance studies, UAV remote sensing has large existing value and potential. The digital photography-based canopy height, biomass, and canopy cover are highly correlated with field measurements during forest recovery (Zahawi et al., 2015). UAV-based photogrammetry has been increasingly useful for disturbance assessment with a wide range of choices in digital cameras and development of image processing algorithms. The visible images acquired from UAVs can provide sub-meter measurements of forest properties, including forest composition (Alonzo et al., 2018; Bourgoïn et al., 2020), tree crown area

(Chadwick et al., 2020; Panagiotidis et al., 2017), canopy height (S. J. Chen et al., 2017; Krause et al., 2019; Larrinaga & Brotons, 2019; Mohan et al., 2017; Panagiotidis et al., 2017), and forest cover (Rossi et al., 2018). The photography-based 3D point cloud, often generated by structure from motion (SfM), is especially useful in modeling understory structures. SfM-based point clouds in disturbed forests identified lower height with homogeneous textures of the logged forest canopy (Bourgoin et al., 2020). Another study showed that the canopy height model and vegetation indices could be regressed to characterize post-fire pine regrowth (Larrinaga & Brotons, 2019). Saarinen et al. (2018) suggested that integrated use of the structural and spectral datasets could reliably estimate understory biodiversity. These high-resolution forest structures demonstrate reliable estimations compared with ground-based data (Rossi et al., 2018; Tomastik et al., 2017) and lidar-based point clouds (McNicol et al., 2021; Wallace et al., 2016). Processing resolution may limit accuracy of UAV-based canopy structure models.

2.3.3. UAV Thermal Sensing of Disturbance

UAV-based thermal data can be used to estimate vegetation water stress that shows strong correlations with ground-based measurements (Baluja et al., 2012; Bellvert et al., 2015; Bian et al., 2019; Javadian et al., 2022; Santesteban et al., 2017). Stomatal conductance derived from leaf surface temperature can inform how different species respond to water stress conditions at a leaf level, potentially useful for understanding how stomatal activities respond to varying drought intensity (Ludovisi et al., 2017; Smigaj et al., 2017). Similarly, significantly lower increases in canopy temperature and water stress in a thinned ponderosa pine forest support greater resiliency to drought than an untreated forest (Sankey & Tatum, 2022). Determination of wet- and dry-end temperature and mean temperature of the canopy surface is also crucial for estimating physiological status. Relationships between forest structure and canopy surface temperature were also used to evaluate diurnal surface temperature and water stress from satellite thermal products (Javadian et al., 2022).

2.4. Ground

Ground-based remote sensing has been increasingly available with smaller, lighter, and cheaper sensor systems. Recent advances in sensor technology have allowed ecosystem monitoring with opportunities including very high (millimeters to centimeters) and adjustable spatial and temporal resolution, ready availability, and very low cost. High maneuverability and versatility of sensor systems enhance the usability in field observations with various purposes and customizations. Because the sensing distance to the object is fairly close, product calibration and validation is more readily available with in-situ observations, but spatial coverage is limited by accessibility and time available to manually operate the equipment. Particularly with different viewing angles and geometry due to relatively low observation height, ground-based remote sensing is valuable for observing understory attributes especially in dense canopy that the other platforms cannot readily observe. With sensor size reduction for general use, sensors embedded in portable devices (i.e., smartphones and tablets) make field observation even more readily available (Luetzenburg et al., 2021; Tavani et al., 2022).

2.4.1. Ground Spectral Imaging of Disturbance

Ground spectral imaging is a relatively underexplored realm in forest research because observation of the top of the canopy surface is not readily available in many cases. With technological advances in hyperspectral imaging, however, physiological traits of the canopy can be detected with hundreds of spectral bands. This benefit can leverage the PhenoCam Network, the nationwide field photograph network covering multiple ecotones and species composition (Richardson, 2019; Richardson et al., 2018), by providing regular data acquisition of the forest canopy with more specific spectral information. A portable spectroradiometer can detect early stage insect infestation because of the difficulties in discrimination otherwise.

2.4.2. Ground Lidar and Photogrammetry of Disturbance

Examples of a standalone ground-based remote sensing survey include utilization of terrestrial laser scanning (TLS) to generate microtopography (Harman et al., 2014; Nouwakpo et al., 2016; Stovall, Diamond, et al., 2019), vegetation structure (Ashcroft et al., 2014; Grau et al., 2017; Kong et al., 2016; Richardson et al., 2014), and soil erosion and transport (Ballesteros-Canovas et al., 2015; Eitel et al., 2011; Longoni et al., 2016) models at very high resolution (i.e., millimeters to centimeters). Due to deployment height and viewing angle, TLS is particularly specialized in monitoring understory vegetation structure, including tree stems (Heinzel & Huber, 2017) and biomass (Li et al., 2021), evaluating post-disturbance understory changes (Li et al., 2021), and refining

other laser scanning platforms (Crespo-Peremarch et al., 2018, 2020; Luscombe et al., 2015). TLS enhances the conventional method that empirically estimates biomass from structural properties of vegetation (e.g., canopy size, density, species composition). Plant structure derived from laser scanning products (i.e., canopy height, understory cover, and foliage diversity) correlates strongly with biomass measurements, and thus suggests great potential in biomass change mapping (Hall et al., 2011) and carbon budget estimation (Harman et al., 2014; Singhal et al., 2021; Stovall et al., 2018). Very specific vertical profiling from TLS can predict species richness and ultimately inform change in biodiversity (Anderson et al., 2021). Nevertheless, the operational barriers (e.g., labor intensiveness, limited observation height above the land surface, obstruction of the object during the horizontal sensing) constrain regular data acquisition especially over a large area.

2.4.3. Ground Thermal Sensing of Disturbance

Despite limited capability in observing tall forest canopy, ground-based thermal sensing has been increasingly used in forest monitoring with benefits including constant viewing geometry and no need for atmospheric correction on attenuation and cloud contamination (Hwang et al., 2023). Liu et al. (2020) used canopy leaf surface temperature from multiple thermal sensors to estimate CWSI in Mediterranean forests. Estimated CWSI has an exponential relationship with soil moisture and a linear relationship with soil water potential. This relationship between CWSI and soil moisture was used in a wheat field to inversely estimate root zone soil moisture, which has high spatio-temporal variability and is difficult to measure with contemporary remote sensing capabilities (Akuraju et al., 2021).

2.4.4. Ground Radar Remote Sensing of Disturbance

Ground radar remote sensing, including ground penetrating radar (GPR), has received relatively little attention in forest disturbance monitoring. However, it may provide useful information in post-disturbance forest regrowth because underground attributes such as the regulation of root water uptake and distribution of root systems influence physiological responses (Manoli et al., 2017). GPR is capable of mapping underground attributes, including soil profiles (Huisman et al., 2003; Lambot et al., 2002), tree root systems (Alani & Lantini, 2020), and root biomass (Guo et al., 2013). Coherence between remotely sensed canopy and root structure at a 3–4 m scale (and larger for old stands) may better capture pre- and post-disturbance belowground forest structures for comparison (Hardiman et al., 2017).

3. Examples of Observing CZ Response to Disturbance

The accelerating pace of natural and human-caused disturbances in the western US, including flooding (Brunner et al., 2020), wildfire (Dennison et al., 2014), and drought (Anderegg et al., 2015), has given opportunities to observe CZ response and vegetation recovery. Less than 15 years old, the National Science Foundation (NSF) funded Critical Zone Observatories (CZO) and the Critical Zone Collaborative Network (CZCN) have experienced substantial disturbances over their short lifetimes. Here, we discuss examples of large flooding events, intense fires, lower severity lightning-caused fires, forest restoration, and drought effects. These examples combine different sensors and platforms across multiple disturbance types, which illustrate the potential application of certain technologies for some types of disturbances but not others. Overall, these case studies demonstrate the uniqueness of different types of disturbances, local site issues that impact vegetation recovery and remote sensing platforms, and illustrate opportunities for better observations across scales using new remote sensing capabilities.

3.1. Biogeomorphic Responses to Flooding and Fire

Flooding can cause significant geomorphic changes on hillslopes and within river corridors (channels and floodplains) (Coe et al., 2014; Magilligan et al., 2015), and fire can result in increased sediment and water yields, enhanced deposition in river corridors, and more frequent debris flows (McGuire et al., 2021; Rathburn et al., 2018; Smith et al., 2011; Warrick et al., 2012). Geomorphic changes alter the physical template on which ecosystems respond to disturbance; for example, disturbance frequency and type controls the spatial organization of riparian plant assemblages in river corridors (Gurnell et al., 2016). In addition, disturbances such as fires and floods influence the partitioning of organic carbon (OC) stored in sediment, vegetation, and downed large wood (>1 m in length and >0.1 m in diameter) within watersheds (Lininger et al., 2021; Rathburn et al., 2017).

Quantification of these changes needs disaggregated observation to address ecogeomorphic responses as follows: (a) how flood events erode hillslopes and redeposit sediment, (b) how vegetation controls patterns of erosion and deposition, and (c) vegetation reestablishment patterns in erosion or deposition zones.

An extreme precipitation event that occurred over multiple days on the Colorado Front Range in September 2013 caused substantial geomorphic changes on hillslopes and in river corridors. Over the course of the event, rainfall totals exceeded 450 mm in some areas (Gochis et al., 2015), causing over 1100 landslides and debris flows identified through examination of high-resolution (0.5 m) spectral satellite imagery (Coe et al., 2014). Many studies used repeat high resolution lidar datasets taken pre- and post-flood to assess topographic changes using digital elevation models of difference (DoDs). For example, debris flows that occurred during the precipitation event resulted in an average of ~10 mm of basin-wide lowering over an area of 102 km² (Anderson et al., 2015). In addition to hillslope failures, DoDs allowed for quantification of deposition and erosion in river corridors along the Front Range (Sholtes et al., 2018).

That same 2013 flood also influenced the partitioning and storage of OC in sediment and large wood. In the North St. Vrain watershed, pre- and post-flood lidar dataset, along with field data demonstrated that the flood mobilized significant amounts of sediment and associated OC from hillslopes and the river corridor, resulting in increasing deposition in downstream reservoirs (Rathburn et al., 2017). In addition to deposition in reservoirs, the flood eroded standing trees on hillslopes and in the valley bottom, depositing large wood into accumulations on floodplains in multiple drainages (Guiney & Lininger, 2022; Lininger et al., 2021). In a watershed impacted by both the 2013 flood and a recent upstream fire, the amount of large wood deposited on the floodplain was significantly greater when compared with a watershed that experienced the 2013 flood without a recent fire (Guiney & Lininger, 2022).

Remote sensing data have proven to be effective in determining the impact of human activities, such as beaver removal, beaver reintroduction, and anthropogenic structures (e.g., beaver dam analogs), on river corridor response to wildfire and flooding. Beavers influence biogeomorphic interactions including riparian water table, regulate water storage and flow, modify vegetation composition and abundance, and promote sediment deposition and associated carbon (Larsen et al., 2021; Norman et al., 2022). The presence of beavers and their associated structures, such as abandoned beaver dams and channel-spanning log jams (accumulations), can attenuate sediment fluxes following wildfires in unconfined, physically complex river corridors within mountain stream networks (Wohl et al., 2022). In the western US, river corridors with beaver activity maintained higher NDVI during large wildfires compared to those without beaver activity, indicating how beavers create refugia during wildfire (Fairfax & Whittle, 2020). Lidar datasets, multispectral data, and a combination of both can help assess the ecogeomorphic impact of disturbance, including the role of beavers in mediating disturbances, sediment and OC fluxes during flooding, and the influence of erosion and deposition on riparian and hillslope forest structure.

3.2. High Severity Fire

High severity fire in the western US often accompanies drought and different pathways of vegetation regrowth that adapt to local hydrometeorological conditions (Savage et al., 2013). Here, we define burn severity as the degree of fire-induced change to vegetation and soil conditions (Ebel et al., 2018; Parks et al., 2018; Robichaud et al., 2007). Along with forest type, severity of fire affects forest recovery and carbon flux trajectories (Ghimire et al., 2012). However, understanding of these post-disturbance recovery processes is lacking despite decades of remote sensing-based diagnoses. Detailed monitoring of changes in forest structure helps better understand both immediate forest cover loss as well as the multi-year to multi-decadal response of the forest to high severity fires. Research questions include: (a) How does vegetation regrowth vary across high severity fire areas? (b) How do standing dead trees interfere with regrowth detection? (c) How does high severity fire change snow accumulation and ablation?

Different sensor types and platforms depict different degrees of post-fire vegetation regrowth with two high severity fire cases. Two stand-replacing wildfires, the Las Conchas Fire (2011) and Thompson Ridge Fire in (2013), impacted the aspen- and mixed conifer-dominated Rabbit and Redondo Mountain sites in the Jemez CZO in New Mexico, respectively (Figure 3). Both the multispectral and lidar metrics visually show vegetation loss and regrowth associated with the high severity fire (Figures 4 and 5). The fine-resolution airborne metrics visually demonstrate spatially variable degrees of forest regrowth after high severity fire. Various platforms

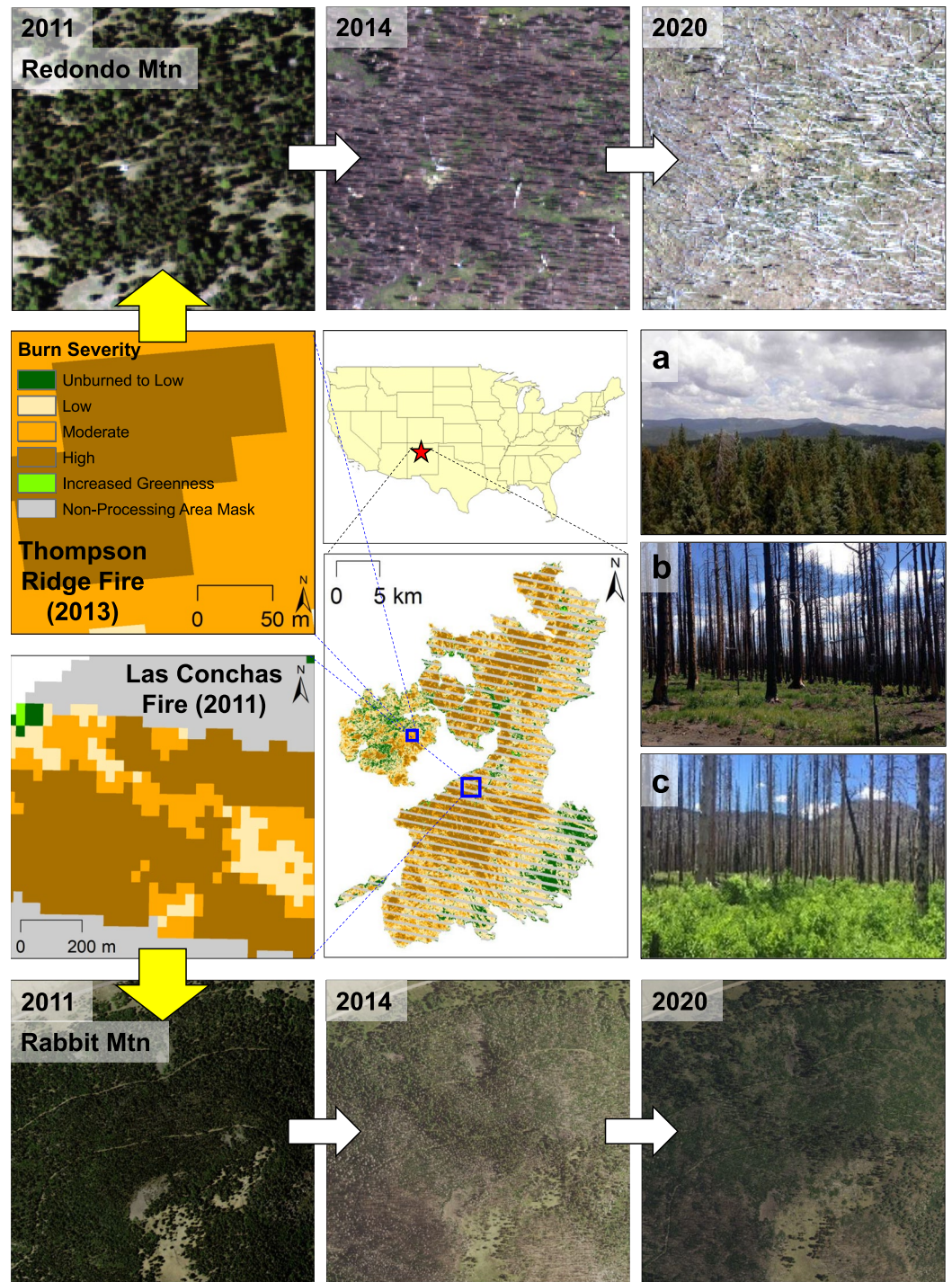


Figure 3. Redondo Mountain (top) and Rabbit Mountain (bottom) in Jemez CZO were affected by Thompson Ridge Fire in 2013 and Las Conchas Fire in 2011, respectively. Gray stripes of the Landsat burn severity map from the Monitoring Trends in Burn Severity (MTBS) program (Eidenshink et al., 2007) indicate non-processing area due to the Scan Line Corrector failure on the Landsat 7 Enhanced Thematic Mapper Plus (ETM+) sensor. NAIP aerial images illustrate the areas before the Thompson Ridge Fire and Las Conchas Fire in (2011), 1/3 years after the fires (2014), and 7/9 years after the fires (2020). Site photographs illustrate the subalpine conifer area in Redondo Mountain (a) before the fire, post-fire understory regrowth (b) a year after the fire with standing dead trees and emergent ground cover, and (c) 3 years after the fire with only tree boles remaining and heterogeneous seedling reestablishment.

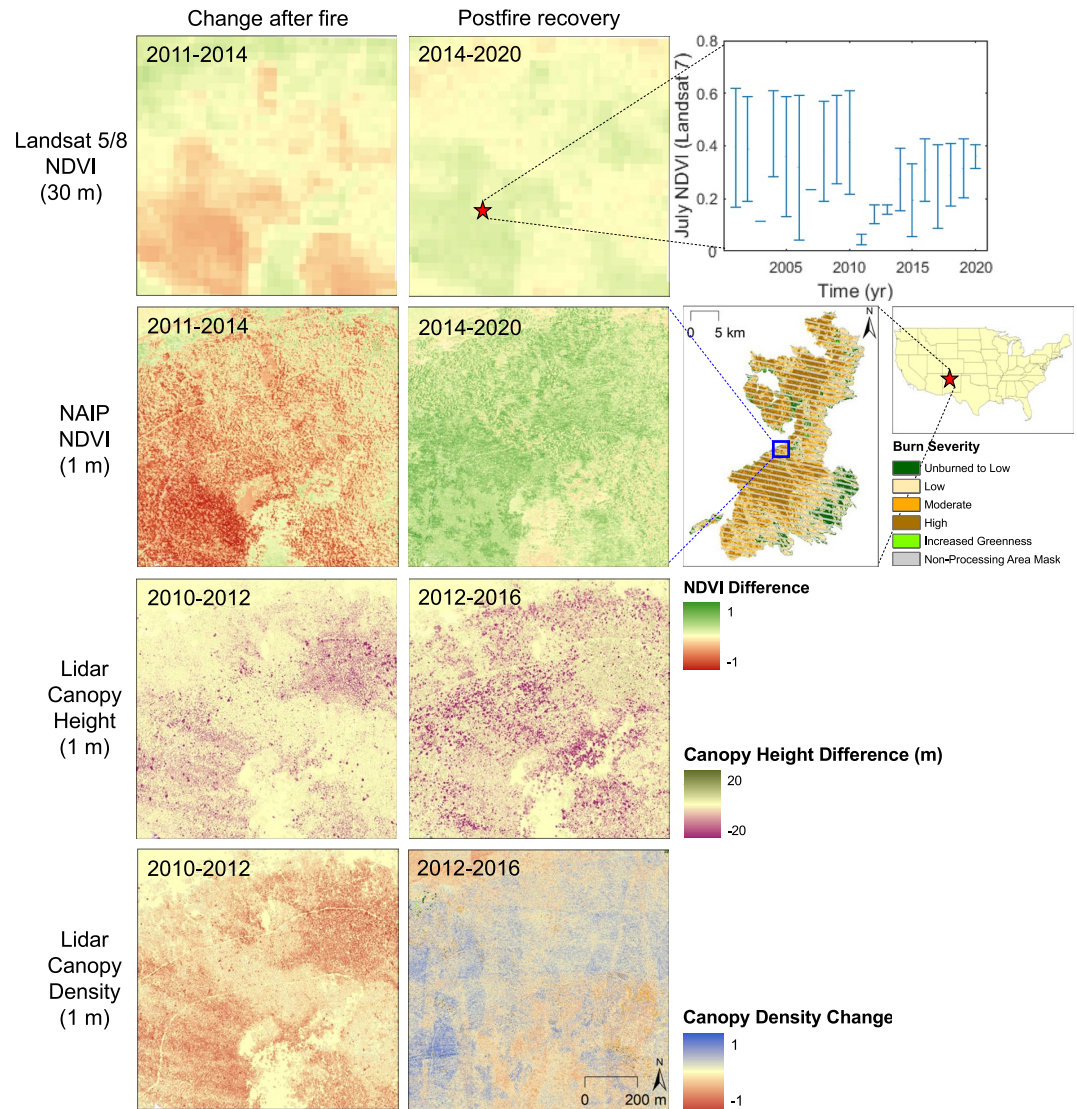


Figure 4. Spatial distribution of vegetation metrics in Rabbit Mountain indicating postfire vegetation loss (left panel of the maps) and regrowth (right panel) from the Las Conchas fire in 2011. Gray stripes of the MTBS burn severity map indicate non-processing area due to the Scan Line Corrector failure on the Landsat 7 ETM+ sensor. The Landsat 7 NDVI range in July indicates a stark decrease by fire and gradual post-fire recovery. The lidar canopy density map during the regrowth period represents the understory vegetation density (<2 m above the land surface).

show different observation capabilities with respect to the observation height and angle. In particular, National Agriculture Imagery Program (NAIP) NDVI maps detect areas of fire loss and post-fire vegetation regrowth in some areas that coarser-resolution Landsat NDVI maps do not. The lidar-based canopy height model may depict misleading information on burn severity and post-fire regrowth, suggesting the importance of comparing multiple vegetation metrics to understand the full story of post-disturbance recovery. Both airborne and ground observations show post-fire regrowth of understory vegetation. However, substantial loss in canopy height does not directly correlate biomass loss and decrease in NDVI at the same period, especially with respect to wildfire.

Vegetation structure metrics derived from the lidar data are useful in evaluating vegetation change and modeling post-fire understory vegetation succession. Changes in canopy height and density present physical change in forest structure and spatially agree with aerial photographs. In particular, canopy density change depicts large areas of regrowth compared with post-fire changes, whereas canopy height decreases in most areas both due to fire and during the regrowth period (Figures 4 and 5). Canopy density change maps present contrasting patterns in response to fire and subsequent regrowth. Canopy height difference maps illustrate the fire-induced canopy

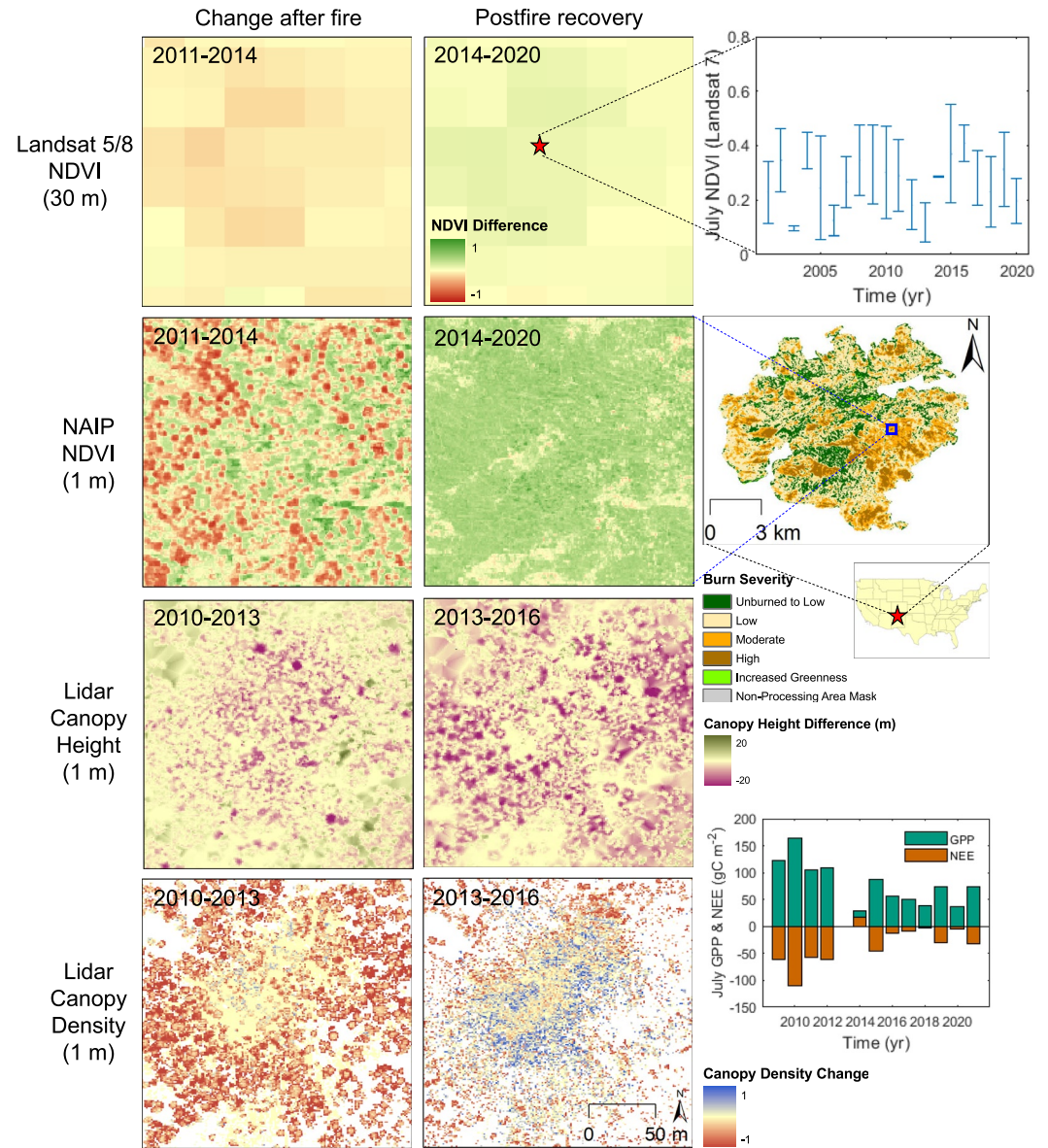


Figure 5. Spatial distribution of vegetation metrics in Redondo Mountain indicating vegetation loss (left panel of the maps) and regrowth (right panel) from the Thompson Ridge fire in 2013. July GPP and net ecosystem exchange (NEE) observations from the eddy covariance tower indicate a stark decrease by fire and gradual post-fire recovery. The lidar canopy density map during the regrowth period represents the understory vegetation density (<2 m above the land surface).

loss. However, post-fire vegetation regrowth was captured to a limited extent in the given area due to falling of large fire-damaged trees that potentially created a spatially heterogeneous regrowth pattern. The ground-based TLS data provided a more detailed structure of understory vegetation with operational flexibility, which would be ideal for monitoring post-disturbance vegetation regrowth. The fine-resolution remote sensing could reduce uncertainties in physiology and biomass changes, which can supplement larger-scale products.

The NAIP NDVI difference maps visually demonstrate burned and regrowing areas, suggesting their ability in disaggregating coarser-resolution Landsat NDVI. Especially near the fire perimeter, NAIP provided spatially detailed information on change in canopy greenness. Compared with the lidar maps, the NAIP NDVI maps may be less sensitive to vegetation growth because once established, canopy cover masks understory growth. The maximum NAIP NDVI values in the scene recovered to 0.50 in 2014 due to understory vegetation reestablishment and then gradually increased to 0.65 in 2020. Landsat time series data show the burn damage and vegetation

regrowth at annual timesteps (Figure 4). A Landsat NDVI range in July at the Rabbit Mountain site plummeted from 0.22 to 0.61 in 2010 to 0.03–0.07 in 2011, before gradually increasing to 0.31–0.40 from regrowth in 2020. July peak values decreased from 0.63 (2001) to 0.43 (2016). The NAIP NDVI difference maps in the Redondo Mountain site provide detailed information of vegetation loss and regrowth due to the Thompson Ridge Fire in 2013 (Figure 5). Continuous ground-based observation indicates a large reduction in carbon sequestration and ecosystem productivity in the years following the fire. Carbon sink strength in the 6 years following the fire was approximately 1/8 of the total carbon sequestration in the 6 years prior to the burn (Figure 5). Recovery of vegetation following the fire was hindered by drier than average years in 2016, 2017, and 2018 prior to the monsoon. Without canopy obstructions from large trees due to the fire loss, this high-resolution product visually detects understory vegetation regeneration that the coarser-resolution Landsat NDVI failed to differentiate.

3.3. Restored Low-Severity Fire Regime

Many forested areas in the Sierra Nevada of California were historically adapted to frequent, mixed-severity wildfires started by lightning or Native American ignitions (Van Wagtenonk, 2007). Widespread fire suppression over the last century has altered forest characteristics that affect fuel loads, fire behavior, and ecohydrological processes. Data and modeling efforts based in the Illilouette Creek Basin (ICB) in Yosemite National Park, where fire use policies have been implemented to restore a natural wildfire regime since 1972, suggest that these policies reduced fire hazards and increased annual streamflow production through large changes in landscape-scale forest cover and structure (Stephens et al., 2021). Despite 80–100 years of fire exclusion policies from ~1880 to 1972, the frequency of contemporary fire activity in ICB is similar to the pre-fire exclusion period (~1700–1880 C.E.) using dated fire scars (Collins & Stephens, 2007). Since 1974, only 14% of the total burned area in the basin has been classified as high severity, despite more than fifteen fires covering approximately 80 km² (over half of the basin area and 75% of the vegetated area) (Boisrame et al., 2019). The return of natural fire to the ICB has allowed investigation into the processes driving natural fire-vegetation dynamics. Assessments of landscape-scale vegetation change using aerial photography during the managed fire period revealed that in the ICB, the proportion of the basin comprised of conifer forest decreased from 82% to 62%, and was replaced by shrublands and meadows (Boisrame, Thompson, Kelly, et al., 2017). The change in forest composition resulted in markedly lower surface fuel loads (Collins et al., 2016) and increasing wetness and runoff-precipitation ratio (Boisrame, Thompson, Collins, & Stephens, 2017). Both short-term (year to few years after fire) and long-term (decades after fire) vegetation change due to mixed-severity fire needs comprehensive assessment to specifically address (a) how vegetation regrowth responds to fire in different landscape positions, (b) the net effects of low severity fire on water and energy budgets over different time scales, and (c) how resilient remaining forests are to high severity fire.

Wildfire manipulates forest biomass and carbon dynamics over decades (Sato et al., 2016). The northwestern part of the watershed has been exposed to two major mixed-severity fires since 2000: the Meadow Fire in 2004 and Empire Fire in 2017 (Figure 6). Vegetation cover maps using National Aerial Photography Program (NAPP) and NAIP images display substantial changes in vegetation type patches from before the Meadow Fire through 2020. The moderate-high severity burned areas were dominated by sparse vegetation for a few years after the fire and then by the shrub expansion (Figure 6). Shrub-dominated areas then largely returned at high severity, likely due to the spatially continuous fuel load these shrubs provided. The Landsat data demonstrate their value in temporally consistent data acquisition for long-term monitoring of vegetation disturbance and regrowth (Figure 6). NDVI throughout several decades presents fire-induced vegetation loss and regeneration with the relative chlorophyll content and associated physiological attributes. Nevertheless, the spectral vegetation index did not explain the change in species composition. This change in composition is important because a complete loss of tree cover (as occurred in the 2004 high severity areas) and a complete loss of shrub cover (as occurred in 2017 high severity areas) have different implications in terms of carbon loss (Gonzalez et al., 2015) and changes to the local water budget (Bart et al., 2016; Boisrame et al., 2018, 2019). However, these differing vegetation changes are both interpreted as high severity from Landsat (severity maps in Figure 6). A combination of satellite products and finer-scale aerial imagery provide a much more nuanced understanding of wildfire's impacts in this basin than using only a single data product.

Short-term changes in vegetation loss and reestablishment due to fire highlight a need for detailed observations in temporal, spatial and spectral resolutions. The focal area in ICB displays vegetation loss and regrowth

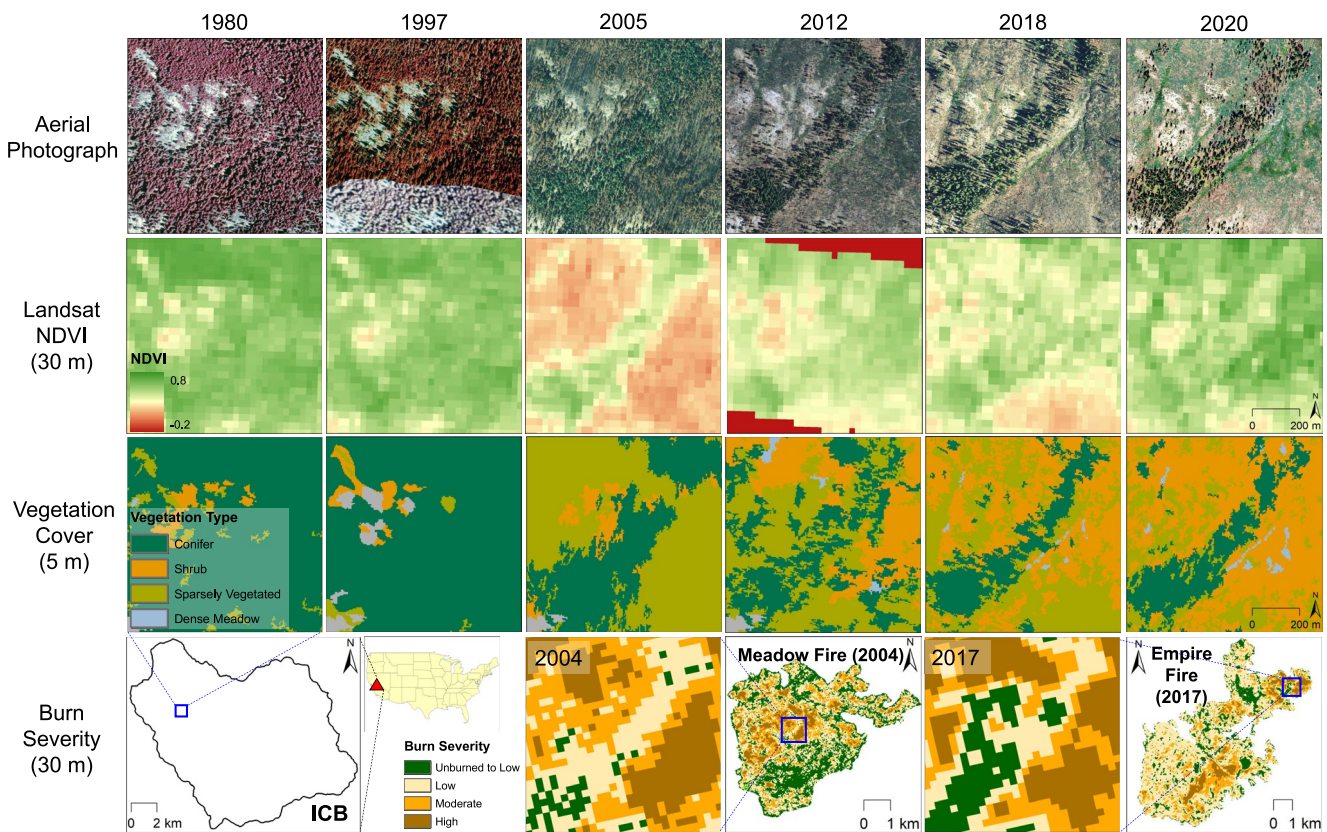


Figure 6. Long-term trends of aerial photograph (first row—photos prior to 2005 are color infrared NAPP images from USGS, others are true color NAIP imagery from USDA), Landsat NDVI (second row) and aerial photography-based vegetation cover (third row; Boisrime, Thompson, Collins, & Stephens, 2017; Boisrime, Thompson, Kelly, et al., 2017) in the Illilouette Creek Basin (ICB). From 1980 to 2018, the inset region experienced multiple mixed-severity fires including the 2004 Meadow Fire and 2017 Empire Fire.

from the 2017 Empire Fire (Figures 7i–7k). Post-fire vegetation change of two higher-resolution vegetation indices spatially agrees with the Landsat burn severity map (Figure 7). In particular, the chlorophyll carotenoid index (CCI), acquired from airborne hyperspectral band images, may be useful in capturing changes in biomass and species (Figures 7a and 7b). Compared with NDVI (which indicates the chlorophyll content), CCI is a carotenoid-sensitive vegetation index that measures carotenoid pigments and thus provides improved monitoring of gross primary productivity (GPP) phenology of conifer trees (Gamon et al., 2016). While Airborne Visible/Infrared Imaging Spectroradiometer (AVIRIS) CCI and NDVI show similar spatial patterns in terms of their disturbance (Figures 7a and 7c), they capture very different recovery patterns (Figures 7b and 7d), ostensibly capturing different components of the vegetation recovery. Comparing NDVI from AVIRIS (Figures 7c and 7d) and Landsat (Figures 7e and 7f) illustrates the ability of the higher resolution AVIRIS to capture more detailed patterns of disturbance, recovery, and post-fire mortality or stress. These small-scale effects of fire on vegetation cover are important to capture as they can have important impacts on biodiversity (Turner, 1989), as well as hydrologic processes such as snow water storage (Lundquist et al., 2013).

3.4. Forest Thinning

Forest thinning may result in increases in short-term water yields, although increases in evaporation and water use by remaining trees typically mean that these gains are often negligible (Tague et al., 2019). How forest thinning translates into these proposed benefits at specific locations and given a wide range of fuel treatment characteristics remains highly uncertain—and likely varies not only across broad regional bioclimatic gradients but also within local management units (e.g., within a first order watershed) with slope, aspect, prior vegetation, and subsurface characteristics (Burke et al., 2021; Hanan et al., 2021; Hunter & Robles, 2020). Substantial research is

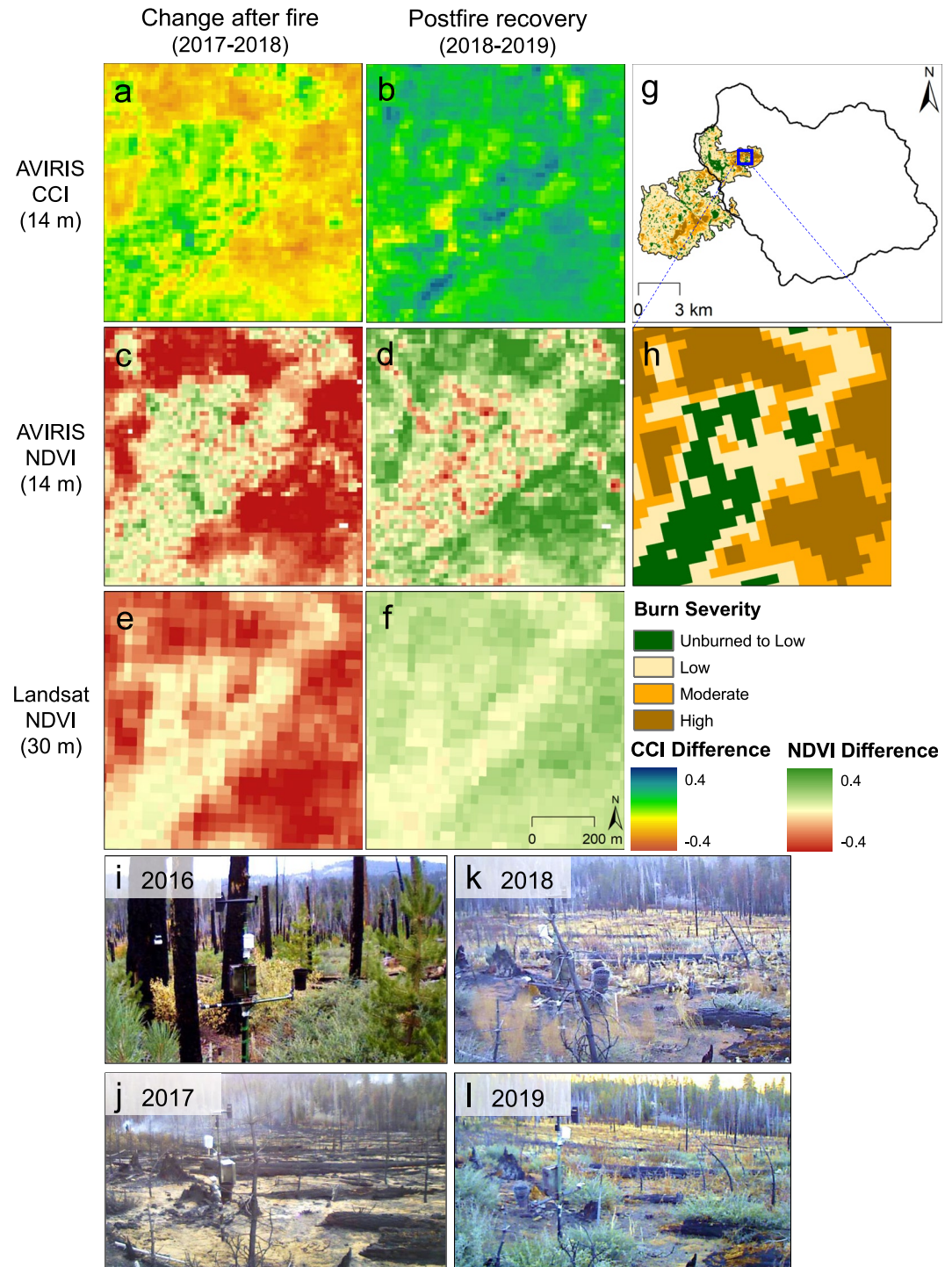


Figure 7. Spatial distribution of (a, b) AVIRIS CCI difference, (c, d) AVIRIS NDVI difference, (e, f) Landsat NDVI difference, and (g, h) burn severity in Illilouette Creek Basin indicating vegetation loss (the left column) and regrowth (the middle column) from the 2017 Empire Fire. The MTBS burn severity maps indicate a variety of vegetation loss within the scene. Site photos show a shrub field (i) before the fire (2016), (j) immediately after the fire (November 2017), (k) 1 year after the fire (2018), and (l) 2 years after the fire (2019).

still needed to (a) better characterize fuel treatments themselves, including their intensity, spatial extent and how they change the canopy structure, (b) monitor how vegetation recovers following fuel treatments and similarly following fire and other disturbances, and (c) link these changes in canopy structure with response variables of interest including the productivity and growth of remaining trees but also hydrologic variables including snow accumulation, snowmelt, and streamflow. Remote sensing can facilitate improved characterization of how fuel treatments actually alter forest structure, how forest structure then evolves, and the impacts on remaining trees and CZ processes to address research questions including: (a) What are the best areas to thin to promote water and low intensity wildlife, while reducing fuels? (b) How does understory respond to forest removal? (c) Are the remaining trees more resilient to drought and water stress following removal of nearby trees? Linking remote sensing of fuel treatment with measurements of response variables of interest, such as burn severity (Petrakis et al., 2018) or hydrologic variables such as snowpacks (Belmonte et al., 2021), can provide insight into fuel treatment impacts. Assimilating remote sensing of canopy structure (Hanan et al., 2018) and fuel treatment changes to canopy structure into process-based models (Saksa et al., 2020) can also improve our estimates of fuel treatment benefits and their spatial-temporal heterogeneity.

We show how different remote sensing-based measurements characterize fuel treatment changes to forest structure at Sagehen Creek Experimental Forest (SCEF), a 36.4-km² watershed located in the Tahoe National Forest, central Sierra Nevada, California. SCEF has been managed by the US Forest Service to survey forest structure and test innovative forest management strategies for conducting fuels treatments. Vegetation treatments were applied to over 10.5 km², in various combinations of mechanical thinning, mastication, and underburning. Spectral vegetation indices estimate substantial thinning between 2014 and 2020 (Figure 8). In addition to canopy loss with thinning, canopy height metrics derived from lidar show growth in untreated forests and in remaining conifers in the treated area (Figures 8a and 8b). Coarse-scale vegetation indices, such as Landsat NDVI (Figure 8c), do not resolve these tree scale responses. Spatial distribution of the airborne NDVI (Figure 8d) resembles those of the lidar canopy difference metrics (Figures 8a and 8b). The availability of high-resolution lidar data allows forest thinning treatment to be represented as not only a change in leaf area index (LAI) but also how thinning impacts canopy gaps, and distributions of remaining tree heights. This more realistic representation of canopy structural changes, particularly the inclusion of gaps, can have important implications for ecohydrological estimates, including changes in snowpack, increased transpiration of remaining trees and evaporative losses (Tsamir et al., 2019).

Hyperspectral imagery offers the potential to revolutionize our understanding of coupled ecohydrological responses of mountain ecosystems to drought, extreme fire, and snowpack change. In evergreen conifers, such as those common throughout ICB (Figure 7) and SCEF (Figure 8), the foliage changes minimally throughout the year because there is little seasonal variation in chlorophyll content, making satellite remote sensing of photosynthetic phenology challenging. NDVI can only measure the greenness of trees, which does not vary much across seasons, while CCI is a proven method of tracking conifer phenology by measuring carotenoid pigments, which vary by a factor of ~2–3 throughout the year (Wong et al., 2019). Remotely sensed CCI has provided a method of observing evergreen photosynthetic activity from optical remote sensing across multiple spatial scales. Studies have used AVIRIS (Green et al., 1998) and demonstration satellite missions (e.g., Hyperion) (Middleton et al., 2013) to calculate CCI, but there is currently no frequent global coverage CCI product. Proposed satellite-based imaging spectrometers could help monitor CCI changes from space, but we are currently using airborne platforms to provide CCI temporal and spatial coverage.

3.5. Drought and Water Stress

Understanding and predicting the drivers of water stress on plant health and productivity is critical in light of increasing drought events from climate change (Meehl & Tebaldi, 2004). Derived estimates of plant phenology and gross primary productivity from satellite remote sensing depend solely on the spectral reflectance of the surface, and do not consider soil water conditions (Lowman & Barros, 2016, 2018). However, satellite estimates may be improved by assimilating the data into models that incorporate soil water stress (Lowman & Barros, 2018). This approach can potentially reinforce remote sensing observation of physiological responses to water stress. Specific research questions include: (a) How do data assimilation and phenology modeling improve remote sensing observation of drought? (b) How is water stress linked to forest growth and mortality? (c) How does a changing climate affect forest vulnerability to water stress?

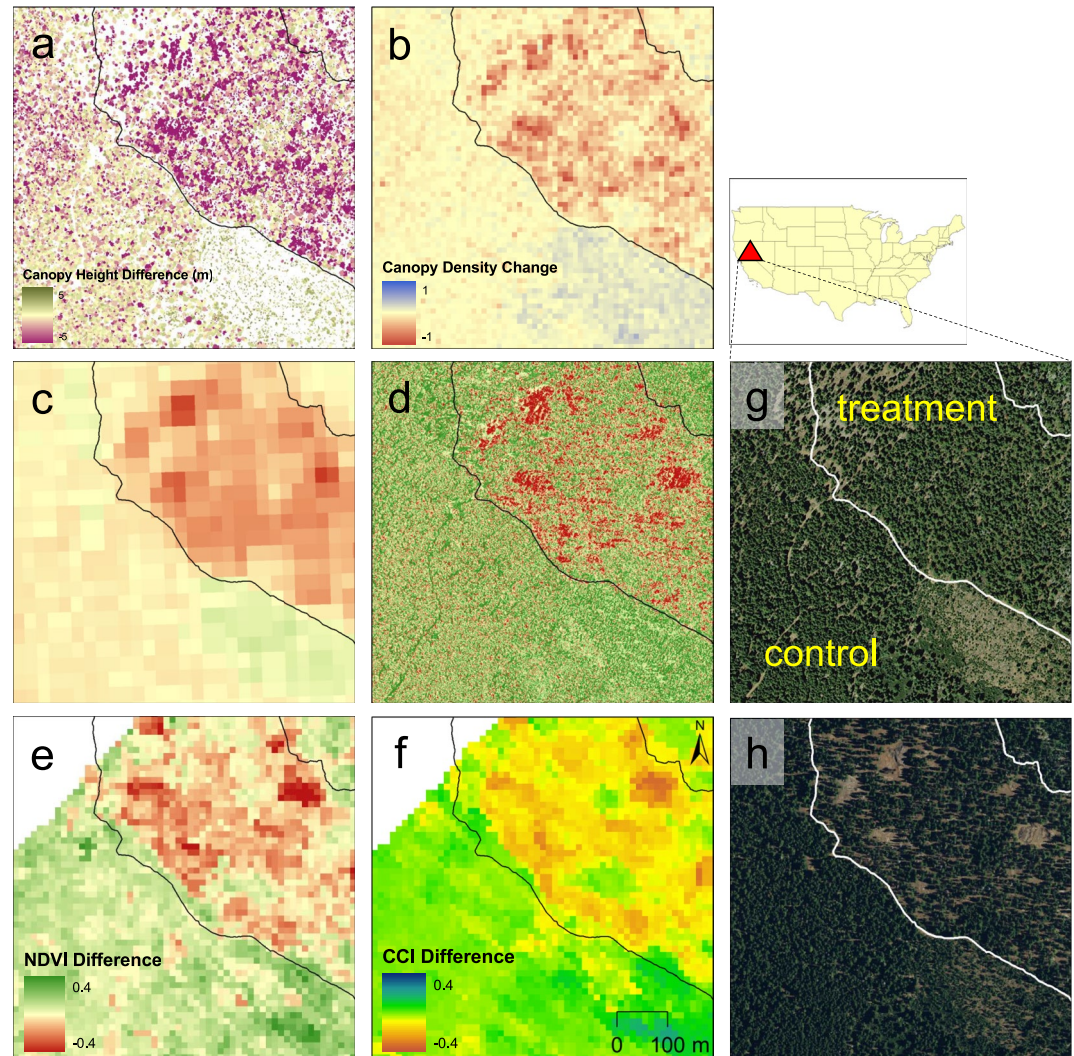


Figure 8. Spatial distribution of the 2014–2020 difference in (a) lidar-based canopy height, (b) lidar-based canopy density, (c) Landsat NDVI, (d) NAIP NDVI, (e) AVIRIS NDVI, and (f) AVIRIS CCI in Sagehen Creek Experimental Forest. The NAIP true color composites visually illustrate progressive changes in tree density from (g) 2014 to (h) 2020.

We present a drought case at the Mountainair Pinyon-Juniper Woodland AmeriFlux site (US-Mpj) in New Mexico to investigate how changes in atmospheric aridity and soil moisture during drought influence plant photosynthetic pathways. This analysis combines data assimilation and phenology modeling techniques to determine the ranges of VPD and soil moisture that indicate water stress limitations on photosynthesis, but not complete plant mortality (Lowman & Barros, 2018). Specifically, by assimilating MODIS fraction of absorbed photosynthetically active radiation (FPAR) and LAI data to a prognostic phenology model using a dual parameter-state Ensemble Kalman Filter, we estimate threshold values at which photosynthesis shuts down at minimum VPD (VPD_{min}) and soil moisture (SM_{min}), and when photosynthesis is uninhibited at maximum VPD (VPD_{max}) and soil moisture (SM_{max}). These limits define the range for suboptimal photosynthetic function and differ from wilting point, the soil moisture level at which cavitation occurs in plants, and field capacity, a soil hydraulic property. AmeriFlux and MODIS GPP data were used to evaluate changes in plant photosynthesis rates. This analysis used soil moisture data from the root-zone soil moisture merging project (SMERGE) and climate data for temperature, specific humidity, and vapor pressure from Phase 2 of the North American Land Data Assimilation System (NLDAS-2) Forcing File A, both at 0.125° spatial resolution. The years 2013–2015 were selected as the assimilation period, as it encompassed both wet and dry conditions for the US-Mpj site. Results for a dry (2013) and wet (2015) water year demonstrate how this technique may be used to determine primary drivers for reduced photosynthesis during drought.

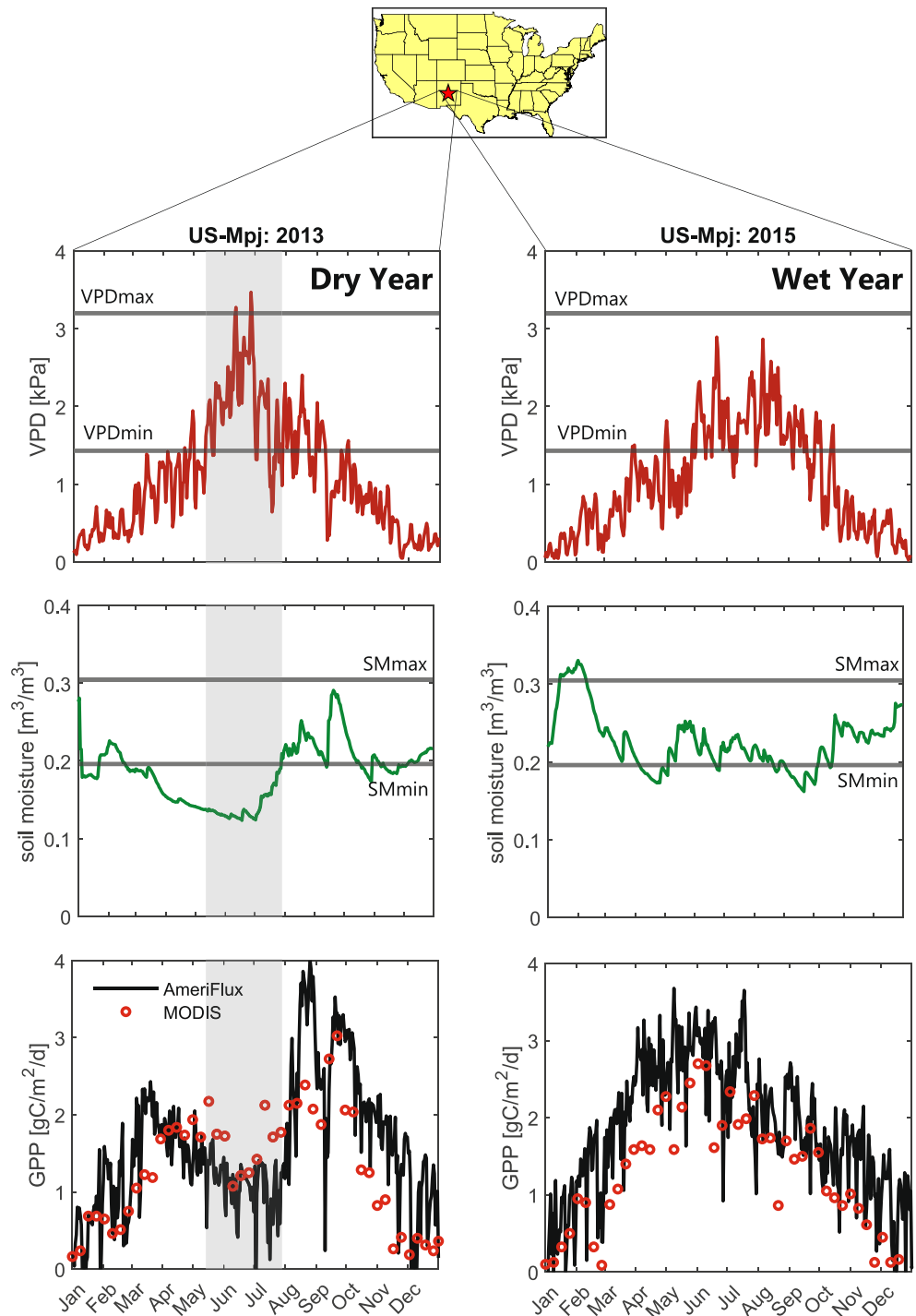


Figure 9. Time series of vapor pressure deficit (VPD), soil moisture, and gross primary productivity (GPP) for a forested mountain site in New Mexico (US-Mpj) in 2013 (dry year) and 2015 (wet year). The horizontal gray lines mark the suboptimal range for photosynthesis determined by assimilating MODIS FPAR/LAI data to a phenology forecasting model. Gray shading in 2013 plots highlights a period of drought stress.

The modeling technique determined the ranges of VPD and soil moisture between which stomata are completely open ($VPD_{max} = 3.20$ kPa, $SM_{max} = 0.30$ $m^3 m^{-3}$) and fully closed ($VPD_{min} = 1.43$ kPa, $SM_{min} = 0.20$ $m^3 m^{-3}$) for the corresponding NLDAS grid cell. Between mid-May and late July in 2013, soil moisture fell below SM_{min} and VPD exceeded VPD_{max} (Figure 9). Both soil water stress and dry atmospheric conditions contributed to near

and complete shutdown of photosynthesis during this period (Figure 9). Soil water stress remained below SM_{min} for an extended period between February and July, and for shorter periods in September, October, and November. In June, there were two short periods where VPD exceeded VPD_{max} . In both cases, soil water stress served as the primary driver for reductions in plant photosynthesis rates. The AmeriFlux GPP data show that photosynthesis rates were severely reduced during the period where both soil moisture falls below SM_{min} and VPD exceeds VPD_{max} (Figure 9). The MODIS GPP data did not show the same reduction in plant productivity, because the satellite remote sensing product did not account for changes in soil moisture that influence plant photosynthesis (Lowman & Barros, 2016, 2018).

During the 2015 wet year, there were no sustained mid-season reductions in GPP (Figure 9). Zero and near-zero reductions in GPP in the growing season only occurred during the dry year (2013) when both VPD exceeded VPD_{max} and soil moisture fell below SM_{min} (Figure 9). In 2015, there were no periods where VPD exceeded VPD_{max} , hence the area was never under combined soil moisture and atmospheric stress. There were short periods throughout 2015 where soil moisture fell below SM_{min} , and these were associated with small, short duration drops in GPP. The regional-scale estimates may have greater uncertainty in mountainous regions with averages over highly complex topography, where vegetation conditions can change rapidly along altitudinal gradients within a single pixel (Bolstad et al., 2001; Giorgi & Avissar, 1997).

4. Recommendations for Future Research and Application

Exploring the disturbance cases with new remote sensing approaches in Section 3 highlights new opportunities for observing CZ response to disturbance. The case studies demonstrate the value of new sensor-platform combinations to spatially resolve disturbance severity, post-disturbance change, and intensive forest management at multiple time scales. Given the importance of forest management and disaster prevention, there is a growing need for regular observation campaigns, which requires federal and state governments to cooperate with both public (e.g., NASA, US Department of Agriculture) and private (e.g., Airborne Snow Observatories, Inc, Planet Labs) stakeholders to ensure continuous funding and maintenance of these monitoring programs. Technological advances in sensors and platforms reinforced detection of specific physiological responses and understory vegetation regrowth. In-situ observations and data analysis techniques helped identify forest recovery processes and refine ecohydrological modeling. In this section, we suggest how these advances can be integrated with existing knowledge and resources. In particular, we discuss how new findings from new platform-sensor combinations can be incorporated into broadening our observational capabilities in CZ processes.

4.1. New Data Analysis With New or Existing Sensors

Advances in sensor technologies enable estimation of environmental metrics that until now were only possible through field or lab analysis at much finer scales. This data acquisition can be achieved by innovative sensor and algorithm development. New variables including canopy water content from microwave data (Konings et al., 2017, 2019) and subsurface water storage from gravimetry sensors (Geruo et al., 2017; Yang et al., 2014) complement existing campaigns with new algorithms. Ground-based remote sensing data including a cosmic-ray neutron probe (Andreasen et al., 2017; Desilets et al., 2010) and soil moisture retrieval from global positioning system (GPS) signals (Larson, 2016; Larson et al., 2008) can not only evaluate intensive forest management but unravel drivers of forest regrowth processes.

With capabilities of observing very narrow bandwidths, hyperspectral data have the potential to capture signals that conventional remote sensing instruments cannot detect. Hyperspectral imagery has been increasingly used to refine predictability of physiological activities with detailed estimation of fuel type and condition, vegetation recovery process (Veraverbeke et al., 2018), vegetation health (Tane et al., 2018), water stress, and carbon uptake (Asner et al., 2004). Ongoing and upcoming hyperspectral missions including Copernicus Hyperspectral Imaging Mission for the Environment (CHIME), HISUI, High-resolution Temperature and Spectral Emissivity Mapping (HiTeSEM), Surface Biology and Geology (SBG), Environmental Mapping and Analysis Program (EnMAP), PRISMA, and Fluorescence Explorer (FLEX) are expected to contribute to reliable assessment of vulnerability to disturbance, disturbance intensity, and post-disturbance forest recovery.

4.2. Data Fusion Across Multiple Sensors and Platforms

Multiple sensor types can acquire land surface and vegetation variables that are not available to estimate from a single remote sensing source. However, effective implementation of the multi-sensor integration is relatively underexplored due to inconsistent spatio-temporal resolution and coverage, and different monitoring trajectories. Data fusion of multiple platform products continuously improves with increasing data availability. Past data fusion techniques have used the same sensor types (e.g., multispectral images) to produce spatially and temporally disaggregated images in an extended period (Gao et al., 2006; Ghosh et al., 2020; Hilker et al., 2009; Roy et al., 2008; Schmidt et al., 2015; Yang et al., 2020; Zhu et al., 2010). For instance, modern platform sensors have fine spatio-temporal resolutions that can be harmonized and merged with satellite products that have long observation records to derive biophysical variables and to evaluate historical disturbance processes and responses at various scales.

Because CZ processes develop across the atmosphere-land surface-subsurface continuum, the complexity of responses and interactions with disturbance needs comprehensive investigation. Integration of multiple sensors or platforms can provide advantages such as (a) greater capability of addressing complex environmental feedback to disturbance facilitated by multivariate retrievals (Hao & AghaKouchak, 2013; Hao & Singh, 2015), (b) extensive spatio-temporal coverage of the remote sensing data (van Leeuwen et al., 2006), (c) deployment of multiple sensors, especially with small satellite constellations (McCabe, Aragon, et al., 2017; Woellert et al., 2011), for real-time observation with higher spatio-temporal resolution (Gao et al., 2006; McCabe, Rodell, et al., 2017; Pohl & van Genderen, 1998; Zhu et al., 2010), and (d) more robust analysis with cross validation and reduced uncertainty (Jiao et al., 2021). Previous and current airborne campaigns, including the Airborne Snow Observatory (ASO), Global Airborne Observatory (GAO), National Center for Airborne Laser Mapping (NCALM), SnowEx, and the National Ecological Observatory Network (NEON) Airborne Observation Platform (AOP), use lidar and spectral sensors to monitor changes in land surface (e.g., soil, snow) and vegetation properties. In particular, recently launched airborne forest monitoring campaigns (e.g., NEON AOP) are based on simultaneous data acquisition of spectral (for physiological attributes) and laser (for biophysical attributes) data in the same flight (Table 2). Moreover, the private sector plays a vital role in increasing spatio-temporal coverage and improving the reliability of data fusion through UAV and ground observation projects to meet the growing demand for high-resolution products. For example, value-added information on water supply forecasting for reservoirs (e.g., Airborne Snow Observatories, Inc.) and agriculture (Weiss et al., 2020) are stimulating new companies and technologies.

Simultaneous observations with multiple sensors may also result in estimating new variables that have not yet been possible to acquire with a single instrument. The remaining questions include a direct/indirect connection between biophysical and biochemical attributes from new sensor combinations, such as post-disturbance changes in forest structure (Meng et al., 2018; Sankey et al., 2017), sediment/nutrient transport (Sankey et al., 2021), canopy water content (Asner et al., 2015; Paz-Kagan et al., 2018; Swatantran et al., 2011), habitat characteristics (Vogeler et al., 2016), and canopy water stress (Coates et al., 2015; Sankey & Tatum, 2022) using hyperspectral data. Upcoming satellite missions including SBG, HyTI, CHIME, and BIOMASS, which are expected to provide extensive observations of the land surface and vegetation with a variety of sensor suites. In particular, hyperspectral missions have the great potential for detailed observation of plant responses to disturbance in combination with lidar (Degerickx et al., 2018; Ramirez et al., 2018; Sankey et al., 2018; Shivers et al., 2019; Sobejano-Paz et al., 2020). Because each platform has unique benefits, innovative methods can be applied to leverage these opportunities.

4.3. Increasing the Value of Ground-Based Observations

Few field networks effectively integrate remote sensing into larger CZ understanding or are used rigorously for remote sensing validation efforts. Furthermore, advances in remote sensing in CZ science often demand integrative approaches with other tools (e.g., physically based models) and observations (e.g., in-situ observations and multiple remote sensing products). Substantial ground truth data from in-situ surveys are required for remote sensing modeling of environmental variables and change detection (Steininger, 2000). Despite a wide variety of ground-based observations, remote sensing-based investigation of the forest response to disturbance is limited due to the lack of coordinated use of multidisciplinary data collection. For modeling regional tree species with different physiological traits during their growth stages, empirical or allometric approaches often

depend heavily on ground-based observations of canopy height and diameter at breast height (DBH) (Badreldin & Sanchez-Azofeifa, 2015). Growing remote sensing capabilities with technological advances enable estimation of new ecohydrological and biogeochemical variables that can ultimately be incorporated with in-situ measurements to provide greater value, such as species richness (Anderson et al., 2021). Because different platforms and sensors have different capabilities in elucidating ecohydrological processes in the CZ, a long record of continuous ground-based observations at a dense network of core watersheds is necessary. The recently launched CZCN is designed to promote centralized field and remote data collection for comparative interdisciplinary studies. As ground-based data are rarely available for selected core sites, intensive site-based investigations would effectively enhance ecohydrological modeling and verify remote sensing estimation. The network will be extremely useful to expand opportunities for remote sensing campaigns and greater availability of ground-based observations (Harpoled et al., 2015).

4.4. Disturbance Modeling

Greater diversity of remote sensing data and estimated variables can improve the prediction of the disturbance models. Dynamic forest modeling is typically based on the assumption that vegetation distribution is uniform in its maturity and physiological attributes across the watershed (Ajami et al., 2014; Shi et al., 2013). Incorporation of the distributed physiological status can improve model performance for heterogeneous landscape and non-steady-state conditions (Hanan et al., 2018). Remote sensing data from a new sensor-platform combination can resolve these spatial and temporal constraints and ultimately enhance the modeling accuracy and understanding of the environmental processes over multiple spatial and temporal scales. In specific, benefits of the high-resolution remote sensing data (e.g., PlanetScope and airborne/UAV data) include more reliable model calibration of ecophysiological parameters with regard to disturbance histories (Francini et al., 2020). A remotely sensed vegetation variable (e.g., LAI, stem wood) can help initialize the model conditions and biogeochemical pools (Hanan et al., 2018). Data assimilation can improve model initialization of disturbance histories (Luo et al., 2011). Remote sensing-based analysis can be used to evaluate modeled forest response to disturbance.

Along with exponentially increasing data volume and processing capabilities, emerging big data tools (e.g., data assimilation, machine learning, cloud computing) can produce reliable products over decades or longer. These methods are especially useful to estimate physiological responses to disturbance, such as vegetation health (Tane et al., 2018), forest mortality (Hart & Veblen, 2015; Rao et al., 2019), and carbon transfer (Williams et al., 2005; Yan et al., 2016), in areas with a lack of established biophysical relationships. The enhanced environmental monitoring with extensive coverage would ultimately benefit more robust forest management and disturbance assessment (Skole et al., 2021).

4.5. Synthesis: Putting It All Together to Improve Understanding of Disturbance

Synthesis of these conceptual and technical developments would contribute to comprehensive understanding of how CZ structure interacts with disturbance in montane forests. In this paper, we have shown how remote sensing can be used to provide insight into how climatic and human-driven disturbances (e.g., fire, drought, flood, and direct human modification of forests) can alter CZ structure. Most of this work has focused on how disturbance changes montane forest structure (e.g., cover, height, density) and species composition, or in the case of flood-driven erosion, how surface topography changes. A key contribution of remote sensing is the ability to track post-disturbance changes to vegetation and surface topography over time. The field is poised to link surface CZ structural changes with CZ function—carbon sequestration, water use, habitat provisioning by combining remote sensing with other datasets and models. From our examples, it is clear that disturbance intensity (e.g., a high-severity fire vs. a low-intensity thinning or drought event) and location within the heterogeneous montane forest landscapes (e.g., locations along regional climate gradients and locally between south- and north-facing aspects, or in locations with deep vs. shallow soils) interact to determine how the CZ functions regrow and evolve over time following disturbance. While many disturbances initially increase runoff and reduce evapotranspiration, magnitude and persistence of this effect varies with both disturbance intensity and local biogeoclimatic setting (Hanan et al., 2021; Tague & Moritz, 2019). More work is needed to develop a comprehensive theory of disturbance impacts that considers these space-time complexities. High spatio-temporal resolution remote sensing will be an essential for evolving this comprehensive picture.

Finally, we acknowledge that what is missing from this work is the integration of the subsurface. Some recent work has clearly showed that subsurface CZ structure can play a key role determining forest responses to disturbances (Callahan et al., 2022; Tague & Moritz, 2019). However, a myriad of unresolved questions in the CZ are based on two-way connections between subsurface properties and physiological response (Bloschl et al., 2019; Brantley et al., 2017; Fan, 2015). We know little, for example, about how multi-decade disturbance frequencies such as fire regimes, might influence subsurface weathering through impacts on root networks of different vegetation communities that are altered by fire. While direct remote sensing of the subsurface structure, particularly in steep forested montane regions, poses a challenge, regular remote sensing observations (e.g., subdaily, daily, or weekly) over decades can help to inform co-evolution models by offering trajectories of vegetation change. For instance, California Forest Observatory integrates a variety of satellite remote sensing sources (e.g., atmosphere, vegetation, topography) to provide a regional forest monitoring system.

Data Availability Statement

The ground-based GPP and NEE data from eddy covariance towers are available from AmeriFlux (Litvak, 2022a, 2022b). The aerial image-based vegetation cover data are available through Boisrame, Thompson, Kelly, et al. (2017). The Landsat burn severity data are available from the MTBS program (Eidenshink et al., 2007). The MODIS GPP, Landsat NDVI, NAIP, and NLDAS-2 climate data are available from Google Earth Engine (Gorelick et al., 2017). The SMERGE soil moisture data are available from NASA Earthdata (Crow & Tobin, 2018). The AVIRIS data are available from the AVIRIS Data Products Portal (Vane et al., 1993). The lidar data are available from OpenTopography (NCALM, 2012, 2014; USGS, 2022) and Oak Ridge National Laboratory Distributed Active Archive Center (Xu et al., 2018).

Acknowledgments

This research is supported by NSF Collaborative Research award # 2012669 and # 2011346. We acknowledge the following AmeriFlux sites for their data records: US-Vcm and US-Mpj. In addition, funding for AmeriFlux data resources was provided by the U.S. Department of Energy's Office of Science.

References

- Abatzoglou, J. T., & Williams, A. P. (2016). Impact of anthropogenic climate change on wildfire across Western US forests. *Proceedings of the National Academy of Sciences of the United States of America*, 113(42), 11770–11775. <https://doi.org/10.1073/pnas.1607171113>
- Abdollahnejad, A., & Panagiotidis, D. (2020). Tree species classification and health status assessment for a mixed broadleaf-conifer forest with UAS multispectral imaging. *Remote Sensing*, 12(22), 3722. <https://doi.org/10.3390/rs12223722>
- Ackerman, S. A., Strabala, K. I., Menzel, W. P., Frey, R. A., Moeller, C. C., & Gumley, L. E. (1998). Discriminating clear sky from clouds with MODIS. *Journal of Geophysical Research*, 103(D24), 32141–32157. <https://doi.org/10.1029/1998jd200032>
- Ajami, H., McCabe, M. F., Evans, J. P., & Stisen, S. (2014). Assessing the impact of model spin-up on surface water-groundwater interactions using an integrated hydrologic model. *Water Resources Research*, 50(3), 2636–2656. <https://doi.org/10.1002/2013wr014258>
- Akuraju, V. R., Ryu, D., & George, B. (2021). Estimation of root-zone soil moisture using crop water stress index (CWSI) in agricultural fields. *GIScience and Remote Sensing*, 58(3), 340–353. <https://doi.org/10.1080/15481603.2021.1877009>
- Alani, A. M., & Lantini, L. (2020). Recent advances in tree root mapping and assessment using non-destructive testing methods: A focus on ground penetrating radar. *Surveys in Geophysics*, 41(3), 605–646. <https://doi.org/10.1007/s10712-019-09548-6>
- Allison, R. S., Johnston, J. M., Craig, G., & Jennings, S. (2016). Airborne optical and thermal remote sensing for wildfire detection and monitoring. *Sensors*, 16(8), 1310. <https://doi.org/10.3390/s16081310>
- Almeida, R., Rosenqvist, A., Shimabukuro, Y. E., & Silva-Gomez, R. (2007). Detecting deforestation with multitemporal L-band SAR imagery: A case study in Western Brazilian Amazonia. *International Journal of Remote Sensing*, 28(6), 1383–1390. <https://doi.org/10.1080/01431160600754591>
- Alonzo, M., Andersen, H. E., Morton, D. C., & Cook, B. D. (2018). Quantifying boreal forest structure and composition using UAV structure from motion. *Forests*, 9(3), 119. <https://doi.org/10.3390/f9030119>
- Altenau, E. H., Pavelsky, T. M., Moller, D., Lion, C., Pitcher, L. H., Allen, G. H., et al. (2017). AirSWOT measurements of river water surface elevation and slope: Tanana River, AK. *Geophysical Research Letters*, 44(1), 181–189. <https://doi.org/10.1002/2016gl071577>
- Anderegg, W. R. L., Hicke, J. A., Fisher, R. A., Allen, C. D., Aukema, J., Bentz, B., et al. (2015). Tree mortality from drought, insects, and their interactions in a changing climate. *New Phytologist*, 208(3), 674–683. <https://doi.org/10.1111/nph.13477>
- Anderegg, W. R. L., Konings, A. G., Trugman, A. T., Yu, K. L., Bowling, D. R., Gabbitas, R., et al. (2018). Hydraulic diversity of forests regulates ecosystem resilience during drought. *Nature*, 561(7724), 538–541. <https://doi.org/10.1038/s41586-018-0539-7>
- Anderson, C. T., Dietz, S. L., Pokswinski, S. M., Jenkins, A. M., Kaeser, M. J., Hiers, J. K., & Pelc, B. D. (2021). Traditional field metrics and terrestrial LiDAR predict plant richness in southern pine forests. *Forest Ecology and Management*, 491, 119118. <https://doi.org/10.1016/j.foreco.2021.119118>
- Anderson, S. W., Anderson, S. P., & Anderson, R. S. (2015). Exhumation by debris flows in the 2013 Colorado Front Range storm. *Geology*, 43(5), 391–394. <https://doi.org/10.1130/g36507.1>
- Andreasen, M., Jensen, K. H., Desilets, D., Zreda, M., Bogen, H. R., & Looms, M. C. (2017). Cosmic-ray neutron transport at a forest field site: The sensitivity to various environmental conditions with focus on biomass and canopy interception. *Hydrology and Earth System Sciences*, 21(3), 1875–1894. <https://doi.org/10.5194/hess-21-1875-2017>
- Arnett, J., Coops, N. C., Gergel, S. E., Falls, R. W., & Baker, R. H. (2014). Detecting stand-replacing disturbance using RapidEye imagery: A Tasseled Cap transformation and modified disturbance index. *Canadian Journal of Remote Sensing*, 40(1), 1–14. <https://doi.org/10.1080/07038992.2014.899878>
- Arroyo, L. A., Pascual, C., & Manzanera, J. A. (2008). Fire models and methods to map fuel types: The role of remote sensing. *Forest Ecology and Management*, 256(6), 1239–1252. <https://doi.org/10.1016/j.foreco.2008.06.048>

- Ashcroft, M. B., Gollan, J. R., & Ramp, D. (2014). Creating vegetation density profiles for a diverse range of ecological habitats using terrestrial laser scanning. *Methods in Ecology and Evolution*, 5(3), 263–272. <https://doi.org/10.1111/2041-210x.12157>
- Asner, G. P., Anderson, C. B., Martin, R. E., Knapp, D. E., Tupayachi, R., Sinca, F., & Malhi, Y. (2014). Landscape-scale changes in forest structure and functional traits along an Andes-to-Amazon elevation gradient. *Biogeosciences*, 11(3), 843–856. <https://doi.org/10.5194/bg-11-843-2014>
- Asner, G. P., Martin, R. E., Anderson, C. B., & Knapp, D. E. (2015). Quantifying forest canopy traits: Imaging spectroscopy versus field survey. *Remote Sensing of Environment*, 158, 15–27. <https://doi.org/10.1016/j.rse.2014.11.011>
- Asner, G. P., Nepstad, D., Cardinot, G., & Ray, D. (2004). Drought stress and carbon uptake in an Amazon forest measured with spaceborne imaging spectroscopy. *Proceedings of the National Academy of Sciences of the United States of America*, 101(16), 6039–6044. <https://doi.org/10.1073/pnas.0400168101>
- Badreldin, N., & Sanchez-Azofeifa, A. (2015). Estimating forest biomass dynamics by integrating multi-temporal Landsat satellite images with ground and airborne LiDAR data in the coal valley mine, Alberta, Canada. *Remote Sensing*, 7(3), 2832–2849. <https://doi.org/10.3390/rs70302832>
- Bae, S., Muller, J., Forster, B., Hilmers, T., Hochrein, S., Jacobs, M., et al. (2022). Tracking the temporal dynamics of insect defoliation by high-resolution radar satellite data. *Methods in Ecology and Evolution*, 13(1), 121–132. <https://doi.org/10.1111/2041-210x.13726>
- Baguskas, S. A., Peterson, S. H., Bookhagen, B., & Still, C. J. (2014). Evaluating spatial patterns of drought-induced tree mortality in a coastal California pine forest. *Forest Ecology and Management*, 315, 43–53. <https://doi.org/10.1016/j.foreco.2013.12.020>
- Bales, R. C., Goulden, M. L., Hunsaker, C. T., Conklin, M. H., Hartsough, P. C., O'Geen, A. T., et al. (2018). Mechanisms controlling the impact of multi-year drought on mountain hydrology. *Scientific Reports*, 8(1), 690. <https://doi.org/10.1038/s41598-017-19007-0>
- Ballesteros-Canovas, J. A., Corona, C., Stoffel, M., Lucia-Vela, A., & Bodoque, J. M. (2015). Combining terrestrial laser scanning and root exposure to estimate erosion rates. *Plant and Soil*, 394(1–2), 127–137. <https://doi.org/10.1007/s11104-015-2516-3>
- Baluja, J., Diago, M. P., Balda, P., Zorer, R., Meggio, F., Morales, F., & Tardaguila, J. (2012). Assessment of vineyard water status variability by thermal and multispectral imagery using an unmanned aerial vehicle (UAV). *Irrigation Science*, 30(6), 511–522. <https://doi.org/10.1007/s00271-012-0382-9>
- Bart, R. R., Tague, C. L., & Moritz, M. A. (2016). Effect of tree-to-shrub type conversion in lower Montane Forests of the Sierra Nevada (USA) on streamflow. *PLoS One*, 11(8), e0161805. <https://doi.org/10.1371/journal.pone.0161805>
- Bellvert, J., Marsal, J., Girona, J., & Zarco-Tejada, P. J. (2015). Seasonal evolution of crop water stress index in grapevine varieties determined with high-resolution remote sensing thermal imagery. *Irrigation Science*, 33(2), 81–93. <https://doi.org/10.1007/s00271-014-0456-y>
- Belmonte, A., Sankey, T., Biederman, J., Bradford, J., Goetz, S., & Kolb, T. (2021). UAV-based estimate of snow cover dynamics: Optimizing semi-arid forest structure for snow persistence. *Remote Sensing*, 13(5), 1036. <https://doi.org/10.3390/rs13051036>
- Bian, J., Zhang, Z. T., Chen, J. Y., Chen, H. Y., Cui, C. F., Li, X. W., et al. (2019). Simplified evaluation of cotton water stress using high resolution unmanned aerial vehicle thermal imagery. *Remote Sensing*, 11(3), 267. <https://doi.org/10.3390/rs11030267>
- Bloschl, G., Bierkens, M. F. P., Chambel, A., Cudennec, C., Destouni, G., Fiori, A., et al. (2019). Twenty-three unsolved problems in hydrology (UPH) - A community perspective. *Hydrological Sciences Journal*, 64(10), 1141–1158. <https://doi.org/10.1080/02626667.2019.1620507>
- Boisrame, G., Thompson, S., Collins, B., & Stephens, S. (2017). Managed wildfire effects on forest resilience and water in the sierra Nevada. *Ecosystems*, 20(4), 717–732. <https://doi.org/10.1007/s10021-016-0048-1>
- Boisrame, G., Thompson, S., Kelly, M., Cavalli, J., Wilkin, K., & Stephens, S. (2017). Vegetation change during 40 years of repeated managed wildfires in the Sierra Nevada, California. *Forest Ecology and Management*, 402, 241–252. <https://doi.org/10.1016/j.foreco.2017.07.034>
- Boisrame, G., Thompson, S., & Stephens, S. (2018). Hydrologic responses to restored wildfire regimes revealed by soil moisture-vegetation relationships. *Advances in Water Resources*, 112, 124–146. <https://doi.org/10.1016/j.advwatres.2017.12.009>
- Boisrame, G., Thompson, S., Tague, C., & Stephens, S. (2019). Restoring a natural fire regime alters the water balance of a sierra Nevada catchment. *Water Resources Research*, 55(7), 5751–5769. <https://doi.org/10.1029/2018wr024098>
- Bolstad, P. V., Vose, J. M., & McNulty, S. G. (2001). Forest productivity, leaf area, and terrain in southern Appalachian deciduous forests. *Forest Science*, 47(3), 419–427.
- Bolton, D. K., Coops, N. C., & Wulder, M. A. (2015). Characterizing residual structure and forest recovery following high-severity fire in the Western boreal of Canada using Landsat time-series and airborne lidar data. *Remote Sensing of Environment*, 163, 48–60. <https://doi.org/10.1016/j.rse.2015.03.004>
- Boucher, P. B., Hancock, S., Orwig, D. A., Duncanson, L., Armston, J., Tang, H., et al. (2020). Detecting change in forest structure with simulated GEDI lidar waveforms: A case study of the Hemlock woolly adelgid (HWA: *Adelges tsugae*) infestation. *Remote Sensing*, 12(8), 1304. <https://doi.org/10.3390/rs12081304>
- Bourgoin, C., Betbeder, J., Couteron, P., Blanc, L., Dessard, H., Oszward, J., et al. (2020). UAV-based canopy textures assess changes in forest structure from long-term degradation. *Ecological Indicators*, 115, 106386. <https://doi.org/10.1016/j.ecolind.2020.106386>
- Bouvet, A., Mermoz, S., Toan, T. L., Villard, L., Mathieu, R., Naidoo, L., & Asner, G. P. (2018). An above-ground biomass map of African savannahs and woodlands at 25 m resolution derived from ALOS PALSAR. *Remote Sensing of Environment*, 206, 156–173. <https://doi.org/10.1016/j.rse.2017.12.030>
- Brantley, S. L., Eissenstat, D. M., Marshall, J. A., Godsey, S. E., Balogh-Brunstad, Z., Karwan, D. L., et al. (2017). Reviews and syntheses: On the roles trees play in building and plumbing the critical zone. *Biogeosciences*, 14(22), 5115–5142. <https://doi.org/10.5194/bg-14-5115-2017>
- Brodrick, P. G., & Asner, G. P. (2017). Remotely sensed predictors of conifer tree mortality during severe drought. *Environmental Research Letters*, 12(11), 115013. <https://doi.org/10.1088/1748-9326/aa8f55>
- Brunner, M. I., Papalexiou, S., Clark, M. P., & Gilleland, E. (2020). How probable is widespread flooding in the United States? *Water Resources Research*, 56(10). <https://doi.org/10.1029/2020wr028096>
- Burke, W. D., Tague, C., Kennedy, M. C., & Moritz, M. A. (2021). Understanding how fuel treatments interact with climate and biophysical setting to affect fire, water, and forest health: A process-based modeling approach. *Frontiers in Forests and Global Change*, 3. <https://doi.org/10.3389/ffgc.2020.591162>
- Callahan, R. P., Riebe, C. S., Sklar, L. S., Pasquet, S., Ferrier, K. L., Hahms, W. J., et al. (2022). Forest vulnerability to drought controlled by bedrock composition. *Nature Geoscience*, 15(9), 714–719. <https://doi.org/10.1038/s41561-022-01012-2>
- Campbell, M. J., Dennison, P. E., Hudak, A. T., Parham, L. M., & Butler, B. W. (2018). Quantifying understory vegetation density using small-footprint airborne lidar. *Remote Sensing of Environment*, 215, 330–342. <https://doi.org/10.1016/j.rse.2018.06.023>
- Chadwick, K. D., Brodrick, P. G., Grant, K., Goulden, T., Henderson, A., Falco, N., et al. (2020). Integrating airborne remote sensing and field campaigns for ecology and Earth system science. *Methods in Ecology and Evolution*, 11(11), 1492–1508. <https://doi.org/10.1111/2041-210x.13463>
- Chen, J., Shiyomi, M., Hori, Y., & Yamamura, Y. (2008). Frequency distribution models for spatial patterns of vegetation abundance. *Ecological Modelling*, 211(3–4), 403–410. <https://doi.org/10.1016/j.ecolmodel.2007.09.017>

- Chen, Q., Gong, P., Baldocchi, D., & Tian, Y. Q. (2007). Estimating basal area and stem volume for individual trees from lidar data. *Photogrammetric Engineering & Remote Sensing*, 73(12), 1355–1365. <https://doi.org/10.14358/pers.73.12.1355>
- Chen, S. J., McDermid, G. J., Castilla, G., & Linke, J. (2017). Measuring vegetation height in linear disturbances in the boreal forest with UAV photogrammetry. *Remote Sensing*, 9(12), 1257. <https://doi.org/10.3390/rs9121257>
- Chen, Y. W., Hakala, T., Karjalainen, M., Feng, Z. Y., Tang, J., Litkey, P., et al. (2017). UAV-borne profiling radar for forest research. *Remote Sensing*, 9(1), 58. <https://doi.org/10.3390/rs9010058>
- Clark, J. S., Iverson, L., Woodall, C. W., Allen, C. D., Bell, D. M., Bragg, D. C., et al. (2016). The impacts of increasing drought on forest dynamics, structure, and biodiversity in the United States. *Global Change Biology*, 22(7), 2329–2352. <https://doi.org/10.1111/gcb.13160>
- Coates, A. R., Dennison, P. E., Roberts, D. A., & Roth, K. L. (2015). Monitoring the impacts of severe drought on Southern California Chaparral species using hyperspectral and thermal infrared imagery. *Remote Sensing*, 7(11), 14276–14291. <https://doi.org/10.3390/rs71114276>
- Coe, J. A., Kean, J. W., Godt, J. W., Baum, R. L., Jones, E. S., Gochis, D., & Anderson, G. S. (2014). New insights into debris-flow hazards from an extraordinary event in the Colorado Front Range. *Geological Society of America Today*, 24(10), 4–10. <https://doi.org/10.1130/gsatg214a.1>
- Collins, B. M., Lydersen, J. M., Fry, D. L., Wilkin, K., Moody, T., & Stephens, S. L. (2016). Variability in vegetation and surface fuels across mixed-conifer-dominated landscapes with over 40 years of natural fire. *Forest Ecology and Management*, 381, 74–83. <https://doi.org/10.1016/j.foreco.2016.09.010>
- Collins, B. M., & Stephens, S. L. (2007). Fire scarring patterns in Sierra Nevada wilderness areas burned by multiple wildland fire use fires. *Fire Ecology*, 3(2), 53–67. <https://doi.org/10.4996/fireecology.0302053>
- Condon, L. E., Markovich, K. H., Kelleher, C. A., McDonnell, J. J., Ferguson, G., & McIntosh, J. C. (2020). Where is the bottom of a watershed? *Water Resources Research*, 56(3). <https://doi.org/10.1029/2019wr026010>
- Crespo-Peremarch, P., Fournier, R. A., Nguyen, V. T., van Lier, O. R., & Ruiz, L. A. (2020). A comparative assessment of the vertical distribution of forest components using full-waveform airborne, discrete airborne and discrete terrestrial laser scanning data. *Forest Ecology and Management*, 473, 118268. <https://doi.org/10.1016/j.foreco.2020.118268>
- Crespo-Peremarch, P., Tompalski, P., Coops, N. C., & Ruiz, L. A. (2018). Characterizing understory vegetation in Mediterranean forests using full-waveform airborne laser scanning data. *Remote Sensing of Environment*, 217, 400–413. <https://doi.org/10.1016/j.rse.2018.08.033>
- Crow, W., & Tobin, K. (2018). Smerge-Noah-CCI root zone soil moisture 0–40 cm L4 daily 0.125 x 0.125 degree V2.0. [Dataset]. <https://doi.org/10.5067/PAVQY1KHTMUT>
- Cuevas-Gonzalez, M., Gerard, F., Balzter, H., & Riano, D. (2009). Analysing forest recovery after wildfire disturbance in boreal Siberia using remotely sensed vegetation indices. *Global Change Biology*, 15(3), 561–577. <https://doi.org/10.1111/j.1365-2486.2008.01784.x>
- Curtis, P. G., Slay, C. M., Harris, N. L., Tyukavina, A., & Hansen, M. C. (2018). Classifying drivers of global forest loss. *Science*, 361(6407), 1108–1111. <https://doi.org/10.1126/science.aau3445>
- Dale, V. H., Joyce, L. A., McNulty, S., Neilson, R. P., Ayres, M. P., Flannigan, M. D., et al. (2001). Climate change and forest disturbances: Climate change can affect forests by altering the frequency, intensity, duration, and timing of fire, drought, introduced species, insect and pathogen outbreaks, hurricanes, windstorms, ice storms, or landslides. *BioScience*, 51(9), 723–734. [https://doi.org/10.1641/0006-3568\(2001\)051\[0723:ccafd\]2.0.co;2](https://doi.org/10.1641/0006-3568(2001)051[0723:ccafd]2.0.co;2)
- Dash, J. P., Watt, M. S., Pearse, G. D., Heaphy, M., & Dungey, H. S. (2017). Assessing very high resolution UAV imagery for monitoring forest health during a simulated disease outbreak. *ISPRS Journal of Photogrammetry and Remote Sensing*, 131, 1–14. <https://doi.org/10.1016/j.isprsjprs.2017.07.007>
- Degerickx, J., Roberts, D. A., McFadden, J. P., Hermy, M., & Somers, B. (2018). Urban tree health assessment using airborne hyperspectral and LiDAR imagery. *International Journal of Applied Earth Observation and Geoinformation*, 73, 26–38. <https://doi.org/10.1016/j.jag.2018.05.021>
- Dennison, P. E., Brewer, S. C., Arnold, J. D., & Moritz, M. A. (2014). Large wildfire trends in the Western United States, 1984–2011. *Geophysical Research Letters*, 41(8), 2928–2933. <https://doi.org/10.1002/2014gl059576>
- Desilets, D., Zreda, M., & Ferre, T. P. A. (2010). Nature's neutron probe: Land surface hydrology at an elusive scale with cosmic rays. *Water Resources Research*, 46(11). <https://doi.org/10.1029/2009wr008726>
- Dolan, K., Masek, J. G., Huang, C. Q., & Sun, G. Q. (2009). Regional forest growth rates measured by combining ICESat GLAS and Landsat data. *Journal of Geophysical Research*, 114(G2). <https://doi.org/10.1029/2008jg000893>
- Dorado-Roda, I., Pascual, A., Godinho, S., Silva, C. A., Botequim, B., Rodriguez-Gonzalez, P., et al. (2021). Assessing the accuracy of GEDI data for canopy height and aboveground biomass estimates in mediterranean forests. *Remote Sensing*, 13(12), 2279. <https://doi.org/10.3390/rs13122279>
- Ebel, B. A. (2020). Temporal evolution of measured and simulated infiltration following wildfire in the Colorado Front Range, USA: Shifting thresholds of runoff generation and hydrologic hazards. *Journal of Hydrology*, 585, 124765. <https://doi.org/10.1016/j.jhydrol.2020.124765>
- Ebel, B. A., & Moody, J. A. (2017). Synthesis of soil-hydraulic properties and infiltration timescales in wildfire-affected soils. *Hydrological Processes*, 31(2), 324–340. <https://doi.org/10.1002/hyp.10998>
- Ebel, B. A., Romero, O. C., & Martin, D. A. (2018). Thresholds and relations for soil-hydraulic and soil-physical properties as a function of burn severity 4 years after the 2011 Las Conchas Fire, New Mexico, USA. *Hydrological Processes*, 32(14), 2263–2278. <https://doi.org/10.1002/hyp.13167>
- Eidenshink, J., Schwind, B., Brewer, K., Zhu, Z.-L., Quayle, B., & Howard, S. (2007). A project for monitoring trends in burn severity. *Fire Ecology*, 3(1), 3–21. <https://doi.org/10.4996/fireecology.0301003>
- Eitel, J. U. H., Williams, C. J., Vierling, L. A., Al-Hamdan, O. Z., & Pierson, F. B. (2011). Suitability of terrestrial laser scanning for studying surface roughness effects on concentrated flow erosion processes in rangelands. *Catena*, 87(3), 398–407. <https://doi.org/10.1016/j.catena.2011.07.009>
- Fairfax, E., & Whittle, A. (2020). Smokey the Beaver: Beaver-dammed riparian corridors stay green during wildfire throughout the Western United States. *Ecological Applications*, 30(8). <https://doi.org/10.1002/eap.2225>
- Falkowski, M. J., Evans, J. S., Martinuzzi, S., Gessler, P. E., & Hudak, A. T. (2009). Characterizing forest succession with lidar data: An evaluation for the Inland Northwest, USA. *Remote Sensing of Environment*, 113(5), 946–956. <https://doi.org/10.1016/j.rse.2009.01.003>
- Fan, Y. (2015). Groundwater in the Earth's critical zone: Relevance to large-scale patterns and processes. *Water Resources Research*, 51(5), 3052–3069. <https://doi.org/10.1002/2015wr017037>
- Fassnacht, F. E., Latifi, H., Ghosh, A., Joshi, P. K., & Koch, B. (2014). Assessing the potential of hyperspectral imagery to map bark beetle-induced tree mortality. *Remote Sensing of Environment*, 140, 533–548. <https://doi.org/10.1016/j.rse.2013.09.014>
- Field, J. P., Breshears, D. D., Law, D. J., Villegas, J. C., Lopez-Hoffman, L., Brooks, P. D., et al. (2015). Critical zone services: Expanding context, constraints, and currency beyond ecosystem services. *Vadose Zone Journal*, 14(1), 1–7. <https://doi.org/10.2136/vzj2014.10.0142>

- Fisher, J. B., Lee, B., Purdy, A. J., Halverson, G. H., Dohlen, M. B., Cawse-Nicholson, K., et al. (2020). ECOSTRESS: NASA's next generation mission to measure evapotranspiration from the International Space Station. *Water Resources Research*, 56(4). <https://doi.org/10.1029/2019wr026058>
- Francini, S., D'Amico, G., Vangi, E., Borghi, C., & Chirici, G. (2022). Integrating GEDI and Landsat: Spaceborne lidar and four decades of optical imagery for the analysis of forest disturbances and biomass changes in Italy. *Sensors*, 22(5), 2015. <https://doi.org/10.3390/s22052015>
- Francini, S., McRoberts, R. E., Giannetti, F., Mencucci, M., Marchetti, M., Mugnozza, G. S., & Chirici, G. (2020). Near-real time forest change detection using PlanetScope imagery. *European Journal of Remote Sensing*, 53(1), 233–244. <https://doi.org/10.1080/22797254.2020.1806734>
- Frazier, A. E., & Hemingway, B. L. (2021). A technical review of Planet smallsat data: Practical considerations for processing and using PlanetScope imagery. *Remote Sensing*, 13(19), 3930. <https://doi.org/10.3390/rs13193930>
- Freeman, M. P., Stow, D. A., & Roberts, D. A. (2016). Object-based image mapping of conifer tree mortality in San Diego county based on multitemporal aerial ortho-imagery. *Photogrammetric Engineering & Remote Sensing*, 82(7), 571–580. <https://doi.org/10.14358/pers.82.7.571>
- Frolking, S., Milliman, T., Palace, M., Wisser, D., Lammers, R., & Fahnestock, M. (2011). Tropical forest backscatter anomaly evident in Sea Winds scatterometer morning overpass data during 2005 drought in Amazonia. *Remote Sensing of Environment*, 115(3), 897–907. <https://doi.org/10.1016/j.rse.2010.11.017>
- Frolking, S., Palace, M. W., Clark, D. B., Chambers, J. Q., Shugart, H. H., & Hurtt, G. C. (2009). Forest disturbance and recovery: A general review in the context of spaceborne remote sensing of impacts on aboveground biomass and canopy structure. *Journal of Geophysical Research*, 114(G2). <https://doi.org/10.1029/2008jg000911>
- Gabban, A., San-Miguel-Ayaz, J., & Viegas, D. X. (2006). On the suitability of the use of normalized difference vegetation index for forest fire risk assessment. *International Journal of Remote Sensing*, 27(22), 5095–5102. <https://doi.org/10.1080/01431160500185656>
- Gamon, J. A., Huemmrich, K. F., Wong, C. Y. S., Ensminger, I., Garrity, S., Hollinger, D. Y., et al. (2016). A remotely sensed pigment index reveals photosynthetic phenology in evergreen conifers. *Proceedings of the National Academy of Sciences of the United States of America*, 113(46), 13087–13092. <https://doi.org/10.1073/pnas.1606162113>
- Gao, F., Masek, J., Schwaller, M., & Hall, F. (2006). On the blending of the Landsat and MODIS surface reflectance: Predicting daily Landsat surface reflectance. *IEEE Transactions on Geoscience and Remote Sensing*, 44(8), 2207–2218. <https://doi.org/10.1109/tgrs.2006.872081>
- Garrity, S. R., Allen, C. D., Brumby, S. P., Gangodagamage, C., McDowell, N. G., & Cai, D. M. (2013). Quantifying tree mortality in a mixed species woodland using multitemporal high spatial resolution satellite imagery. *Remote Sensing of Environment*, 129, 54–65. <https://doi.org/10.1016/j.rse.2012.10.029>
- Gartner, P., Forster, M., & Kleinschmit, B. (2016). The benefit of synthetically generated RapidEye and Landsat 8 data fusion time series for riparian forest disturbance monitoring. *Remote Sensing of Environment*, 177, 237–247. <https://doi.org/10.1016/j.rse.2016.01.028>
- Gerhards, M., Schlerf, M., Rascher, U., Udelhoven, T., Juszczak, R., Alberti, G., et al. (2018). Analysis of airborne optical and thermal imagery for detection of water stress symptoms. *Remote Sensing*, 10(7), 1139. <https://doi.org/10.3390/rs10071139>
- Geruo, A., Velicogna, I., Kimball, J. S., Du, J. Y., Kim, Y., & Njoku, E. (2017). Satellite-observed changes in vegetation sensitivities to surface soil moisture and total water storage variations since the 2011 Texas drought. *Environmental Research Letters*, 12(5), 054006. <https://doi.org/10.1088/1748-9326/aa6965>
- Ghimire, B., Williams, C. A., Collatz, G. J., & Vanderhoof, M. (2012). Fire-induced carbon emissions and regrowth uptake in Western U.S. forests: Documenting variation across forest types, fire severity, and climate regions. *Journal of Geophysical Research*, 117(G3). <https://doi.org/10.1029/2011jg001935>
- Ghosh, R., Gupta, P. K., Tolpekin, V., & Srivastav, S. K. (2020). An enhanced spatiotemporal fusion method - implications for coal fire monitoring using satellite imagery. *International Journal of Applied Earth Observation and Geoinformation*, 88, 102056. <https://doi.org/10.1016/j.jag.2020.102056>
- Giorgi, F., & Avissar, R. (1997). Representation of heterogeneity effects in Earth system modeling: Experience from land surface modeling. *Reviews of Geophysics*, 35(4), 413–437. <https://doi.org/10.1029/97rg01754>
- Gochis, D., Schumacher, R., Friedrich, K., Doesken, N., Kelsch, M., Sun, J. Z., et al. (2015). The Great Colorado flood of September 2013. *Bulletin of the American Meteorological Society*, 96(9), 1461–1487. <https://doi.org/10.1175/bams-d-13-00241.1>
- Goetz, S. J., Sun, M., Baccini, A., & Beck, P. S. A. (2010). Synergistic use of spaceborne lidar and optical imagery for assessing forest disturbance: An Alaska case study. *Journal of Geophysical Research*, 115(G2). <https://doi.org/10.1029/2008jg000898>
- Gonzalez, P., Battles, J. J., Collins, B. M., Robards, T., & Saah, D. S. (2015). Aboveground live carbon stock changes of California wildland ecosystems, 2001–2010. *Forest Ecology and Management*, 348, 68–77. <https://doi.org/10.1016/j.foreco.2015.03.040>
- Gorelick, N., Hancher, M., Dixon, M., Ilyushchenko, S., Thau, D., & Moore, R. (2017). Google Earth Engine: Planetary-scale geospatial analysis for everyone. *Remote Sensing of Environment*, 202, 18–27. <https://doi.org/10.1016/j.rse.2017.06.031>
- Grau, E., Durrieu, S., Fournier, R., Gastellu-Etchegorry, J. P., & Yin, T. G. (2017). Estimation of 3D vegetation density with Terrestrial Laser Scanning data using voxels. A sensitivity analysis of influencing parameters. *Remote Sensing of Environment*, 191, 373–388. <https://doi.org/10.1016/j.rse.2017.01.032>
- Green, R. O., Eastwood, M. L., Sarture, C. M., Chrien, T. G., Aronsson, M., Chippendale, B. J., et al. (1998). Imaging spectroscopy and the Airborne Visible Infrared Imaging Spectrometer (AVIRIS). *Remote Sensing of Environment*, 65(3), 227–248. [https://doi.org/10.1016/s0034-4257\(98\)00064-9](https://doi.org/10.1016/s0034-4257(98)00064-9)
- Green, S. M., Dungait, J. A. J., Tu, C., Buss, H. L., Sanderson, N., Hawkes, S. J., et al. (2019). Soil functions and ecosystem services research in the Chinese Karst Critical Zone. *Chemical Geology*, 527, 119107. <https://doi.org/10.1016/j.chemgeo.2019.03.018>
- Gu, Y. X., Brown, J. F., Verdin, J. P., & Wardlow, B. (2007). A five-year analysis of MODIS NDVI and NDWI for grassland drought assessment over the central Great Plains of the United States. *Geophysical Research Letters*, 34(6), L06407. <https://doi.org/10.1029/2006gl029127>
- Gu, Y. X., Hunt, E., Wardlow, B., Basara, J. B., Brown, J. F., & Verdin, J. P. (2008). Evaluation of MODIS NDVI and NDWI for vegetation drought monitoring using Oklahoma Mesonet soil moisture data. *Geophysical Research Letters*, 35(22), L22401. <https://doi.org/10.1029/2008gl035772>
- Guiney, M. R., & Lininger, K. B. (2022). Disturbance and valley confinement: Controls on floodplain large wood and organic matter jam deposition in the Colorado Front Range, USA. *Earth Surface Processes and Landforms*, 47(6), 1371–1389. <https://doi.org/10.1002/esp.5321>
- Guo, L., Chen, J., Cui, X. H., Fan, B. H., & Lin, H. (2013). Application of ground penetrating radar for coarse root detection and quantification: A review. *Plant and Soil*, 362(1–2), 1–23. <https://doi.org/10.1007/s11104-012-1455-5>
- Gurnell, A. M., Corenblit, D., De Jalon, D. G., Del Tanago, M. G., Grabowski, R. C., O'Hare, M. T., & Szewczyk, M. (2016). A conceptual model of vegetation-hydrogeomorphology interactions within river corridors. *River Research and Applications*, 32(2), 142–163. <https://doi.org/10.1002/rra.2928>
- Hall, F. G., Bergen, K., Blair, J. B., Dubayah, R., Houghton, R., Hurtt, G., et al. (2011). Characterizing 3D vegetation structure from space: Mission requirements. *Remote Sensing of Environment*, 115(11), 2753–2775. <https://doi.org/10.1016/j.rse.2011.01.024>

- Hamraz, H., Contreras, M. A., & Zhang, J. (2017). Forest understory trees can be segmented accurately within sufficiently dense airborne laser scanning point clouds. *Scientific Reports*, 7(1), 6770. <https://doi.org/10.1038/s41598-017-07200-0>
- Hanan, E. J., Ren, J. N., Tague, C. L., Kolden, C. A., Abatzoglou, J. T., Bart, R. R., et al. (2021). How climate change and fire exclusion drive wildfire regimes at actionable scales. *Environmental Research Letters*, 16(2), 024051. <https://doi.org/10.1088/1748-9326/abd78e>
- Hanan, E. J., Tague, C., Choate, J., Liu, M. L., Kolden, C., & Adam, J. (2018). Accounting for disturbance history in models: Using remote sensing to constrain carbon and nitrogen pool spin-up. *Ecological Applications*, 28(5), 1197–1214. <https://doi.org/10.1002/eap.1718>
- Hansen, M. C., Egorov, A., Kommareddy, A., Tyukavina, A., Justice, C. O., Thau, D., et al. (2013). High-resolution global maps of 21st-century forest cover change. *Science*, 342(6160), 850–853. <https://doi.org/10.1126/science.1244693>
- Hansen, M. C., Stehman, S. V., & Potapov, P. V. (2010). Quantification of global gross forest cover loss. *Proceedings of the National Academy of Sciences of the United States of America*, 107(19), 8650–8655. <https://doi.org/10.1073/pnas.0912668107>
- Hao, Z., & AghaKouchak, A. (2013). Multivariate standardized drought index: A parametric multi-index model. *Advances in Water Resources*, 57, 12–18. <https://doi.org/10.1016/j.advwatres.2013.03.009>
- Hao, Z., & Singh, V. P. (2015). Drought characterization from a multivariate perspective: A review. *Journal of Hydrology*, 527, 668–678. <https://doi.org/10.1016/j.jhydrol.2015.05.031>
- Hardiman, B. S., Gough, C. M., Butnor, J. R., Bohrer, G., Detto, M., & Curtis, P. S. (2017). Coupling fine-scale root and canopy structure using ground-based remote sensing. *Remote Sensing*, 9(2), 182. <https://doi.org/10.3390/rs9020182>
- Harman, C. J., Lohse, K. A., Troch, P. A., & Sivapalan, M. (2014). Spatial patterns of vegetation, soils, and microtopography from terrestrial laser scanning on two semiarid hillslopes of contrasting lithology. *Journal of Geophysical Research-Biogeosciences*, 119(2), 163–180. <https://doi.org/10.1002/2013jg002507>
- Harpold, A. A., Marshall, J. A., Lyon, S. W., Barnhart, T. B., Fisher, B. A., Donovan, M., et al. (2015). Laser vision: Lidar as a transformative tool to advance critical zone science. *Hydrology and Earth System Sciences*, 19(6), 2881–2897. <https://doi.org/10.5194/hess-19-2881-2015>
- Harris, S., Veraverbeke, S., & Hook, S. (2011). Evaluating spectral indices for assessing fire severity in chaparral ecosystems (Southern California) using MODIS/ASTER (MASTER) airborne simulator data. *Remote Sensing*, 3(11), 2403–2419. <https://doi.org/10.3390/rs3112403>
- Hart, S. J., & Veblen, T. T. (2015). Detection of spruce beetle-induced tree mortality using high- and medium-resolution remotely sensed imagery. *Remote Sensing of Environment*, 168, 134–145. <https://doi.org/10.1016/j.rse.2015.06.015>
- Hartmann, H., Bastos, A., Das, A. J., Esquivel-Muelbert, A., Hammond, W. M., Martinez-Vilalta, J., et al. (2022). Climate change risks to global forest health: Emergence of unexpected events of elevated tree mortality worldwide. *Annual Review of Plant Biology*, 73(1), 673–702. <https://doi.org/10.1146/annurev-arplant-102820-012804>
- Hausner, M. B., Huntington, J. L., Nash, C., Morton, C., McEvoy, D. J., Pilliod, D. S., et al. (2018). Assessing the effectiveness of riparian restoration projects using Landsat and precipitation data from the cloud-computing application ClimateEngine.org. *Ecological Engineering*, 120, 432–440. <https://doi.org/10.1016/j.ecoleng.2018.06.024>
- Heinzel, J., & Huber, M. O. (2017). Detecting tree stems from volumetric TLS data in forest environments with rich understory. *Remote Sensing*, 9(1), 9. <https://doi.org/10.3390/rs9010009>
- Hermosilla, T., Wulder, M. A., White, J. C., & Coops, N. C. (2019). Prevalence of multiple forest disturbances and impact on vegetation regrowth from interannual Landsat time series (1985–2015). *Remote Sensing of Environment*, 233, 111403. <https://doi.org/10.1016/j.rse.2019.111403>
- Hicke, J. A., Allen, C. D., Desai, A. R., Dietze, M. C., Hall, R. J., Hogg, E. H., et al. (2012). Effects of biotic disturbances on forest carbon cycling in the United States and Canada. *Global Change Biology*, 18(1), 7–34. <https://doi.org/10.1111/j.1365-2486.2011.02543.x>
- Hilker, T., Wulder, M. A., Coops, N. C., Linke, J., McDermid, G., Masek, J. G., et al. (2009). A new data fusion model for high spatial- and temporal-resolution mapping of forest disturbance based on Landsat and MODIS. *Remote Sensing of Environment*, 113(8), 1613–1627. <https://doi.org/10.1016/j.rse.2009.03.007>
- Hislop, S., Jones, S., Soto-Berelov, M., Skidmore, A., Haywood, A., & Nguyen, T. H. (2019). A fusion approach to forest disturbance mapping using time series ensemble techniques. *Remote Sensing of Environment*, 221, 188–197. <https://doi.org/10.1016/j.rse.2018.11.025>
- Hook, S. J., Myers, J. E. J., Thome, K. J., Fitzgerald, M., & Kahle, A. B. (2001). The MODIS/ASTER airborne simulator (MASTER) - A new instrument for Earth science studies. *Remote Sensing of Environment*, 76(1), 93–102. [https://doi.org/10.1016/s0034-4257\(00\)00195-4](https://doi.org/10.1016/s0034-4257(00)00195-4)
- Huang, C. Y., Anderegg, W. R. L., & Asner, G. P. (2019). Remote sensing of forest die-off in the Anthropocene: From plant ecophysiology to canopy structure. *Remote Sensing of Environment*, 231, 111233. <https://doi.org/10.1016/j.rse.2019.111233>
- Huesca, M., Ustin, S. L., Shapiro, K. D., Boynton, R., & Thorne, J. H. (2021). Detection of drought-induced blue oak mortality in the Sierra Nevada Mountains, California. *Ecosphere*, 12(6). <https://doi.org/10.1002/ecs2.3558>
- Huisman, J. A., Hubbard, S. S., Redman, J. D., & Annan, A. P. (2003). Measuring soil water content with ground penetrating radar: A review. *Vadose Zone Journal*, 2(4), 476–491. <https://doi.org/10.2136/vzj2003.4760>
- Hunter, M. E., & Robles, M. D. (2020). Tamm review: The effects of prescribed fire on wildfire regimes and impacts: A framework for comparison. *Forest Ecology and Management*, 475, 118435. <https://doi.org/10.1016/j.foreco.2020.118435>
- Hwang, K., Chandler, D. G., & Flerchinger, G. N. (2023). Ground-based infrared thermometry reveals seasonal evapotranspiration patterns in semiarid rangelands. *Hydrological Processes*, 37(3). <https://doi.org/10.1002/hyp.14827>
- Idso, S. B., Reginato, R. J., Jackson, R. D., & Pinter, P. J. (1981). Measuring yield-reducing plant water potential depressions in wheat by infrared thermometry. *Irrigation Science*, 2(4), 205–212. <https://doi.org/10.1007/bf00258374>
- Javadian, M., Smith, W. K., Lee, K., Knowles, J. F., Scott, R. L., Fisher, J. B., et al. (2022). Canopy temperature is regulated by ecosystem structural traits and captures the ecohydrologic dynamics of a semiarid mixed conifer forest site. *Journal of Geophysical Research-Biogeosciences*, 127(2). <https://doi.org/10.1029/2021jg006617>
- Jiao, W., Wang, L., & McCabe, M. F. (2021). Multi-sensor remote sensing for drought characterization: Current status, opportunities and a roadmap for the future. *Remote Sensing of Environment*, 256, 112313. <https://doi.org/10.1016/j.rse.2021.112313>
- Jiao, W. Z., Chang, Q., & Wang, L. X. (2019). The sensitivity of satellite solar-induced chlorophyll fluorescence to meteorological drought. *Earth's Future*, 7(5), 558–573. <https://doi.org/10.1029/2018ef001087>
- Jin, S. M., & Sader, S. A. (2005). MODIS time-series imagery for forest disturbance detection and quantification of patch size effects. *Remote Sensing of Environment*, 99(4), 462–470. <https://doi.org/10.1016/j.rse.2005.09.017>
- Jones, M. O., Kimball, J. S., & Jones, L. A. (2013). Satellite microwave detection of boreal forest recovery from the extreme 2004 wildfires in Alaska and Canada. *Global Change Biology*, 19(10), 3111–3122. <https://doi.org/10.1111/gcb.12288>
- Joshi, N., Mitchard, E. T. A., Broly, M., Schumacher, J., Fernandez-Landa, A., Johannsen, V. K., et al. (2017). Understanding 'saturation' of radar signals over forests. *Scientific Reports*, 7(1), 3505. <https://doi.org/10.1038/s41598-017-03469-3>
- Junttila, S., Vastaranta, M., Hamalainen, J., Latva-kayra, P., Holopainen, M., Clemente, R. H., et al. (2017). Effect of forest structure and health on the relative surface temperature captured by airborne thermal imagery - case study in Norway Spruce-dominated stands in Southern Finland. *Scandinavian Journal of Forest Research*, 32(2), 154–165. <https://doi.org/10.1080/02827581.2016.1207800>

- Kane, V. R., Bakker, J. D., McGaughey, R. J., Lutz, J. A., Gersonde, R. F., & Franklin, J. F. (2010). Examining conifer canopy structural complexity across forest ages and elevations with LiDAR data. *Canadian Journal of Forest Research-Revue Canadienne De Recherche Forestiere*, 40(4), 774–787. <https://doi.org/10.1139/x10-064>
- Kane, V. R., Gersonde, R. F., Lutz, J. A., McGaughey, R. J., Bakker, J. D., & Franklin, J. F. (2011). Patch dynamics and the development of structural and spatial heterogeneity in Pacific Northwest forests. *Canadian Journal of Forest Research*, 41(12), 2276–2291. <https://doi.org/10.1139/x11-128>
- Kane, V. R., North, M. P., Lutz, J. A., Churchill, D. J., Roberts, S. L., Smith, D. F., et al. (2014). Assessing fire effects on forest spatial structure using a fusion of Landsat and airborne LiDAR data in Yosemite National Park. *Remote Sensing of Environment*, 151, 89–101. <https://doi.org/10.1016/j.rse.2013.07.041>
- Karnieli, A., Agam, N., Pinker, R. T., Anderson, M., Imhoff, M. L., Gutman, G. G., et al. (2010). Use of NDVI and land surface temperature for drought assessment: Merits and limitations. *Journal of Climate*, 23(3), 618–633. <https://doi.org/10.1175/2009jcli2900.1>
- Keller, C. K. (2019). Carbon exports from terrestrial ecosystems: A critical-zone framework. *Ecosystems*, 22(8), 1691–1705. <https://doi.org/10.1007/s10021-019-00375-9>
- Kennedy, R. E., Yang, Z. G., & Cohen, W. B. (2010). Detecting trends in forest disturbance and recovery using yearly Landsat time series: 1. LandTrendr - temporal segmentation algorithms. *Remote Sensing of Environment*, 114(12), 2897–2910. <https://doi.org/10.1016/j.rse.2010.07.008>
- Kennedy, R. E., Yang, Z. Q., Cohen, W. B., Pfaff, E., Braaten, J., & Nelson, P. (2012). Spatial and temporal patterns of forest disturbance and regrowth within the area of the Northwest Forest Plan. *Remote Sensing of Environment*, 122, 117–133. <https://doi.org/10.1016/j.rse.2011.09.024>
- Kimm, H., Guan, K. Y., Jiang, C. Y., Peng, B., Gentry, L. F., Wilkin, S. C., et al. (2020). Deriving high-spatiotemporal-resolution leaf area index for agroecosystems in the US Corn Belt using Planet Labs CubeSat and STAIR fusion data. *Remote Sensing of Environment*, 239, 111615. <https://doi.org/10.1016/j.rse.2019.111615>
- Kloucek, T., Komarek, J., Surovy, P., Hrach, K., Janata, P., & Vasicek, B. (2019). The use of UAV mounted sensors for precise detection of bark beetle infestation. *Remote Sensing*, 11(13), 1561. <https://doi.org/10.3390/rs11131561>
- Kokaly, R. F., Rockwell, B. W., Haire, S. L., & King, T. V. V. (2007). Characterization of post-fire surface cover, soils, and burn severity at the Cerro Grande Fire, New Mexico, using hyperspectral and multispectral remote sensing. *Remote Sensing of Environment*, 106(3), 305–325. <https://doi.org/10.1016/j.rse.2006.08.006>
- Kong, F. H., Yan, W. J., Zheng, G., Yin, H. W., Cavan, G., Zhan, W. F., et al. (2016). Retrieval of three-dimensional tree canopy and shade using terrestrial laser scanning (TLS) data to analyze the cooling effect of vegetation. *Agricultural and Forest Meteorology*, 217, 22–34. <https://doi.org/10.1016/j.agrformet.2015.11.005>
- Konings, A. G., Holtzman, N. M., Rao, K., Xu, L., & Saatchi, S. S. (2021). Interannual variations of vegetation optical depth are due to both water stress and biomass changes. *Geophysical Research Letters*, 48(16). <https://doi.org/10.1029/2021gl095267>
- Konings, A. G., Rao, K., & Steele-Dunne, S. C. (2019). Macro to micro: Microwave remote sensing of plant water content for physiology and ecology. *New Phytologist*, 223(3), 1166–1172. <https://doi.org/10.1111/nph.15808>
- Konings, A. G., Yu, Y. F., Xu, L., Yang, Y., Schimel, D. S., & Saatchi, S. S. (2017). Active microwave observations of diurnal and seasonal variations of canopy water content across the humid African tropical forests. *Geophysical Research Letters*, 44(5), 2290–2299. <https://doi.org/10.1002/2016gl072388>
- Krause, S., Sanders, T. G. M., Mund, J. P., & Greve, K. (2019). UAV-based photogrammetric tree height measurement for intensive forest monitoring. *Remote Sensing*, 11(7), 758. <https://doi.org/10.3390/rs11070758>
- Lambot, S., Javaux, M., Hupet, F., & Vanclooster, M. (2002). A global multilevel coordinate search procedure for estimating the unsaturated soil hydraulic properties. *Water Resources Research*, 38(11), 6–1–6–15. <https://doi.org/10.1029/2001wr001224>
- Larrinaga, A. R., & Brotons, L. (2019). Greenness indices from a low-cost UAV imagery as tools for monitoring post-fire forest recovery. *Drones*, 3(1), 6. <https://doi.org/10.3390/drones3010006>
- Larsen, A., Larsen, J. R., & Lane, S. N. (2021). Dam builders and their works: Beaver influences on the structure and function of river corridor hydrology, geomorphology, biogeochemistry and ecosystems. *Earth-Science Reviews*, 218, 103623. <https://doi.org/10.1016/j.earscirev.2021.103623>
- Larson, K. M. (2016). GPS interferometric reflectometry: Applications to surface soil moisture, snow depth, and vegetation water content in the Western United States. *Wiley Interdisciplinary Reviews-Water*, 3(6), 775–787. <https://doi.org/10.1002/wat2.1167>
- Larson, K. M., Small, E. E., Gutmann, E. D., Bilich, A. L., Braun, J. J., & Zavorotny, V. U. (2008). Use of GPS receivers as a soil moisture network for water cycle studies. *Geophysical Research Letters*, 35(24), L24405. <https://doi.org/10.1029/2008gl036013>
- Latifi, H., Dahms, T., Beudert, B., Heurich, M., Kubert, C., & Dech, S. (2018). Synthetic RapidEye data used for the detection of area-based spruce tree mortality induced by bark beetles. *GIScience and Remote Sensing*, 55(6), 839–859. <https://doi.org/10.1080/15481603.2018.1458463>
- Lausch, A., Erasmi, S., King, D. J., Magdon, P., & Heurich, M. (2017). Understanding forest health with remote sensing-Part II-A review of approaches and data models. *Remote Sensing*, 9(2), 129. <https://doi.org/10.3390/rs9020129>
- Lehmann, J. R. K., Nieberding, F., Prinz, T., & Knoth, C. (2015). Analysis of unmanned aerial system-based CIR images in forestry-A new perspective to monitor pest infestation levels. *Forests*, 6(3), 594–612. <https://doi.org/10.3390/f6030594>
- Lettenmaier, D. P., Alsdorf, D., Dozier, J., Huffman, G. J., Pan, M., & Wood, E. F. (2015). Inroads of remote sensing into hydrologic science during the WRR era. *Water Resources Research*, 51(9), 7309–7342. <https://doi.org/10.1002/2015wr017616>
- Lewis, S. A., Robichaud, P. R., Hudak, A. T., Austin, B., & Liebermann, R. J. (2012). Utility of remotely sensed imagery for assessing the impact of salvage logging after forest fires. *Remote Sensing*, 4(7), 2112–2132. <https://doi.org/10.3390/rs4072112>
- Li, S., Wang, T. M., Hou, Z. Y., Gong, Y. A., Feng, L. M., & Ge, J. P. (2021). Harnessing terrestrial laser scanning to predict understory biomass in temperate mixed forests. *Ecological Indicators*, 121, 107011. <https://doi.org/10.1016/j.ecolind.2020.107011>
- Lininger, K. B., Scamardo, J. E., & Guiney, M. R. (2021). Floodplain large wood and organic matter jam formation after a large flood: Investigating the influence of floodplain forest stand characteristics and river corridor morphology. *Journal of Geophysical Research-Earth Surface*, 126(6). <https://doi.org/10.1029/2020jf006011>
- Litvak, M. (2022a). AmeriFlux BASE US-Mpj Mountainair Pinyon-Juniper Woodland, Ver. 20-5. [Dataset]. AmeriFlux AMP. <https://doi.org/10.17190/AMF/1246123>
- Litvak, M. (2022b). AmeriFlux BASE US-Vcm Valles Caldera Mixed Conifer, Ver. 22-5. [Dataset]. AmeriFlux AMP. <https://doi.org/10.17190/AMF/1246121>
- Liu, N., Deng, Z. J., Wang, H. L., Luo, Z. D., Gutierrez-Jurado, H. A., He, X. G., & Guan, H. D. (2020). Thermal remote sensing of plant water stress in natural ecosystems. *Forest Ecology and Management*, 476, 118433. <https://doi.org/10.1016/j.foreco.2020.118433>
- Liu, Y. L., Kumar, M., Katul, G. G., & Porporato, A. (2019). Reduced resilience as an early warning signal of forest mortality. *Nature Climate Change*, 9(11), 880–885. <https://doi.org/10.1038/s41558-019-0583-9>

- Loehman, R. A., Keane, R. E., Holsinger, L. M., & Wu, Z. W. (2017). Interactions of landscape disturbances and climate change dictate ecological pattern and process: Spatial modeling of wildfire, insect, and disease dynamics under future climates. *Landscape Ecology*, *32*(7), 1447–1459. <https://doi.org/10.1007/s10980-016-0414-6>
- Lohberger, S., Stangel, M., Atwood, E. C., & Siegert, F. (2018). Spatial evaluation of Indonesia's 2015 fire-affected area and estimated carbon emissions using Sentinel-1. *Global Change Biology*, *24*(2), 644–654. <https://doi.org/10.1111/gcb.13841>
- Longoni, L., Papini, M., Brambilla, D., Barazzetti, L., Roncoroni, F., Scaioni, M., & Ivanov, V. I. (2016). Monitoring riverbank erosion in mountain catchments using terrestrial laser scanning. *Remote Sensing*, *8*(3), 241. <https://doi.org/10.3390/rs8030241>
- Lowman, L. E. L., & Barros, A. P. (2016). Interplay of drought and tropical cyclone activity in SE US gross primary productivity. *Journal of Geophysical Research-Biogeosciences*, *121*(6), 1540–1567. <https://doi.org/10.1002/2015jg003279>
- Lowman, L. E. L., & Barros, A. P. (2018). Predicting canopy biophysical properties and sensitivity of plant carbon uptake to water limitations with a coupled eco-hydrological framework. *Ecological Modelling*, *372*, 33–52. <https://doi.org/10.1016/j.ecolmodel.2018.01.011>
- Lucas, R., Armston, J., Fairfax, R., Fensham, R., Accad, A., Carreiras, J., et al. (2010). An evaluation of the ALOS PALSAR L-band backscatter-above ground biomass relationship Queensland, Australia: Impacts of surface moisture condition and vegetation structure. *IEEE Journal of Selected Topics in Applied Earth Observations and Remote Sensing*, *3*(4), 576–593. <https://doi.org/10.1109/jstars.2010.2086436>
- Lucas, R. M., Cronin, N., Moghaddam, M., Lee, A., Armston, J., Bunting, P., & Witte, C. (2006). Integration of radar and Landsat-derived foliage projected cover for woody regrowth mapping, Queensland, Australia. *Remote Sensing of Environment*, *100*(3), 388–406. <https://doi.org/10.1016/j.rse.2005.09.020>
- Lucas, R. M., Lee, A. C., & Williams, M. L. (2006). Enhanced simulation of radar backscatter from forests using LiDAR and optical data. *IEEE Transactions on Geoscience and Remote Sensing*, *44*(10), 2736–2754. <https://doi.org/10.1109/tgrs.2006.881802>
- Ludovisi, R., Tauro, F., Salvati, R., Khoury, S., Mugnozza, G. S., & Harfouche, A. (2017). UAV-based thermal imaging for high-throughput field phenotyping of black poplar response to drought. *Frontiers in Plant Science*, *8*. <https://doi.org/10.3389/fpls.2017.01681>
- Luetzenburg, G., Kroon, A., & Bjork, A. A. (2021). Evaluation of the Apple iPhone 12 Pro LiDAR for an application in geosciences. *Scientific Reports*, *11*(1), 22221. <https://doi.org/10.1038/s41598-021-01763-9>
- Lundquist, J. D., Dickerson-Lange, S. E., Lutz, J. A., & Cristea, N. C. (2013). Lower forest density enhances snow retention in regions with warmer winters: A global framework developed from plot-scale observations and modeling. *Water Resources Research*, *49*(10), 6356–6370. <https://doi.org/10.1002/wrcr.20504>
- Luo, Y. Q., Ogle, K., Tucker, C., Fei, S. F., Gao, C., LaDeau, S., et al. (2011). Ecological forecasting and data assimilation in a data-rich era. *Ecological Applications*, *21*(5), 1429–1442. <https://doi.org/10.1890/09-1275.1>
- Luscombe, D. J., Anderson, K., Gatis, N., Wetherelt, A., Grand-Clement, E., & Brazier, R. E. (2015). What does airborne LiDAR really measure in upland ecosystems? *Ecohydrology*, *8*(4), 584–594. <https://doi.org/10.1002/eco.1527>
- Magilligan, F. J., Buraas, E. M., & Renshaw, C. E. (2015). The efficacy of stream power and flow duration on geomorphic responses to catastrophic flooding. *Geomorphology*, *228*, 175–188. <https://doi.org/10.1016/j.geomorph.2014.08.016>
- Mallakpour, I., & Villarini, G. (2016). A simulation study to examine the sensitivity of the Pettitt test to detect abrupt changes in mean. *Hydrological Sciences Journal-Journal Des Sciences Hydrologiques*, *61*(2), 245–254. <https://doi.org/10.1080/02626667.2015.1008482>
- Manoli, G., Huang, C. W., Bonetti, S., Domec, J. C., Marani, M., & Katul, G. (2017). Competition for light and water in a coupled soil-plant system. *Advances in Water Resources*, *108*, 216–230. <https://doi.org/10.1016/j.advwatres.2017.08.004>
- Marselis, S. M., Keil, P., Chase, J. M., & Dubayah, R. (2022). The use of GEDI canopy structure for explaining variation in tree species richness in natural forests. *Environmental Research Letters*, *17*(4), 045003. <https://doi.org/10.1088/1748-9326/ac583f>
- Martin, R. E., Asner, G. P., Francis, E., Ambrose, A., Baxter, W., Das, A. J., et al. (2018). Remote measurement of canopy water content in giant sequoias (*Sequoiadendron giganteum*) during drought. *Forest Ecology and Management*, *419*, 279–290. <https://doi.org/10.1016/j.foreco.2017.12.002>
- Matasci, G., Hermosilla, T., Wulder, M. A., White, J. C., Coops, N. C., Hobart, G. W., & Zald, H. S. J. (2018). Large-area mapping of Canadian boreal forest cover, height, biomass and other structural attributes using Landsat composites and lidar plots. *Remote Sensing of Environment*, *209*, 90–106. <https://doi.org/10.1016/j.rse.2017.12.020>
- McCabe, M. F., Aragon, B., Houborg, R., & Mascaro, J. (2017). CubeSats in hydrology: Ultrahigh-resolution insights into vegetation dynamics and terrestrial evaporation. *Water Resources Research*, *53*(12), 10017–10024. <https://doi.org/10.1002/2017wr022240>
- McCabe, M. F., Rodell, M., Alsdorf, D. E., Miralles, D. G., Uijlenhoet, R., Wagner, W., et al. (2017). The future of Earth observation in hydrology. *Hydrology and Earth System Sciences*, *21*(7), 3879–3914. <https://doi.org/10.5194/hess-21-3879-2017>
- McGuire, L. A., Youberg, A. M., Rengers, F. K., Abramson, N. S., Ganesh, I., Gorr, A. N., et al. (2021). Extreme precipitation across adjacent burned and unburned watersheds reveals impacts of low severity wildfire on debris-flow processes. *Journal of Geophysical Research-Earth Surface*, *126*(4). <https://doi.org/10.1029/2020jfo05997>
- McNicol, I. M., Mitchard, E. T. A., Aquino, C., Burt, A., Carstairs, H., Dassi, C., et al. (2021). To what extent can UAV photogrammetry replicate UAV LiDAR to determine forest structure? A test in two contrasting tropical forests. *Journal of Geophysical Research-Biogeosciences*, *126*(12). <https://doi.org/10.1029/2021jg006586>
- Meddens, A. J. H., & Hicke, J. A. (2014). Spatial and temporal patterns of Landsat-based detection of tree mortality caused by a mountain pine beetle outbreak in Colorado, USA. *Forest Ecology and Management*, *322*, 78–88. <https://doi.org/10.1016/j.foreco.2014.02.037>
- Meddens, A. J. H., Hicke, J. A., & Ferguson, C. A. (2012). Spatiotemporal patterns of observed bark beetle-caused tree mortality in British Columbia and the Western United States. *Ecological Applications*, *22*(7), 1876–1891. <https://doi.org/10.1890/11-1785.1>
- Meddens, A. J. H., Hicke, J. A., & Vierling, L. A. (2011). Evaluating the potential of multispectral imagery to map multiple stages of tree mortality. *Remote Sensing of Environment*, *115*(7), 1632–1642. <https://doi.org/10.1016/j.rse.2011.02.018>
- Meehl, G. A., & Tebaldi, C. (2004). More intense, more frequent, and longer lasting heat waves in the 21st century. *Science*, *305*(5686), 994–997. <https://doi.org/10.1126/science.1098704>
- Melesse, A. M., Nangia, V., Wang, X. X., & McClain, M. (2007). Wetland restoration response analysis using MODIS and groundwater data. *Sensors*, *7*(9), 1916–1933. <https://doi.org/10.3390/s7091916>
- Meng, R., Wu, J., Zhao, F., Cook, B. D., Hanavan, R. P., & Serbin, S. P. (2018). Measuring short-term post-fire forest recovery across a burn severity gradient in a mixed pine-oak forest using multi-sensor remote sensing techniques. *Remote Sensing of Environment*, *210*, 282–296. <https://doi.org/10.1016/j.rse.2018.03.019>
- Middleton, E. M., Ungar, S. G., Mandl, D. J., Ong, L., Frye, S. W., Campbell, P. E., et al. (2013). The Earth Observing One (EO-1) satellite mission: Over a decade in space. *IEEE Journal of Selected Topics in Applied Earth Observations and Remote Sensing*, *6*(2), 243–256. <https://doi.org/10.1109/jstars.2013.2249496>
- Mildrexler, D., Yang, Z. Q., Cohen, W. B., & Bell, D. M. (2016). A forest vulnerability index based on drought and high temperatures. *Remote Sensing of Environment*, *173*, 314–325. <https://doi.org/10.1016/j.rse.2015.11.024>

- Miller, J. D., & Thode, A. E. (2007). Quantifying burn severity in a heterogeneous landscape with a relative version of the delta Normalized Burn Ratio (dNBR). *Remote Sensing of Environment*, 109(1), 66–80. <https://doi.org/10.1016/j.rse.2006.12.006>
- Minor, J., Pearl, J. K., Barnes, M. L., Colella, T. R., Murphy, P. C., Mann, S., & Barron-Gafford, G. A. (2020). Critical Zone Science in the Anthropocene: Opportunities for biogeographic and ecological theory and praxis to drive Earth science integration. *Progress in Physical Geography: Earth and Environment*, 44(1), 50–69. <https://doi.org/10.1177/0309133319864268>
- Mohan, M., Silva, C. A., Klauberg, C., Jat, P., Catts, G., Cardil, A., et al. (2017). Individual tree detection from Unmanned Aerial Vehicle (UAV) derived canopy height model in an open canopy mixed conifer forest. *Forests*, 8(9), 340. <https://doi.org/10.3390/f8090340>
- Momen, M., Wood, J. D., Novick, K. A., Pangle, R., Pockman, W. T., McDowell, N. G., & Konings, A. G. (2017). Interacting effects of leaf water potential and biomass on vegetation optical depth. *Journal of Geophysical Research-Biogeosciences*, 122(11), 3031–3046. <https://doi.org/10.1002/2017jg004145>
- Moody, J. A., Martin, R. G., & Ebel, B. A. (2019). Sources of inherent infiltration variability in postwildfire soils. *Hydrological Processes*, 33(23), 3010–3029. <https://doi.org/10.1002/hyp.13543>
- Musthafa, M., Khati, U., & Singh, G. (2020). Sensitivity of PolSAR decomposition to forest disturbance and regrowth dynamics in a managed forest. *Advances in Space Research*, 66(8), 1863–1875. <https://doi.org/10.1016/j.asr.2020.07.007>
- Nasi, R., Honkavaara, E., Blomqvist, M., Lyytikäinen-Saarenmaa, P., Hakala, T., Viljanen, N., et al. (2018). Remote sensing of bark beetle damage in urban forests at individual tree level using a novel hyperspectral camera from UAV and aircraft. *Urban Forestry and Urban Greening*, 30, 72–83. <https://doi.org/10.1016/j.ufug.2018.01.010>
- Nasi, R., Honkavaara, E., Lyytikäinen-Saarenmaa, P., Blomqvist, M., Litkey, P., Hakala, T., et al. (2015). Using UAV-based photogrammetry and hyperspectral imaging for mapping bark beetle damage at tree-level. *Remote Sensing*, 7(11), 15467–15493. <https://doi.org/10.3390/rs71115467>
- Navarre-Sitchler, A. K., Brantley, S. L., & Rother, G. (2015). How porosity increases during incipient weathering of crystalline silicate rocks. *Pore-Scale Geochemical Processes*, 80(1), 331–354. <https://doi.org/10.2138/rmg.2015.80.10>
- Navarre-Sitchler, A. K., Cole, D. R., Rother, G., Jin, L., Buss, H. L., & Brantley, S. L. (2013). Porosity and surface area evolution during weathering of two igneous rocks. *Geochimica et Cosmochimica Acta*, 109, 400–413. <https://doi.org/10.1016/j.gca.2013.02.012>
- Navarre-Sitchler, A. K., Steefel, C. I., Yang, L., Tomutsa, L., & Brantley, S. L. (2009). Evolution of porosity and diffusivity associated with chemical weathering of a basaltic clast. *Journal of Geophysical Research*, 114(F2), F02016. <https://doi.org/10.1029/2008jf001060>
- NCALM. (2012). Jemez River Basin snow-off LiDAR survey. [Dataset]. <https://doi.org/10.5069/G9RB72JV>
- NCALM. (2014). Jemez River Basin, NM: Post-fire landscape response. [Dataset]. <https://doi.org/10.5069/G9319SVB>
- Neinavaz, E., Schlerf, M., Darvishzadeh, R., Gerhards, M., & Skidmore, A. K. (2021). Thermal infrared remote sensing of vegetation: Current status and perspectives. *International Journal of Applied Earth Observation and Geoinformation*, 102, 102415. <https://doi.org/10.1016/j.jag.2021.102415>
- Newton, A. C., Hill, R. A., Echeverria, C., Golicher, D., Benayas, J. M. R., Cayuela, L., & Hinsley, S. A. (2009). Remote sensing and the future of landscape ecology. *Progress in Physical Geography: Earth and Environment*, 33(4), 528–546. <https://doi.org/10.1177/0309133309346882>
- Ningthoujam, R. K., Tansey, K., Baltzer, H., Morrison, K., Johnson, S. C. M., Gerard, F., et al. (2016). Mapping forest cover and forest cover change with airborne S-band radar. *Remote Sensing*, 8(7), 577. <https://doi.org/10.3390/rs8070577>
- Norman, L. M., Lal, R., Wohl, E., Fairfax, E., Gellis, A. C., & Pollock, M. M. (2022). Natural infrastructure in dryland streams (NIDS) can establish regenerative wetland sinks that reverse desertification and strengthen climate resilience. *Science of the Total Environment*, 849, 157738. <https://doi.org/10.1016/j.scitotenv.2022.157738>
- Nouwakpo, S. K., Weltz, M. A., & McGwire, K. (2016). Assessing the performance of structure-from-motion photogrammetry and terrestrial LiDAR for reconstructing soil surface microtopography of naturally vegetated plots. *Earth Surface Processes and Landforms*, 41(3), 308–322. <https://doi.org/10.1002/esp.3787>
- Okin, G. S., Dong, C. Y., Willis, K. S., Gillespie, T. W., & MacDonald, G. M. (2018). The impact of drought on native Southern California vegetation: Remote sensing analysis using MODIS-derived time series. *Journal of Geophysical Research-Biogeosciences*, 123(6), 1927–1939. <https://doi.org/10.1029/2018jg004485>
- Orem, C. A., & Pelletier, J. D. (2015). Quantifying the time scale of elevated geomorphic response following wildfires using multi-temporal LiDAR data: An example from the Las Conchas fire, Jemez Mountains, New Mexico. *Geomorphology*, 232, 224–238. <https://doi.org/10.1016/j.geomorph.2015.01.006>
- Orem, C. A., & Pelletier, J. D. (2016). The predominance of post-wildfire erosion in the long-term denudation of the Valles Caldera, New Mexico. *Journal of Geophysical Research-Earth Surface*, 121(5), 843–864. <https://doi.org/10.1002/2015jf003663>
- Otkin, J. A., Anderson, M. C., Hain, C., Mladenova, I. E., Basara, J. B., & Svoboda, M. (2013). Examining rapid onset drought development using the thermal infrared-based evaporative stress index. *Journal of Hydrometeorology*, 14(4), 1057–1074. <https://doi.org/10.1175/jhm-d-12-0144.1>
- Panagiotidis, D., Abdollahnejad, A., Surovy, P., & Chiteculo, V. (2017). Determining tree height and crown diameter from high-resolution UAV imagery. *International Journal of Remote Sensing*, 38(8–10), 2392–2410. <https://doi.org/10.1080/01431161.2016.1264028>
- Parks, S. A., Holsinger, L. M., Panunto, M. H., Jolly, W. M., Dobrowski, S. Z., & Dillon, G. K. (2018). High-severity fire: Evaluating its key drivers and mapping its probability across Western US forests. *Environmental Research Letters*, 13(4), 044037. <https://doi.org/10.1088/1748-9326/aab791>
- Pascolini-Campbell, M., Lee, C., Stavros, N., & Fisher, J. B. (2022). ECOSTRESS reveals pre-fire vegetation controls on burn severity for Southern California wildfires of 2020. *Global Ecology and Biogeography*, 31(10), 1976–1989. <https://doi.org/10.1111/geb.13526>
- Paz-Kagan, T., Vaughn, N. R., Martin, R. E., Brodrick, P. G., Stephenson, N. L., Das, A. J., et al. (2018). Landscape-scale variation in canopy water content of giant sequoias during drought. *Forest Ecology and Management*, 419, 291–304. <https://doi.org/10.1016/j.foreco.2017.11.018>
- Pelletier, J. D., Barron-Gafford, G. A., Breshears, D. D., Brooks, P. D., Chorover, J., Durcik, M., et al. (2013). Coevolution of nonlinear trends in vegetation, soils, and topography with elevation and slope aspect: A case study in the sky islands of southern Arizona. *Journal of Geophysical Research-Earth Surface*, 118(2), 741–758. <https://doi.org/10.1002/jgrf.20046>
- Peterson, T. J., Saft, M., Peel, M. C., & John, A. (2021). Watersheds may not recover from drought. *Science*, 372(6543), 745–+. <https://doi.org/10.1126/science.abd5085>
- Petrakis, R. E., Villarreal, M. L., Wu, Z. T., Hetzler, R., Middleton, B. R., & Norman, L. M. (2018). Evaluating and monitoring forest fuel treatments using remote sensing applications in Arizona, USA. *Forest Ecology and Management*, 413, 48–61. <https://doi.org/10.1016/j.foreco.2018.01.036>
- Petroulli, N., Vik, J. O., Mysterud, A., Gaillard, J. M., Tucker, C. J., & Stenseth, N. C. (2005). Using the satellite-derived NDVI to assess ecological responses to environmental change. *Trends in Ecology & Evolution*, 20(9), 503–510. <https://doi.org/10.1016/j.tree.2005.05.011>
- Pitcher, L. H., Pavelsky, T. M., Smith, L. C., Moller, D. K., Altenau, E. H., Allen, G. H., et al. (2019). AirSWOT InSAR mapping of surface water elevations and hydraulic gradients across the Yukon Flats Basin, Alaska. *Water Resources Research*, 55(2), 937–953. <https://doi.org/10.1029/2018wr023274>

- Pohl, C., & van Genderen, J. L. (1998). Multisensor image fusion in remote sensing: Concepts, methods and applications. *International Journal of Remote Sensing*, 19(5), 823–854. <https://doi.org/10.1080/014311698215748>
- Poulos, H. M., Barton, A. M., Koch, G. W., Kolb, T. E., & Thode, A. E. (2021). Wildfire severity and vegetation recovery drive post-fire evapotranspiration in a southwestern Pine-Oak Forest, Arizona, USA. *Remote Sensing in Ecology and Conservation*, 7(4), 579–591. <https://doi.org/10.1002/rse2.210>
- Qi, W., Saarela, S., Armston, J., Stahl, G., & Dubayah, R. (2019). Forest biomass estimation over three distinct forest types using TanDEM-X InSAR data and simulated GEDI lidar data. *Remote Sensing of Environment*, 232, 111283. <https://doi.org/10.1016/j.rse.2019.111283>
- Radeloff, V. C., Helmers, D. P., Kramer, H. A., Mockrin, M. H., Alexandre, P. M., Bar-Massada, A., et al. (2018). Rapid growth of the US wildland-urban interface raises wildfire risk. *Proceedings of the National Academy of Sciences of the United States of America*, 115(13), 3314–3319. <https://doi.org/10.1073/pnas.1718850115>
- Ramirez, F. J. R., Navarro-Cerrillo, R. M., Varo-Martinez, M. A., Quero, J. L., Doerr, S., & Hernandez-Clemente, R. (2018). Determination of forest fuels characteristics in mortality-affected Pinus forests using integrated hyperspectral and ALS data. *International Journal of Applied Earth Observation and Geoinformation*, 68, 157–167. <https://doi.org/10.1016/j.jag.2018.01.003>
- Rao, K., Anderegg, W. R. L., Sala, A., Martinez-Vilalta, J., & Konings, A. G. (2019). Satellite-based vegetation optical depth as an indicator of drought-driven tree mortality. *Remote Sensing of Environment*, 227, 125–136. <https://doi.org/10.1016/j.rse.2019.03.026>
- Rasmussen, C., Pelletier, J. D., Troch, P. A., Swetnam, T. L., & Chorover, J. (2015). Quantifying topographic and vegetation effects on the transfer of energy and mass to the critical zone. *Vadose Zone Journal*, 14(11), 1–16. <https://doi.org/10.2136/vzj2014.07.0102>
- Rathburn, S. L., Bennett, G. L., Wohl, E. E., Briles, C., McElroy, B., & Sutfin, N. (2017). The fate of sediment, wood, and organic carbon eroded during an extreme flood, Colorado Front Range, USA. *Geology*, 45(6), 499–502. <https://doi.org/10.1130/g38935.1>
- Rathburn, S. L., Shahverdian, S. M., & Ryan, S. E. (2018). Post-disturbance sediment recovery: Implications for watershed resilience. *Geomorphology*, 305, 61–75. <https://doi.org/10.1016/j.geomorph.2017.08.039>
- Richardson, A. D. (2019). Tracking seasonal rhythms of plants in diverse ecosystems with digital camera imagery. *New Phytologist*, 222(4), 1742–1750. <https://doi.org/10.1111/nph.15591>
- Richardson, A. D., Hufkens, K., Milliman, T., Aubrecht, D. M., Chen, M., Gray, J. M., et al. (2018). Tracking vegetation phenology across diverse North American biomes using PhenoCam imagery. *Scientific Data*, 5(1), 180028. <https://doi.org/10.1038/sdata.2018.28>
- Richardson, J. J., Moskal, L. M., & Bakker, J. D. (2014). Terrestrial laser scanning for vegetation sampling. *Sensors*, 14(11), 20304–20319. <https://doi.org/10.3390/s141120304>
- Robichaud, P. R., Lewis, S. A., Laes, D. Y. M., Hudak, A. T., Kokaly, R. F., & Zamudio, J. A. (2007). Postfire soil burn severity mapping with hyperspectral image unmixing. *Remote Sensing of Environment*, 108(4), 467–480. <https://doi.org/10.1016/j.rse.2006.11.027>
- Rosette, J. A. B., North, P. R. J., & Suarez, J. C. (2008). Vegetation height estimates for a mixed temperate forest using satellite laser altimetry. *International Journal of Remote Sensing*, 29(5), 1475–1493. <https://doi.org/10.1080/01431160701736380>
- Rossi, F. C., Fritz, A., & Becker, G. (2018). Combining satellite and UAV imagery to delineate forest cover and basal area after mixed-severity fires. *Sustainability*, 10(7), 2227. <https://doi.org/10.3390/su10072227>
- Rother, M. T., & Veblen, T. T. (2016). Limited conifer regeneration following wildfires in dry ponderosa pine forests of the Colorado Front Range. *Ecosphere*, 7(12). <https://doi.org/10.1002/ecs2.1594>
- Rother, M. T., & Veblen, T. T. (2017). Climate drives episodic conifer establishment after fire in dry ponderosa pine forests of the Colorado Front Range, USA. *Forests*, 8(5), 159. <https://doi.org/10.3390/f8050159>
- Roy, D. P., Ju, J., Lewis, P., Schaaf, C., Gao, F., Hansen, M., & Lindquist, E. (2008). Multi-temporal MODIS-Landsat data fusion for relative radiometric normalization, gap filling, and prediction of Landsat data. *Remote Sensing of Environment*, 112(6), 3112–3130. <https://doi.org/10.1016/j.rse.2008.03.009>
- Ruetschi, M., Small, D., & Waser, L. T. (2019). Rapid detection of windthrows using Sentinel-1 C-band SAR data. *Remote Sensing*, 11(2), 115. <https://doi.org/10.3390/rs11020115>
- Saarinen, N., Vastaranta, M., Nasi, R., Rosnell, T., Hakala, T., Honkavaara, E., et al. (2018). Assessing biodiversity in boreal forests with UAV-based photogrammetric point clouds and hyperspectral imaging. *Remote Sensing*, 10(2), 338. <https://doi.org/10.3390/rs10020338>
- Saatchi, S., Asefi-Najafabady, S., Malhi, Y., Aragao, L., Anderson, L. O., Myneni, R. B., & Nemani, R. (2013). Persistent effects of a severe drought on Amazonian forest canopy. *Proceedings of the National Academy of Sciences of the United States of America*, 110(2), 565–570. <https://doi.org/10.1073/pnas.1204651110>
- Saatchi, S. S., Houghton, R. A., Alvala, R., Soares, J. V., & Yu, Y. (2007). Distribution of aboveground live biomass in the Amazon basin. *Global Change Biology*, 13(4), 816–837. <https://doi.org/10.1111/j.1365-2486.2007.01323.x>
- Saksa, P. C., Bales, R. C., Tague, C. L., Battles, J. J., Tobin, B. W., & Conklin, M. H. (2020). Fuels treatment and wildfire effects on runoff from Sierra Nevada mixed-conifer forests. *Ecology*, 101(3). <https://doi.org/10.1002/eco.2151>
- Sankey, J. B., Sankey, T. T., Li, J. R., Ravi, S., Wang, G., Caster, J., & Kasprak, A. (2021). Quantifying plant-soil-nutrient dynamics in rangelands: Fusion of UAV hyperspectral-LiDAR, UAV multispectral-photogrammetry, and ground-based LiDAR-digital photography in a shrub-encroached desert grassland. *Remote Sensing of Environment*, 253, 112223. <https://doi.org/10.1016/j.rse.2020.112223>
- Sankey, T., Donager, J., McVay, J., & Sankey, J. B. (2017). UAV lidar and hyperspectral fusion for forest monitoring in the southwestern USA. *Remote Sensing of Environment*, 195, 30–43. <https://doi.org/10.1016/j.rse.2017.04.007>
- Sankey, T., & Tatum, J. (2022). Thinning increases forest resiliency during unprecedented drought. *Scientific Reports*, 12(1), 9041. <https://doi.org/10.1038/s41598-022-12982-z>
- Sankey, T. T., McVay, J., Swetnam, T. L., McClaran, M. P., Heilman, P., & Nichols, M. (2018). UAV hyperspectral and lidar data and their fusion for arid and semi-arid land vegetation monitoring. *Remote Sensing in Ecology and Conservation*, 4(1), 20–33. <https://doi.org/10.1002/rse2.44>
- Santesteban, L. G., Di Gennaro, S. F., Herrero-Langreo, A., Miranda, C., Royo, J. B., & Matese, A. (2017). High-resolution UAV-based thermal imaging to estimate the instantaneous and seasonal variability of plant water status within a vineyard. *Agricultural Water Management*, 183, 49–59. <https://doi.org/10.1016/j.agwat.2016.08.026>
- Sato, L. Y., Gomes, V. C. F., Shimabukuro, Y. E., Keller, M., Arai, E., Nara dos-Santos, M., et al. (2016). Post-fire changes in forest biomass retrieved by airborne LiDAR in Amazonia. *Remote Sensing*, 8(10), 839. <https://doi.org/10.3390/rs8100839>
- Savage, M., Mast, J. N., & Feddema, J. J. (2013). Double whammy: High-severity fire and drought in ponderosa pine forests of the southwest. *Canadian Journal of Forest Research-Revue Canadienne De Recherche Forestiere*, 43(6), 570–583. <https://doi.org/10.1139/cjfr-2012-0404>
- Savage, S. L., Lawrence, R. L., & Squires, J. R. (2017). Mapping post-disturbance forest landscape composition with Landsat satellite imagery. *Forest Ecology and Management*, 399, 9–23. <https://doi.org/10.1016/j.foreco.2017.05.017>
- Scherrer, D., Bader, M. K. F., & Korner, C. (2011). Drought-sensitivity ranking of deciduous tree species based on thermal imaging of forest canopies. *Agricultural and Forest Meteorology*, 151(12), 1632–1640. <https://doi.org/10.1016/j.agrformet.2011.06.019>

- Schmidt, M., Lucas, R., Bunting, P., Verbesselt, J., & Armston, J. (2015). Multi-resolution time series imagery for forest disturbance and regrowth monitoring in Queensland, Australia. *Remote Sensing of Environment*, 158, 156–168. <https://doi.org/10.1016/j.rse.2014.11.015>
- Senf, C., Muller, J., & Seidl, R. (2019). Post-disturbance recovery of forest cover and tree height differ with management in Central Europe. *Landscape Ecology*, 34(12), 2837–2850. <https://doi.org/10.1007/s10980-019-00921-9>
- Senf, C., Seidl, R., & Hostert, P. (2017). Remote sensing of forest insect disturbances: Current state and future directions. *International Journal of Applied Earth Observation and Geoinformation*, 60, 49–60. <https://doi.org/10.1016/j.jag.2017.04.004>
- Seyednasrollah, B., Domec, J. C., & Clark, J. S. (2019). Spatiotemporal sensitivity of thermal stress for monitoring canopy hydrological stress in near real-time. *Agricultural and Forest Meteorology*, 269, 220–230. <https://doi.org/10.1016/j.agrformet.2019.02.016>
- Shakesby, R. A., & Doerr, S. H. (2006). Wildfire as a hydrological and geomorphological agent. *Earth-Science Reviews*, 74(3–4), 269–307. <https://doi.org/10.1016/j.earscirev.2005.10.006>
- Shi, Y. N., Davis, K. J., Duffy, C. J., & Yu, X. (2013). Development of a coupled land surface hydrologic model and evaluation at a critical zone observatory. *Journal of Hydrometeorology*, 14(5), 1401–1420. <https://doi.org/10.1175/jhm-d-12-0145.1>
- Shivers, S. W., Roberts, D. A., & McFadden, J. P. (2019). Using paired thermal and hyperspectral aerial imagery to quantify land surface temperature variability and assess crop stress within California orchards. *Remote Sensing of Environment*, 222, 215–231. <https://doi.org/10.1016/j.rse.2018.12.030>
- Sholtes, J. S., Yochum, S. E., Scott, J. A., & Bledsoe, B. P. (2018). Longitudinal variability of geomorphic response to floods. *Earth Surface Processes and Landforms*, 43(15), 3099–3113. <https://doi.org/10.1002/esp.4472>
- Singhal, J., Srivastava, G., Reddy, C. S., Rajashekar, G., Jha, C., Rao, P. V., et al. (2021). Assessment of carbon stock at tree level using terrestrial laser scanning vs. Traditional methods in tropical forest, India. *IEEE Journal of Selected Topics in Applied Earth Observations and Remote Sensing*, 14, 5064–5071. <https://doi.org/10.1109/jstars.2021.3076195>
- Skole, D. L., Mbow, C., Mugabowindekwe, M., Brandt, M. S., & Samek, J. H. (2021). Trees outside of forests as natural climate solutions. *Nature Climate Change*, 11(12), 1013–1016. <https://doi.org/10.1038/s41558-021-01230-3>
- Smigaj, M., Gaulton, R., Suarez, J. C., & Barr, S. L. (2017). Use of miniature thermal cameras for detection of physiological stress in conifers. *Remote Sensing*, 9(9), 957. <https://doi.org/10.3390/rs9090957>
- Smith, H. G., Sheridan, G. J., Lane, P. N. J., Nyman, P., & Haydon, S. (2011). Wildfire effects on water quality in forest catchments: A review with implications for water supply. *Journal of Hydrology*, 396(1–2), 170–192. <https://doi.org/10.1016/j.jhydrol.2010.10.043>
- Sobejano-Paz, V., Mikkelsen, T. N., Baum, A., Mo, X. G., Liu, S. X., Koppl, C. J., et al. (2020). Hyperspectral and thermal sensing of stomatal conductance, transpiration, and photosynthesis for soybean and maize under drought. *Remote Sensing*, 12(19), 3182. <https://doi.org/10.3390/rs12193182>
- Spruce, J. P., Hicke, J. A., Hargrove, W. W., Grulke, N. E., & Meddens, A. J. H. (2019). Use of MODIS NDVI products to map tree mortality levels in forests affected by mountain pine beetle outbreaks. *Forests*, 10(9), 811. <https://doi.org/10.3390/f10090811>
- Steininger, M. K. (2000). Satellite estimation of tropical secondary forest above-ground biomass: Data from Brazil and Bolivia. *International Journal of Remote Sensing*, 21(6–7), 1139–1157. <https://doi.org/10.1080/014311600210119>
- Stephens, S. L., Collins, B. M., Fettig, C. J., Finney, M. A., Hoffman, C. M., Knapp, E. E., et al. (2018). Drought, tree mortality, and wildfire in forests adapted to frequent fire. *BioScience*, 68(2), 77–88. <https://doi.org/10.1093/biosci/bix146>
- Stephens, S. L., Thompson, S., Boisrame, G., Collins, B. M., Ponsio, L. C., Rakhmatulina, E., et al. (2021). Fire, water, and biodiversity in the Sierra Nevada: A possible triple win. *Environmental Research Communications*, 3(8), 081004. <https://doi.org/10.1088/2515-7620/ac17e2>
- Stovall, A. E. L., Anderson-Teixeira, K. J., & Shugart, H. H. (2018). Assessing terrestrial laser scanning for developing non-destructive biomass allometry. *Forest Ecology and Management*, 427, 217–229. <https://doi.org/10.1016/j.foreco.2018.06.004>
- Stovall, A. E. L., Diamond, J. S., Slesak, R. A., McLaughlin, D. L., & Shugart, H. (2019). Quantifying wetland microtopography with terrestrial laser scanning. *Remote Sensing of Environment*, 232, 11271. <https://doi.org/10.1016/j.rse.2019.11.1271>
- Stovall, A. E. L., Shugart, H., & Yang, X. (2019). Tree height explains mortality risk during an intense drought. *Nature Communications*, 10(1), 4385. <https://doi.org/10.1038/s41467-019-12380-6>
- Swatantran, A., Dubayah, R., Roberts, D., Hofton, M., & Blair, J. B. (2011). Mapping biomass and stress in the Sierra Nevada using lidar and hyperspectral data fusion. *Remote Sensing of Environment*, 115(11), 2917–2930. <https://doi.org/10.1016/j.rse.2010.08.027>
- Swetnam, T. L., Falk, D. A., Lynch, A. M., & Yool, S. R. (2014). Estimating individual tree mid- and understorey rank-size distributions from airborne laser scanning in semi-arid forests. *Forest Ecology and Management*, 330, 271–282. <https://doi.org/10.1016/j.foreco.2014.07.011>
- Szpakowski, D. M., & Jensen, J. L. R. (2019). A review of the applications of remote sensing in fire ecology. *Remote Sensing*, 11(22), 2638. <https://doi.org/10.3390/rs11222638>
- Tague, C. L., Moritz, M., & Hanan, E. (2019). The changing water cycle: The eco-hydrologic impacts of forest density reduction in Mediterranean (seasonally dry) regions. *Wiley Interdisciplinary Reviews-Water*, 6(4). <https://doi.org/10.1002/wat2.1350>
- Tague, C. L., & Moritz, M. A. (2019). Plant accessible water storage capacity and tree-scale root interactions determine how forest density reductions alter forest water use and productivity. *Frontiers in Forests and Global Change*, 2. <https://doi.org/10.3389/ffgc.2019.00036>
- Takahashi, A., Oguma, H., Shimada, M., Watanabe, M., Yone, Y., & Saigusa, N. (2011). Influence of thinning and windthrow on backscatter of the airborne L-band synthetic aperture radar at a Larch forest in Northern Japan. *Interaction Science*. Paper presented at the Earth Observation for Land-Atmosphere.
- Tanase, M., de la Riva, J., Santoro, M., Perez-Cabello, F., & Kasischke, E. (2011). Sensitivity of SAR data to post-fire forest regrowth in Mediterranean and boreal forests. *Remote Sensing of Environment*, 115(8), 2075–2085. <https://doi.org/10.1016/j.rse.2011.04.009>
- Tanase, M. A., Aponte, C., Mermoz, S., Bouvet, A., Toan, T. L., & Heurich, M. (2018). Detection of windthrows and insect outbreaks by L-band SAR: A case study in the Bavarian Forest National Park. *Remote Sensing of Environment*, 209, 700–711. <https://doi.org/10.1016/j.rse.2018.03.009>
- Tanase, M. A., Santoro, M., Wegmuller, U., de la Riva, J., & Perez-Cabello, F. (2010). Properties of X-C- and L-band repeat-pass interferometric SAR coherence in Mediterranean pine forests affected by fires. *Remote Sensing of Environment*, 114(10), 2182–2194. <https://doi.org/10.1016/j.rse.2010.04.021>
- Tanase, M. A., Villard, L., Pitar, D., Apostol, B., Petrilă, M., Chivulescu, S., et al. (2019). Synthetic aperture radar sensitivity to forest changes: A simulations-based study for the Romanian forests. *Science of the Total Environment*, 689, 1104–1114. <https://doi.org/10.1016/j.scitotenv.2019.06.494>
- Tane, Z., Roberts, D., Koltunov, A., Sweeney, S., & Ramirez, C. (2018). A framework for detecting conifer mortality across an ecoregion using high spatial resolution spaceborne imaging spectroscopy. *Remote Sensing of Environment*, 209, 195–210. <https://doi.org/10.1016/j.rse.2018.02.073>
- Tang, L. N., & Shao, G. F. (2015). Drone remote sensing for forestry research and practices. *Journal of Forestry Research*, 26(4), 791–797. <https://doi.org/10.1007/s11676-015-0088-y>

- Tavani, S., Billi, A., Corradetti, A., Mercuri, M., Bosman, A., Cuffaro, M., et al. (2022). Smartphone assisted fieldwork: Towards the digital transition of geoscience fieldwork using LiDAR-equipped iPhones. *Earth-Science Reviews*, 227, 103969. <https://doi.org/10.1016/j.earscirev.2022.103969>
- Thorne, J. H., Choe, H., Stine, P. A., Chambers, J. C., Holguin, A., Kerr, A. C., & Schwartz, M. W. (2018). Climate change vulnerability assessment of forests in the Southwest USA. *Climatic Change*, 148(3), 387–402. <https://doi.org/10.1007/s10584-017-2010-4>
- Tomastik, J., Mokros, M., Salon, S., Chudy, F., & Tunak, D. (2017). Accuracy of photogrammetric UAV-based point clouds under conditions of partially-open forest canopy. *Forests*, 8(5), 151. <https://doi.org/10.3390/f8050151>
- Treuhaft, R. N., Law, B. E., & Asner, G. P. (2004). Forest attributes from radar interferometric structure and its fusion with optical remote sensing. *BioScience*, 54(6), 561–571. [https://doi.org/10.1641/0006-3568\(2004\)054\[0561:faftris\]2.0.co;2](https://doi.org/10.1641/0006-3568(2004)054[0561:faftris]2.0.co;2)
- Troch, P. A., Lahmers, T., Meira, A., Mukherjee, R., Pedersen, J. W., Roy, T., & Valdes-Pineda, R. (2015). Catchment coevolution: A useful framework for improving predictions of hydrological change? *Water Resources Research*, 51(7), 4903–4922. <https://doi.org/10.1002/2015wr017032>
- Tsamir, M., Gottlieb, S., Preisler, Y., Rotenberg, E., Tatarinov, F., Yakir, D., et al. (2019). Stand density effects on carbon and water fluxes in a semi-arid forest, from leaf to stand-scale. *Forest Ecology and Management*, 453, 117573. <https://doi.org/10.1016/j.foreco.2019.117573>
- Turner, M. G. (1989). Landscape ecology: The effect of pattern on process. *Annual Review of Ecology and Systematics*, 20(1), 171–197. <https://doi.org/10.1146/annurev.es.20.110189.001131>
- USGS. (2022). NM NorthCentral B1 2016. [Dataset]. Retrieved from: https://portal.opentopography.org/usgsDataset?dsid=NM_NorthCentral_B1_2016
- Vanderhoof, M. K., Hawbaker, T. J., Ku, A. D., Merriam, K., Berryman, E., & Cattau, M. (2021). Tracking rates of postfire conifer regeneration vs. deciduous vegetation recovery across the Western United States. *Ecological Applications*, 31(2). <https://doi.org/10.1002/eap.2237>
- van Ewijk, K. Y., Treitz, P. M., & Scott, N. A. (2011). Characterizing forest succession in Central Ontario using lidar-derived indices. *Photogrammetric Engineering & Remote Sensing*, 77(3), 261–269. <https://doi.org/10.14358/pers.77.3.261>
- van Leeuwen, W. J. D., Orr, B. J., Marsh, S. E., & Herrmann, S. M. (2006). Multi-sensor NDVI data continuity: Uncertainties and implications for vegetation monitoring applications. *Remote Sensing of Environment*, 100(1), 67–81. <https://doi.org/10.1016/j.rse.2005.10.002>
- Van Wagtenonk, J. W. (2007). The history and evolution of wildland fire use. *Fire Ecology*, 3(2), 3–17. <https://doi.org/10.4996/fireecology.0302003>
- van Wagtenonk, J. W., Root, R. R., & Key, C. H. (2004). Comparison of AVIRIS and Landsat ETM+ detection capabilities for burn severity. *Remote Sensing of Environment*, 92(3), 397–408. <https://doi.org/10.1016/j.rse.2003.12.015>
- Vane, G., Green, R. O., Chrien, T. G., Enmark, H. T., Hansen, E. G., & Porter, W. M. (1993). The airborne visible/infrared imaging spectrometer (AVIRIS). *Remote Sensing of Environment*, 44(2–3), 127–143.
- Veraverbeke, S., Dennison, P., Gitas, I., Hulley, G., Kalashnikova, O., Katagis, T., et al. (2018). Hyperspectral remote sensing of fire: State-of-the-art and future perspectives. *Remote Sensing of Environment*, 216, 105–121. <https://doi.org/10.1016/j.rse.2018.06.020>
- Veraverbeke, S., Harris, S., & Hook, S. (2011). Evaluating spectral indices for burned area discrimination using MODIS/ASTER (MASTER) airborne simulator data. *Remote Sensing of Environment*, 115(10), 2702–2709. <https://doi.org/10.1016/j.rse.2011.06.010>
- Veraverbeke, S., Stavros, E. N., & Hook, S. J. (2014). Assessing fire severity using imaging spectroscopy data from the Airborne Visible/Infrared Imaging Spectrometer (AVIRIS) and comparison with multispectral capabilities. *Remote Sensing of Environment*, 154, 153–163. <https://doi.org/10.1016/j.rse.2014.08.019>
- Verbesselt, J., Robinson, A., Stone, C., & Culvenor, D. (2009). Forecasting tree mortality using change metrics derived from MODIS satellite data. *Forest Ecology and Management*, 258(7), 1166–1173. <https://doi.org/10.1016/j.foreco.2009.06.011>
- Viana-Soto, A., Garcia, M., Aguado, I., & Salas, J. (2022). Assessing post-fire forest structure recovery by combining LiDAR data and Landsat time series in Mediterranean pine forests. *International Journal of Applied Earth Observation and Geoinformation*, 108, 102754. <https://doi.org/10.1016/j.jag.2022.102754>
- Virlet, N., Lebourgeois, V., Martinez, S., Costes, E., Labbe, S., & Regnard, J. L. (2014). Stress indicators based on airborne thermal imagery for field phenotyping a heterogeneous tree population for response to water constraints. *Journal of Experimental Botany*, 65(18), 5429–5442. <https://doi.org/10.1093/jxb/eru309>
- Vivoni, E. R., Rango, A., Anderson, C. A., Pierini, N. A., Schreiner-McGraw, A. P., Saripalli, S., & Laliberte, A. S. (2014). Ecohydrology with unmanned aerial vehicles. *Ecosphere*, 5(10), art130. <https://doi.org/10.1890/es14-00217.1>
- Vogel, J. C., Yang, Z. Q., & Cohen, W. B. (2016). Mapping post-fire habitat characteristics through the fusion of remote sensing tools. *Remote Sensing of Environment*, 173, 294–303. <https://doi.org/10.1016/j.rse.2015.08.011>
- Wallace, L., Lucieer, A., Malenovsky, Z., Turner, D., & Vopenka, P. (2016). Assessment of forest structure using two UAV techniques: A comparison of airborne laser scanning and Structure from Motion (SfM) point clouds. *Forests*, 7(3), 62. <https://doi.org/10.3390/f7030062>
- Walter, J. A., & Platt, R. V. (2013). Multi-temporal analysis reveals that predictors of mountain pine beetle infestation change during outbreak cycles. *Forest Ecology and Management*, 302, 308–318. <https://doi.org/10.1016/j.foreco.2013.03.038>
- Wang, B., Smith, L. C., Yang, X., Pavelsky, T. M., Altenau, E. H., Gleason, C. J., et al. (2022). Remote sensing of broad-scale controls on large river anabranching. *Remote Sensing of Environment*, 281, 113243. <https://doi.org/10.1016/j.rse.2022.113243>
- Warrick, J. A., Hatten, J. A., Pasternack, G. B., Gray, A. B., Goni, M. A., & Wheatcroft, R. A. (2012). The effects of wildfire on the sediment yield of a coastal California watershed. *Geological Society of America Bulletin*, 124(7–8), 1130–1146. <https://doi.org/10.1130/b30451.1>
- Weiss, M., Jacob, F., & Duveiller, G. (2020). Remote sensing for agricultural applications: A meta-review. *Remote Sensing of Environment*, 236, 111402. <https://doi.org/10.1016/j.rse.2019.111402>
- White, J. C., Hermosilla, T., Wulder, M. A., & Coops, N. C. (2022). Mapping, validating, and interpreting spatio-temporal trends in post-disturbance forest recovery. *Remote Sensing of Environment*, 271, 112904. <https://doi.org/10.1016/j.rse.2022.112904>
- White, J. C., Saarinen, N., Kankare, V., Wulder, M. A., Hermosilla, T., Coops, N. C., et al. (2018). Confirmation of post-harvest spectral recovery from Landsat time series using measures of forest cover and height derived from airborne laser scanning data. *Remote Sensing of Environment*, 216, 262–275. <https://doi.org/10.1016/j.rse.2018.07.004>
- White, J. C., Wulder, M. A., Hermosilla, T., Coops, N. C., & Hobart, G. W. (2017). A nationwide annual characterization of 25 years of forest disturbance and recovery for Canada using Landsat time series. *Remote Sensing of Environment*, 194, 303–321. <https://doi.org/10.1016/j.rse.2017.03.035>
- Williams, A. P., Allen, C. D., Macalady, A. K., Griffin, D., Woodhouse, C. A., Meko, D. M., et al. (2013). Temperature as a potent driver of regional forest drought stress and tree mortality. *Nature Climate Change*, 3(3), 292–297. <https://doi.org/10.1038/nclimate1693>
- Williams, C. A., Collatz, G. J., Masek, J., Huang, C., & Goward, S. N. (2014). Impacts of disturbance history on forest carbon stocks and fluxes: Merging satellite disturbance mapping with forest inventory data in a carbon cycle model framework. *Remote Sensing of Environment*, 151, 57–71. <https://doi.org/10.1016/j.rse.2013.10.034>
- Williams, M., Schwarz, P. A., Law, B. E., Irvine, J., & Kurpius, M. R. (2005). An improved analysis of forest carbon dynamics using data assimilation. *Global Change Biology*, 11(1), 89–105. <https://doi.org/10.1111/j.1365-2486.2004.00891.x>

- Wilson, E. H., & Sader, S. A. (2002). Detection of forest harvest type using multiple dates of Landsat TM imagery. *Remote Sensing of Environment*, 80(3), 385–396. [https://doi.org/10.1016/S0034-4257\(01\)00318-2](https://doi.org/10.1016/S0034-4257(01)00318-2)
- Wing, B. M., Ritchie, M. W., Boston, K., Cohen, W. B., Gitelman, A., & Olsen, M. J. (2012). Prediction of understory vegetation cover with airborne lidar in an interior ponderosa pine forest. *Remote Sensing of Environment*, 124, 730–741. <https://doi.org/10.1016/j.rse.2012.06.024>
- Woellert, K., Ehrenfreund, P., Ricco, A. J., & Hertzfeld, H. (2011). Cubesats: Cost-effective science and technology platforms for emerging and developing nations. *Advances in Space Research*, 47(4), 663–684. <https://doi.org/10.1016/j.asr.2010.10.009>
- Wohl, E., Marshall, A. E., Scamardo, J., White, D., & Morrison, R. R. (2022). Biogeomorphic influences on river corridor resilience to wildfire disturbances in a mountain stream of the Southern Rockies, USA. *Science of the Total Environment*, 820, 153321. <https://doi.org/10.1016/j.scitotenv.2022.153321>
- Wong, C. Y. S., D'Odorico, P., Bhathena, Y., Arain, M. A., & Ensminger, I. (2019). Carotenoid based vegetation indices for accurate monitoring of the phenology of photosynthesis at the leaf-scale in deciduous and evergreen trees. *Remote Sensing of Environment*, 233, 111407. <https://doi.org/10.1016/j.rse.2019.111407>
- Wulder, M. A., Dymond, C. C., White, J. C., Leckie, D. G., & Carroll, A. L. (2006). Surveying mountain pine beetle damage of forests: A review of remote sensing opportunities. *Forest Ecology and Management*, 221(1–3), 27–41. <https://doi.org/10.1016/j.foreco.2005.09.021>
- Xu, Q., Man, A., Fredrickson, M. M., Hou, Z., Pitkanen, J., Wing, B., et al. (2018). LiDAR-derived aboveground biomass and uncertainty for California forests, 2005–2014. [Dataset]. <https://doi.org/10.3334/ORNDAAC/1537>
- Yan, M., Tian, X., Li, Z. Y., Chen, E. X., Wang, X. F., Han, Z. T., & Sun, H. (2016). Simulation of forest carbon fluxes using model incorporation and data assimilation. *Remote Sensing*, 8(7), 567. <https://doi.org/10.3390/rs8070567>
- Yang, Y., Anderson, M., Gao, F., Hain, C., Noormets, A., Sun, G., et al. (2020). Investigating impacts of drought and disturbance on evapotranspiration over a forested landscape in North Carolina, USA using high spatiotemporal resolution remotely sensed data. *Remote Sensing of Environment*, 238, 111018. <https://doi.org/10.1016/j.rse.2018.12.017>
- Yang, Y. T., Long, D., Guan, H. D., Scanlon, B. R., Simmons, C. T., Jiang, L., & Xu, X. (2014). GRACE satellite observed hydrological controls on interannual and seasonal variability in surface greenness over mainland Australia. *Journal of Geophysical Research-Biogeosciences*, 119(12), 2245–2260. <https://doi.org/10.1002/2014jg002670>
- Young, D. J. N., Stevens, J. T., Earles, J. M., Moore, J., Ellis, A., Jirka, A. L., & Latimer, A. M. (2017). Long-term climate and competition explain forest mortality patterns under extreme drought. *Ecology Letters*, 20(1), 78–86. <https://doi.org/10.1111/ele.12711>
- Yu, X. W., Hyypä, J., Vastaranta, M., Holopainen, M., & Viitala, R. (2011). Predicting individual tree attributes from airborne laser point clouds based on the random forests technique. *ISPRS Journal of Photogrammetry and Remote Sensing*, 66(1), 28–37. <https://doi.org/10.1016/j.isprsjprs.2010.08.003>
- Zahawi, R. A., Dandois, J. P., Holl, K. D., Nadwodny, D., Reid, J. L., & Ellis, E. C. (2015). Using lightweight unmanned aerial vehicles to monitor tropical forest recovery. *Biological Conservation*, 186, 287–295. <https://doi.org/10.1016/j.biocon.2015.03.031>
- Zhu, X., Chen, J., Gao, F., Chen, X., & Masek, J. G. (2010). An enhanced spatial and temporal adaptive reflectance fusion model for complex heterogeneous regions. *Remote Sensing of Environment*, 114(11), 2610–2623. <https://doi.org/10.1016/j.rse.2010.05.032>
- Zolkos, S. G., Goetz, S. J., & Dubayah, R. (2013). A meta-analysis of terrestrial aboveground biomass estimation using lidar remote sensing. *Remote Sensing of Environment*, 128, 289–298. <https://doi.org/10.1016/j.rse.2012.10.017>